Isolierung und Strukturaufklärung von Naturstoffen aus Pilzen der Gattungen *Mycena*, *Megacollybia* und *Tricholomopsis*

Dissertation

zur Erlangung des Grades
Doktor der Naturwissenschaften
(Dr. rer. nat)

dem Fachbereich 2 (Biologie / Chemie)
der Universität Bremen
am 12. Januar 2018 vorgelegt

von

Michèle-Laure Lieunang Watat

1. Gutachter: Prof. Dr. Peter Spiteller

2. Gutachter: Prof. Dr. Franz-Peter Montforts

Datum des Kolloquiums: 08. Februar 2018

Meiner Familie gewidmet

„*In the multitude of my anxieties within me,*
your comforts delight my soul.“
Ps. 94: 19

ERKLÄRUNG

Die vorliegende Doktorarbeit wurde in der Zeit von Juni 2012 bis Dezember 2017 im Fachbereich 2 (Biologie / Chemie) der Universität Bremen unter der Betreuung von Prof. Dr. Peter Spiteller angefertigt.

Ich erkläre hiermit, dass ich die Doktorarbeit mit dem Titel

Isolierung und Strukturaufklärung von Naturstoffen aus Pilzen der Gattungen *Mycena*, *Megacollybia* und *Tricholomopsis*

selbstständig verfasst und geschrieben habe und außer den angegebenen Quellen keine weiteren Hilfsmittel verwendet habe. Die Stellen, die wörtlich oder sinngemäß aus anderen Werken entnommen wurde, habe ich unter Angabe der Quellen als solche kenntlich gemacht.

Bremen, den 12. Januar 2018

Michèle-Laure Lieunang Watat

DANKSAGUNG

Ich möchte mich bei Prof. Dr. Peter Spiteller ganz herzlich bedanken für die freundliche Aufnahme in seine Arbeitsgruppe und den Zugang zu diesem vielseitigen Forschungsgebiet, die Freiheit bei der Wahl und Bearbeitung der Themen, das Verständnis, die Geduld und Motivation bei den zahlreichen Rückschlägen.

Ebenso bedanke ich mich bei Prof. Dr. Franz-Peter Montforts für die Übernahme des Zweitgutachtens.

Außerdem möchte ich mich bei Dorit Kemken und Dr. Thomas Dülcks für ihr Engagement und ihre Hilfestellung bei massenspektrometrischen Fragestellungen bedanken.

Bei Dr. Wieland Willker und Johannes Stelten bedanke ich mich für die Hilfe bei der Messung und Auswertung von NMR-Spektren.

Meine Kolleginnen und Kollegen der Arbeitsgruppe gilt mein besonderer Dank für die Bereitschaft, meine Fragen zu beantworten und die Hilfsbereitschaft bei Labortätigkeiten sowie das angenehme Arbeitsklima und die Einführung in die Pilzkunde. Vielen lieben Dank an Ingrid Killer für die ermutigenden Worte.

Ebenfalls bedanke ich mich bei Prof. Dr. Michael Spiteller, Dr. Marc Lamshöft und Dr. Sebastian Zühlke von der TU Dortmund für die Durchführung der HR-LCMS-Messungen.

Für das Korrekturlesen dieser Dissertation und die hilfreiche Anregungen bedanke ich mich bei Claire Klindt, Julia Lohmann und Dr. Thomas Dülcks.

Meine tiefste Dankbarkeit gilt meinen Schwestern und Freundinnen Stella Tsakeng, Nadine Ngantcha und Armelle Monthé sowie meinen Engeln Léa Audrey, Joëlle Clara, Noé und Clara Shanice für die bedingungslose Liebe und den nötigen Rückhalt in den schwierigsten Momenten. Vielen Dank an Sigrid Schulz für die trostreichen Worte.

Zu guter Letzt möchte ich mich bei meinen Eltern für die Liebe, Unterstützung und Aufmunterung bedanken.

TABLE OF CONTENTS

I ABBREVIATIONS

ATP	Adenosine triphosphate
br	Broad
Bull.	Jean Baptiste François Bulliard
^{13}C	Carbon-13
CD_3OD	Deuteromethanol
CID	Collision-Induced Dissociation
COSY	Correlation Spectroscopy
°C	Degree Celsius
d	Doublet
DAHP	3-Deoxy-D-arabino-heptulosonic acid 7-phosphate
DBE	Double Bond Equivalents
DHQ	3-Dehydroquinic acid
D_2O	Deuterium oxide
DMSO	Dimethyl sulfoxide
Ø	Diameter
δ	Chemical shift
ec	Endcapped
EPSP	Enolpyruvylshikimate-3-phosphate
ESI	Electrospray ionisation
Fr.	Elias Magnus Fries
g	Gram
^{1}H	Proton
h	Hour(s)
H_2O	Hydrogen oxide

HMBC	Heteronuclear Multiple Bond Coherence
HOAc	Acetic acid
HPLC	High Performance Liquid Chromatography
HR	High Resolution
HSQC	Heteronuclear Single Quantum Coherence
Hz	Hertz
J	Coupling constant
K	Kelvin
Kotl.	František Kotlaba
LB	Luria-Bertani-Agar
LC	Liquid Chromatography
m/z	Mass-to-charge ratio
max	Maximum
MeOH	Methanol
MHz	Megahertz
min	Minute(s)
MS	Mass Spectrometry
nm	Nanometer
NMR	Nuclear Magnetic Resonance
NOE	Nuclear Overhauser Effect
NOESY	Nuclear Overhauser Effect Spectroscopy
p	*Para*
PEP	Phosphoenolpyruvate
Pers.	Christian Hendrik Persoon
Pouz.	Zdeněk Pouzar

ppm	Parts per million
PRPP	Pentosephosphate phosphoribosyl pyrophosphate
ROESY	Rotating-frame nuclear Overhauser Effect Spectroscopy
RP	Reversed-phase
Scop.	Johann Anton Scopoli
Sing.	Rolf Singer
SPE	Solid Phase Extraction
UV	Ultraviolet
v/v	Volume per volume
Vis	Visible
λ	Wavelength

II ZUSAMMENFASSUNG

In der vorliegenden Arbeit wurden neue Sekundärmetabolite aus den höheren Pilzen *Mycena epipterygia*, *Megacollybia platyphylla* und *Tricholomopsis decora* isoliert und deren Strukturen aufgeklärt. Um festzustellen, ob diese die Pilze gegen Bakterien oder Fraßfeinde schützen können, wurde die ökologische Rolle der isolierten Naturstoffe untersucht. Darüber hinaus wurden weitere NMR-Daten für die vollständige Charakterisierung von Mycenarubin C aufgenommen, das von Peters [58] erstmals aus *Mycena rosea* isoliert wurde.

Es ist bekannt, dass Mycenarubin C (**33**) aus der Reaktion von Mycenarubin A (**31**) mit Formaldehyd entsteht, wobei Formaldehyd nach Verletzung des Fruchtkörpers enzymatisch freigesetzt wird. Diese Information wurde verwendet, um die Menge an Mycenarubin C, die aus den Pilzen isoliert werden kann, durch Behandlung mit einer Formaldehydlösung, zu optimieren. Die gewünschte Verbindung konnte dadurch in hoher Reinheit und ausreichender Menge isoliert werden, um die notwendigen Experimente zur vollständigen Charakterisierung durchzuführen.

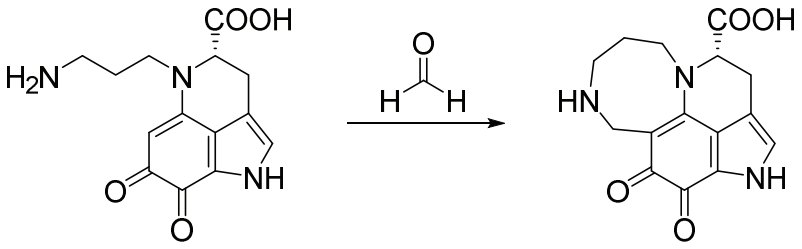

Mycenarubin A (**31**) Mycenarubin C (**33**)

Des Weiteren konnten zwei gelbe Verbindungen aus einem anderen Pilz der Gattung *Mycena*, nämlich aus *Mycena epipterygia*, isoliert werden. Mit Hilfe von HR-(+)-ESIMS-Messungen wurden die Summenformel und Informationen über Fragmente der ersten mit A bezeichneten Verbindung erhalten. NMR-Messungen zeigten die Anwesenheit von mehr als einer Verbindung in der Probe, was die Auswertung verschiedener Spektren erschwerte. Versuche die Probe durch Größenausschlußchromatographie oder die Verwendung verschiedener Lösungsmittel und Gradientenprogramme bei der HPLC-Trennung aufzureinigen, blieben erfolglos. Die zweite Verbindung, die mit B bezeichnet wurde, zeigte die gleiche Masse und ähnliche Fragmentierungsmuster wie Verbindung A. Da sich die Retentionszeiten beider Verbindungen nur wenig unterscheiden (0.5 min), konnte eine vollständige Trennung auf einer C_{18}ec Säule nicht erreicht werden. Dies und die Tatsache, dass beide Verbindungen die

gleiche Masse und das gleiche Fragmentierungsmuster zeigten, deutete auf eine *E*/*Z*-Isomerie hin. Weitere Untersuchungen wurden durch fehlendes Pilzmaterial erschwert. Um eine ausreichende Menge an den Verbindungen A und B für weitere Untersuchungen zu erhalten, müssten große Mengen an Fruchtkörpern zur Isolierung verwendet werden, da es sich bei *Mycena epipterygia* um einen sehr kleinen Pilz handelt.

Megacollybia platyphylla lieferte die zwei neuen Chorisminsäurederivate 3-(1-Carboxyvinyloxy)-5-hydroxy-4-methoxybenzoesäure (**42**) und 3-(1-Carboxyvinyloxy)-4,5-dihydroxybenzoesäure (**43**). Ihre Strukturen wurden aufgeklärt und ihre biologische Aktivität getestet. Obwohl verwandte Verbindungen antibakterielle Aktivität aufgewiesen, zeigten **42** und **43** keine hemmende Wirkung gegen die getesteten Organismen. Auch gegen die Gartenkresse *Lepidium sativum* konnte keine herbizide Wirkung nachgewiesen werden.

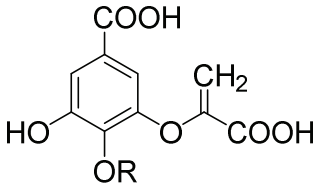

42: R = CH_3

43: R = H

Eine orangene Verbindung, die als D bezeichnet wurde, konnte aus dem Pilz *Tricholomopsis decora* isoliert werden. ESIMS-Messungen zeigten ein $[M+H]^+$-Ion bei *m/z* 804. Die Generierung einer Summenformel durch HR-(+)-ESIMS-Messungen erwies sich jedoch als sehr anspruchsvoll, da sechs Formeln als potentielle Kandidaten erkannt wurden. Durch die Anwendung der sieben Regeln zur heuristischen Filterung von Summenformeln und vor allem durch den Vergleich der Isotopenmuster konnte eine Summenformel postuliert werden. Aufgrund der sehr geringen Ausbeute, die nach der HPLC-Trennung erhalten wurde, ergaben NMR-Messungen keine schlüssigen Ergebnisse. Weitere Analysen wurden wieder wegen Pilzmangels unterbrochen. Für weitere Untersuchungen wären große Mengen an Fruchtkörpern von *Tricholomopsis decora* erforderlich, da Verbindung D nur in sehr geringer Menge im Pilz vorkommt.

II SUMMARY

In the present work, new secondary metabolites were isolated from the higher fungi *Mycena epipterygia*, *Megacollybia platyphylla* and *Tricholomopsis decora* and their structure elucidated. Their ecological role was investigated by testing their antibacterial and herbicidal activity, so as to determine if they protect the fungi against bacteria or predators. In addition, more NMR data were collected for the full characterization of mycenarubin C [58], first isolated from *Mycena rosea* by Peters.

Mycenarubin C (**33**) has been known to evolve from the reaction of mycenarubin A (**31**) with formaldehyde, the latter being enzymatically released after injury of the fruiting body of *Mycena rosea*. This information was used to optimise the amount of mycenarubin C isolated from the fungi by treating the raw extract with a formaldehyde solution. The desired compound could then be isolated in high purity and the necessary experiments for its full characterization were performed.

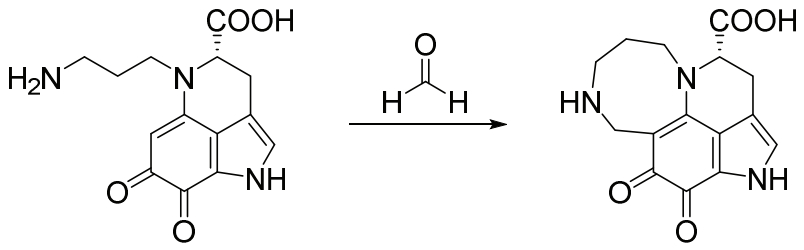

Mycenarubin A (**31**) Mycenarubin C (**33**)

Subsequently, two new yellow compounds were isolated from *Mycena epipterygia*, another fungus of the genus *Mycena*. The molecular formula, as well as information about fragments of the first compound, denoted A, could be obtained from HR-(+)-ESI-MS measurements. NMR experiments revealed the presence of more than one compound in the sample, making it difficult to interpret the different spectra. Attempts to clean the sample by size exclusion chromatography or the use of different solvents and gradient programmes for the HPLC separation remained unsuccessful. The second compound, denoted B, exhibited the same mass and similar fragmentation pattern as compound A in HR-(+)-ESI-MS measurements. A distinct separation of both compounds on a C_{18}ec column could not be achieved as they eluted in an interval of 0.5 min. Further investigations were hindered due to lack of more mushroom material. To obtain sufficient amount of both compounds for further investigation, large quantities of fruiting bodies would be required since *Mycena epipterygia* is a small fungus.

Megacollybia platyphylla delivered two new chorismic acid derivatives, 3-(1-carboxyvinyloxy)-5-hydroxy-4-methoxybenzoic acid (**42**) and 3-(1-carboxyvinyloxy)-4, 5-dihydroxybenzoic acid (**43**). Their structures were fully characterized and their biological activity tested. Even though related compounds were found to exhibit antibacterial activity, compounds **42** and **43** neither showed inhibitory activity against the tested organisms nor did they exhibit herbicidal activity against the garden cress *Lepidium sativum*.

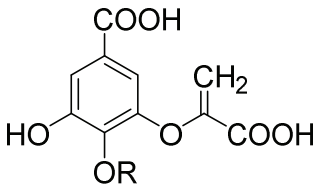

42: R = CH_3

43: R = H

An orange compound, denoted D, was isolated from the fungus *Tricholomopsis decora*. ESI-MS measurements exhibited an $[M+H]^+$ ion at *m/z* 804. Generating a molecular formula from such a high molecular mass proved to be very challenging, since six formulas were retained as potential candidates. By applying of the "seven golden rules for heuristic filtering of molecular formulas" and mostly due to the comparison of isotopic patterns, a molecular formula could be postulated. NMR experiments did not generate conclusive results due to the very low yield obtained from the HPLC separation. Further probing here again was interrupted due to shortage of the mushroom. Large quantities of fruiting bodies of *Tricholomopsis decora* would be needed for further investigations because compound D seems to occur in very low amount in the fungus.

III INTRODUCTION

With the increasing resistance of pathogens against existing antibiotics and the concern of the effect of synthetic chemicals on the environment, scientists have been called upon to develop new compounds that fulfil the conditions of being environmentally friendly, and against which infectious agents would difficultly develop resistance. Historically, natural products have been used since ancient times and in folklore for the treatment of many diseases and illnesses,[1] and therefore play a dominant role in the discovery of new lead compounds.[2, 3] Plants and fungi have been good sources for these lead structures. A well known example is the anti-inflammatory agent acetylsalicylic acid (aspirin), derived from salicin, a natural product isolated from the bark of the willow tree.[4] From fungal source, the strobilurins A and B (Figure 1) identified in 1976 from cultures of the pinecone cap *Strobilurus tenacellus*, which showed strong fungicidal effect on a number of fungi, are a good example.[5, 6] They served as model for the synthesis of derivatives which equally exhibited antifungal activities.[5]

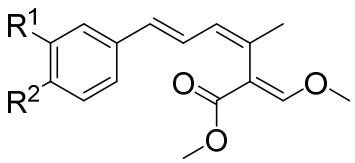

1: $R^1 = R^2 = H$

2: $R^1 = OCH_3$, $R^2 = Cl$

Figure 1: Strobilurin A (**1**) and B (**2**).

These examples and many others encouraged the further screening of plants and fungi for new lead compounds.

There is a very large spectrum of natural products owing to the fact that the mechanism used for biosynthesis is unique to an organism. Moreover, less than ten percent of the world´s biodiversity has been evaluated for potential biological activity.[1] Despite these observations, it is becoming more and more difficult to isolate new lead structures. This is probably due to the fact that readily accessible organisms have already been well investigated.[7] Therefore less accessible organisms, which have nevertheless been observed to be successful in their mode of living, have to be considered. The fruiting bodies of higher fungi or rather mushrooms fall in this category of organisms.

1 Fungi and their Metabolites

Fungi are a large and successful group of non-photosynthetic organisms. Experts assume about 1.5 million species, of which only 70,000 to 100,000 are classified.[8] They range in size from the unicellular yeasts to the large toadstools, puffballs and stinkhorns, and occupy a very wide range of habitats, both aquatic and terrestrial.[9] The diversity in size, habitat, colour and mode of living enhances diversity in metabolites, which in turn, enables a wide range of application for fungi and their metabolites.

Traditionally, fungi were regarded as plants, but modern classifications place them in a separate kingdom. The two largest groups of this kingdom are the Ascomycota and the Basidiomycota, which together are often referred to as “higher fungi”.[9] Their well-developed septate hyphae compact usually at some stage of development to form tissues, which then appear above the ground in the late summer and autumn as fruiting bodies. The variety of these fruiting bodies is reflected in their metabolites, which are products of different biosynthetic pathways from primary and secondary metabolisms.

Primary metabolism involves the biosynthesis and breakdown of compounds essential to all living organisms. [1] Primary metabolites, such as amino acids, sugars and proteins which are products of different pathways engaged in primary metabolism, are directly involved in the growth, development and reproduction, and therefore perform a physiological function in fungi.

The shikimate pathway is one of such biosynthetic pathways. It provides a route to the essential amino acids tryptophan (**15**), phenylalanine (**18**) and tyrosine (**20**) via the central intermediates shikimic (**8**) and chorismic (**11**) acids. [10] These aromatic amino acids serve not only as building blocks for the synthesis of proteins, but also as precursors for a wide range of secondary metabolites.[11] The shikimate pathway is of importance to this work, since the products of this pathway act as precursor to compounds described herein. Moreover, the amino acids **15**, **18** and **20** resulting from this pathway are frequently found in mushroom extracts.

1.1 The Shikimate Pathway

The biosynthesis of the aromatic amino acids tryptophan (**15**), phenylalanine (**18**) and tyrosine (**20**) proceeds via the shikimate pathway to chorismic acid (**9**).[12, 13] At this point the pathway branches, one branch leading to **15** and the other to **18** and **20**.

The shikimate pathway, also known as the chorismate biosynthesis pathway, converts two metabolites, phosphoenolpyruvate (PEP) (**3**) and erythrose 4-phosphate (**4**), into chorismic acid (**11**). It begins with the DAHP synthase-catalysed Aldol-like reaction of **3** and **4** to form 3-deoxy-D-arabino-heptulosonic acid 7-phophate (**5**) (Scheme 1). In the following step, **5** is transformed to 3-dehydroquinic acid (DHQ) (**6**) in a ring-closure reaction catalysed by the enzyme DHQ synthase. **6** is then dehydrated to form 3-dehydroshikimic acid (**7**), which is thus reduced to shikimic acid (**8**).

In an ATP-dependent reaction, **8** is phosphorylated to shikimic acid-3-phosphate (**9**), which couples with **3** to give 5-enolpyruvylshikimate-3-phosphate (EPSP) (**10**). The latter finally loses phosphoric acid to yield chorismic acid (**11**), which is the branch point in the biosynthesis of aromatic amino acids.

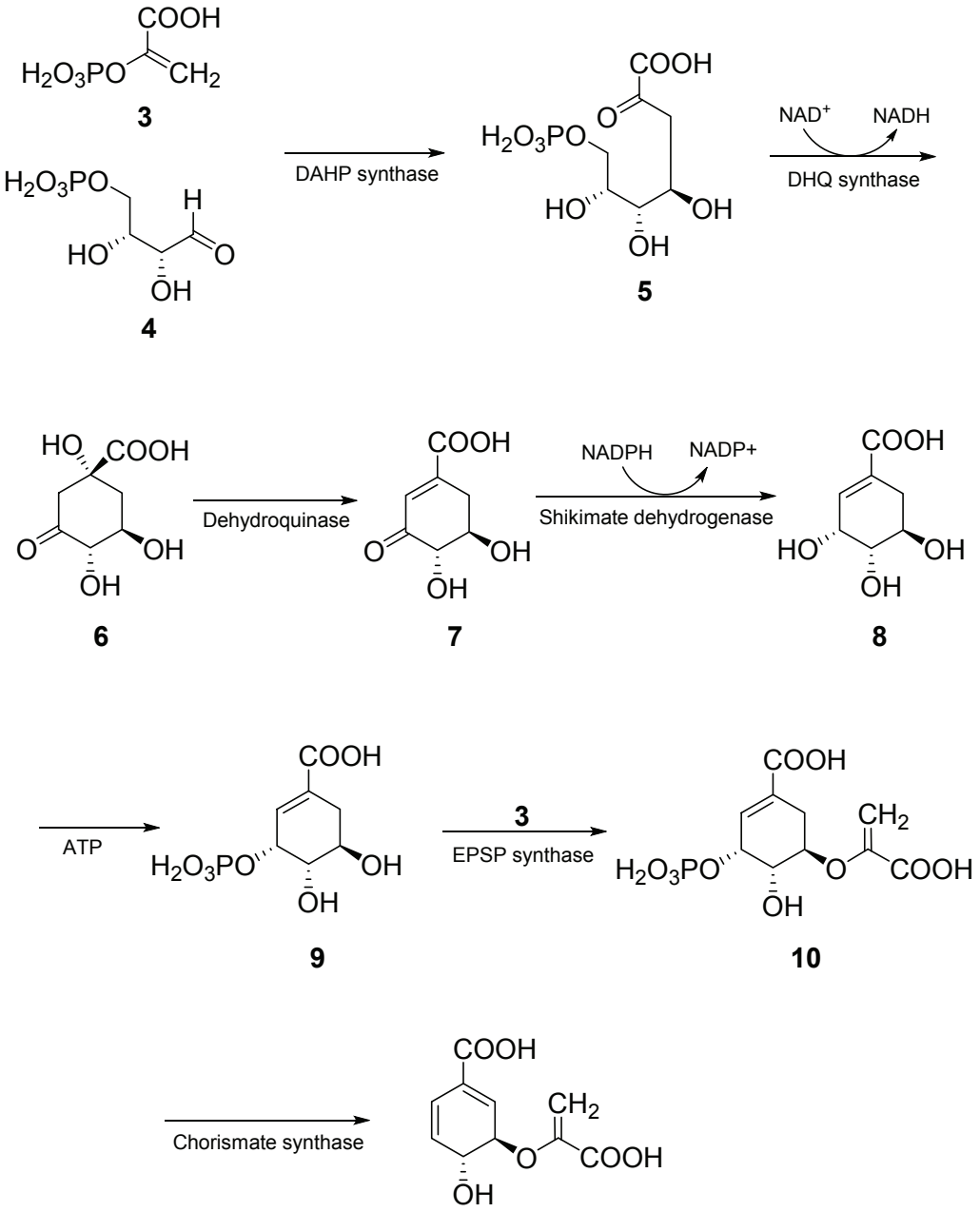

Scheme 1: Biosynthesis of chorismic acid (**11**).

1.2 Biosynthesis of Tryptophan

The principal precursor for the biosynthesis of tryptophan (**17**) is chorismic acid (**11**). In the first step, anthranilate synthase transfers the amino group from glutamine to **11**, which is thus converted to anthranilic acid (**12**) under elimination of the pyruvate rest (Scheme 2).

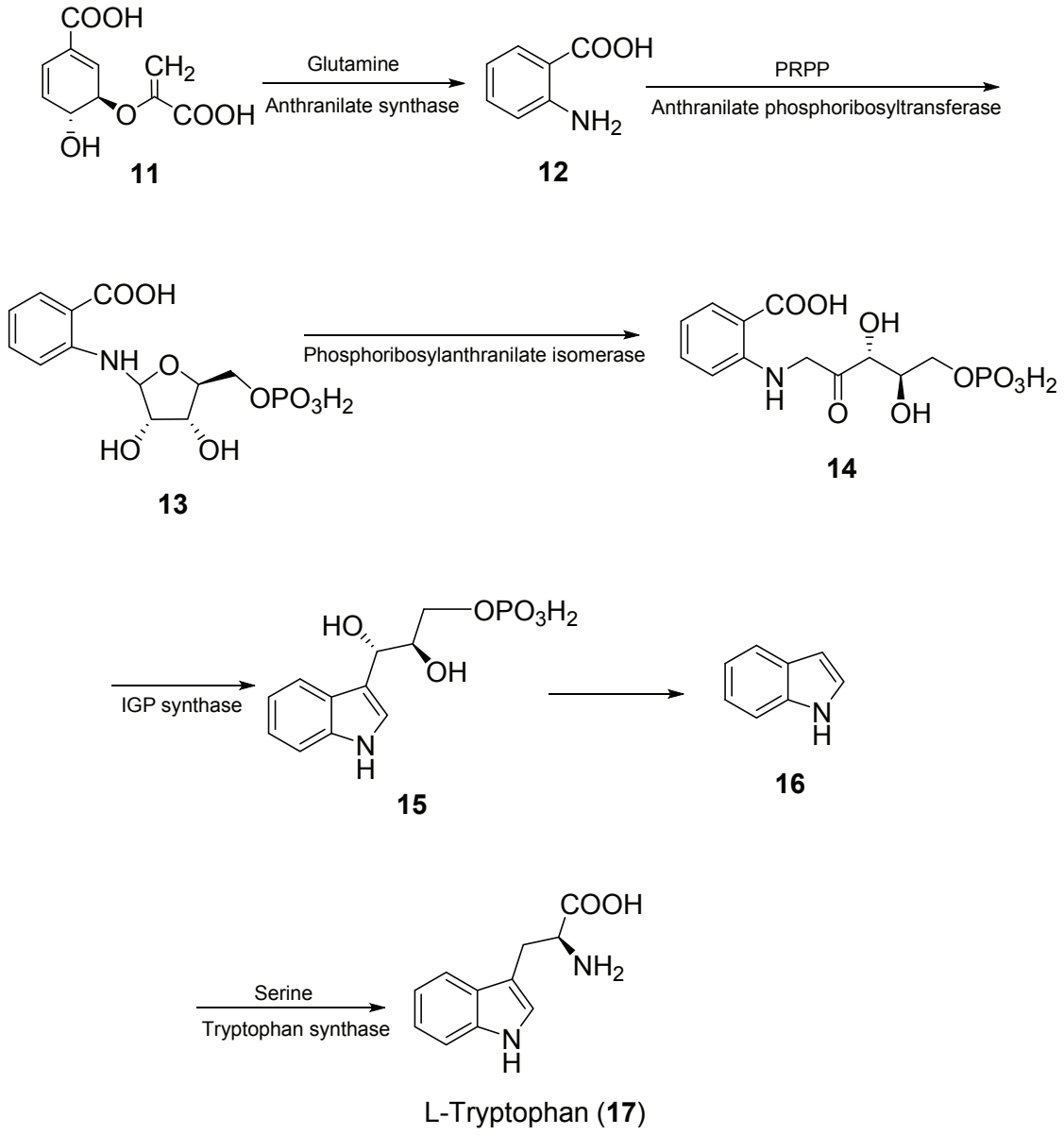

Scheme 2: Biosynthesis of Tryptophan (**17**).

Anthranilic acid (**12**) then reacts with the pentosephosphate phosphoribosyl pyrophosphate (PRPP) to N-(5-phosphoribosyl)-anthranilate (**13**). The ribose ring of **13** is opened by Amadori rearrangement, and subjected to reductive decarboxylation to yield indole-3-glycerinephosphate (**15**), which is transformed to indole (**16**) by elimination of glyceraldehydes-3-phosphate. The last step involves the tryptophan synthase catalysed reaction of **16** with serine to obtain tryptophan (**17**).

1.3 Biosynthesis of Phenylalanine and Tyrosine

Phenylalanine (**20**) and tyrosine (**22**) are also synthesised from **11**, with prephenic acid (**18**) being the common intermediate (Scheme 3). Prephenic acid (**18**) is synthesised from **11** by a chorismate mutase-catalysed Claisen rearrangement. The pathway branches at this point, one leading to **20** and the other to **22**.

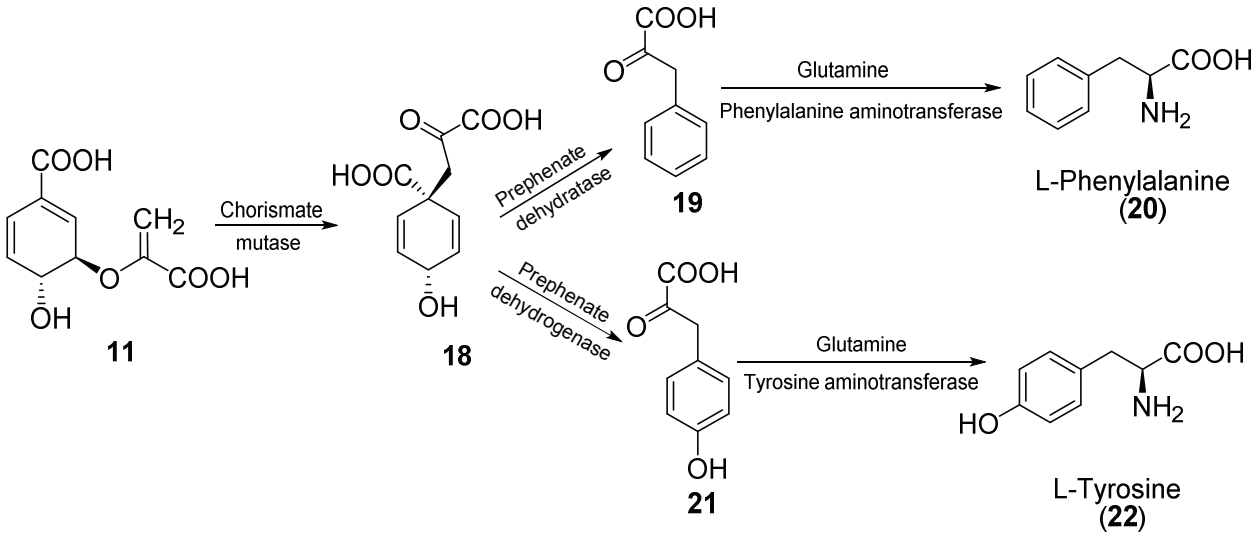

Scheme 3: Biosynthesis of Phenylalanine (**20**) and Tyrosine (**22**).

In order to achieve **20**, prephenic acid (**18**) is converted to phenylpyruvic acid (**19**), which is transaminated in the final step using glutamine as amino group donor. In the case of **22**, prephenic acid is converted to *p*-hydroxyphenylpyruvic acid (**21**) before equally undergoing transamination in the final step.

2 Secondary Metabolites

The term natural product refers to any naturally occurring compound, but is generally taken to mean secondary metabolite in natural products chemistry.[14] Secondary metabolites are organic products of secondary metabolism, which consist of low-molecular weight compounds that are usually regarded as not being essential for life.[15–17] They are biosynthetically derived from primary metabolites. Unlike primary metabolites however, they do not play a direct role in growth, development and reproduction. This apparent absence of primary function, coupled with the effect of secondary metabolites on other organisms, suggests an important role in ecological interactions with other organisms. This interaction may occur in two ways; either in a mutualistic interaction, hereby attracting beneficial organisms, for example, for pollination and scattering of spores and pollen grains (mostly in plants), or in an antagonistic interaction, thus acting as repellent against predators, pathogens or competitors. For this reason, many fungal secondary metabolites exhibit useful biological activities and are of interest to the pharmaceutical, food and agrochemical industries.[18]

Although chemically diverse, all secondary metabolites are produced by a few common biosynthetic pathways,[19] utilizing precursors formed during primary metabolism. The intermediates undergo numerous enzyme-catalyzed reactions leading to diverse chemical structures. Thus, the majority of secondary metabolites are conveniently classified based on their biosynthetic origin.[14] Fungal secondary metabolites can be divided into four main classes; terpenes, polyketides, shikimic acid derived and amino acid derived compounds. Moreover, hybrid metabolites composed of moieties from different classes are common, such as meroterpenes, which are fusions of terpenes and polyketides.[15]

2.1 Functions and Uses of Secondary Metabolites

Secondary metabolites are produced either as a result of the organism adapting to its surrounding environment, or as a possible defence mechanism against predators to assist in the survival of the organism.[20, 21] They are frequently revealed by their colour, smell or taste,[22] and therefore determine our sensory perception of unique characteristics of the organisms in which they are produced.[23] These characteristics find application in many areas. The pigments responsible for the colours of some fungi found application in food colouring,[25] in the textile industry for wool[26] and leather colouring,[27] as well as for wood colouring.[28] Secondary metabolites have also been used as antibiotics against bacteria. The most famous example is that of penicillin, discovered in 1928 by Alexander Fleming from the fungus *Penicillium notatum*.[1, 24] Till today penicillin antibiotics such as penicillin G (Figure 2), still find wide medical application in the treatment of infections caused by bacteria such as staphylococci

and streptococci. The discovery and development of penicillin caused widespread attention on fungal metabolites. [19]

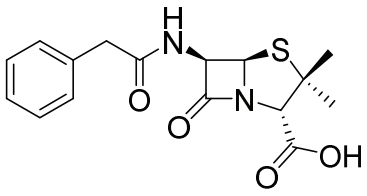

Figure 2: Penicillin G (**23**).

The isolation and structure elucidation of secondary metabolites is very often motivated by the search for bioactive compounds as lead structures for drug development, insecticidal or fungicidal agents. The ecological role of these metabolites however is not well understood. After being received with scepticism decades earlier, chemical ecology began to prosper in the 1960s as the importance of plant secondary metabolites in the interaction of plants with their environment could be proven. [23, 29] Since then, the chemical ecology of plants including their chemical defence has been studied extensively. [30–34] In contrast, the chemical ecology of higher fungi has not enjoyed such interest. Even though the chemical ecology of higher fungi has not yet been extensively investigated as that of plants, fungal secondary metabolites are thought to play a role in the defence mechanism against organisms competing for the same habitat, or in their symbiotic or parasitic interaction.[35] Fungi should therefore also exhibit chemical defence strategies as observed in plants.

Higher fungi are exposed to competitors and enemies at two levels, the mycelia and the fruiting bodies. [36] The mycelia compete with other fungi and bacteria to secure nutrient resources and space for themselves. They thus release fungicidal or antibacterial agents, which eliminate potential rivals. The strobilurins which have been isolated from a number of basidiomycetes, for example from the genera *Strobilurus*, *Oudemansiella* and *Mycena*, have been observed to play the role of securing nutrients for the producers.[37] Meanwhile, the fruiting bodies defend themselves from their potential predators by producing toxins and pungent or bitter compounds.

2.2 Chemical Defence Mechanisms

Just like other living organisms, fungi have developed a variety of defence strategies to protect themselves from predators like mammals and insects, as well as infection from parasitic fungi and bacteria. Chemical defence mechanisms involve the production of chemical compounds and toxins [38] that discourage and in some cases harm the predator. At least three chemical defence mechanisms are known so far; constitutive, induced and wound-activated chemical defence mechanisms. [36]

2.3 Constitutive Chemical Defence

The constitutive chemical defence mechanism involves secondary metabolites that are present in the mushroom in their bioactive form. [36] This defence mechanism is generally determined by observing the response of an organism against its predators. The secondary metabolites involved render the fruiting bodies of fungi toxic, bitter, or generate a pungent smell that prevents attack or ingestion. The fly agaric *Amanita muscaria* is well known for its hallucinogenic properties. The toxic constituents of the mushroom were found to be ibotenic acid (**24**), muscimol (**25**) and muscarine (**26**). [36, 39] The bitter taste of the bitter webcap *Cortinarius infractus*, which has been attributed to the indole alkaloid infractopicrin (**27**), makes the mushroom inedible to humans and many mammals,[36, 40] meanwhile the azepine alkaloid chalciporone (**28**) is responsible for the pungent, peppery taste of the peppery bolete *Chalciporus piperatus*.[41–43]

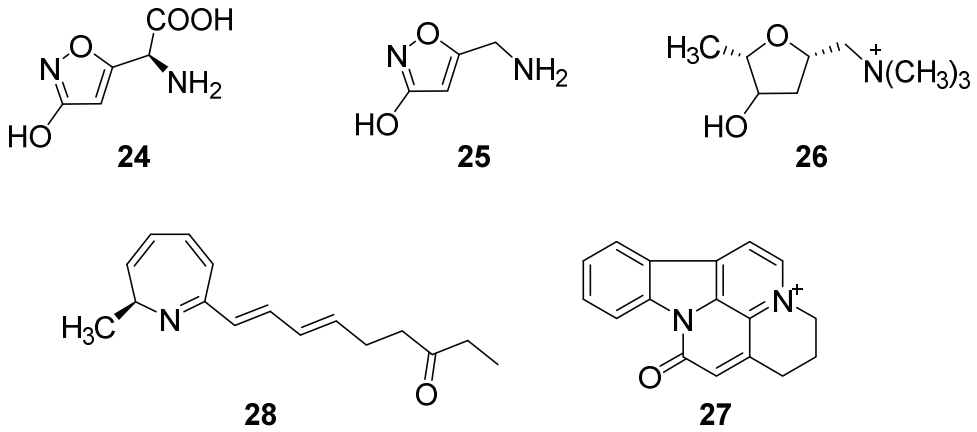

Figure 3: Some compounds involved in constitutive chemical defence in higher fungi: ibotenic acid (**24**), muscimol (**25**), muscarine (**26**), infractopicrin (**27**) and chalciporone (**28**).

2.4 Wound-activated Chemical defence

In wound-activated chemical defence, inactive precursors are converted to active compounds by the action of enzymes stimulated upon injury. It can be detected by comparing the metabolic profile of intact and mechanically wounded fruiting bodies. The metabolic profile of the injured fruiting bodies usually shows an increase or appearance of the active agents, while by the intact fruiting bodies, the precursors are exhibited. Depending on the enzymes involved in the conversion, three main types of wound-activated defence mechanisms are known for fungi: hydrolysis of esters with hydrolytic enzymes being involved, oxidation of phenols with phenol oxidases responsible for the conversion, and lipid peroxidation which takes advantage of lipoxygenases.[36] A wound-activated chemical defence mechanism has been observed in *Mycena galopus* (Scheme 4), where the inactive benzoxepine ester (**29**) is converted to the active benzoxepine alcohol (**30**) upon injury.[44] Compound **30** exhibits fungicidal activity. *Aleurodiscus amorphous*[36, 45] and *Marasmius oreades*[46] have also been found to display wound-activated chemical defence mechanisms, with the release of hydrogen cyanide, which is a toxin to potential predators. Many *Lactarius* and *Russula* species are also known to develop wound-activated chemical defence.[36, 47]

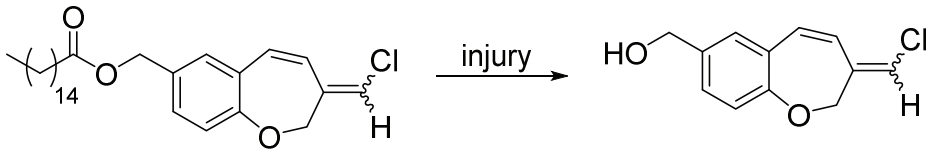

29 **30**

Scheme 4: Wound-activated chemical defence in fruiting bodies of *M. galopus*.[36]

2.5 Induced Chemical Defence

The induced chemical defence strategy is based on the *de novo* synthesis or the significant increase of bioactive compounds initiated on demand.[36, 48] The response of the organism to injury often takes long as compared to wound-activated defence, where the response is instant. This has the disadvantage that induced chemical defence is not convenient for the immediate deterring of enemies. However, valuable resources are being saved, since the biosynthesis of defence compounds, which is energy-consuming, is only initiated on demand.[36] Detecting induced chemical defence metabolism implies the monitoring of the metabolite pattern of stressed organisms. An increase of the defence compounds is generally observed with time. Induced chemical defence is very common to plants[49–52] but barely

investigated in fungi. The production of strobilurins has however been shown to increase considerably, when competing fungi are present in the mycelia cultures. This indicates the presence of an induced chemical defence mechanism in the mycelium of *Strobilurus tenacellus*. [36, 53]

IV AIM AND SCOPE OF WORK

Secondary metabolites were earlier regarded as being waste products of primary metabolism. The study of secondary metabolites began with the isolation of morphine from the opium poppy, and interest grew after it was shown that they play an important role in the survival of the organism in its environment. The increasing interest in natural products is above all to find new bioactive compounds to serve as lead structures for the development of new antibiotics, pesticides and herbicides. Secondary metabolites provide unique structural diversity and therefore opportunities for the discovery of lead compounds.

Although many bioactive compounds have been isolated from a variety of organisms, their function to the producer organism is yet to be elucidated in many cases. The more secondary metabolites are identified and isolated from an organism, the better the relation between them and thereby their mode of functioning is understood. This in turn leads to the understanding of the function of these compounds to the organism. Wound-activated chemical defence mechanism clearly illustrates this situation, where the isolation of the bioactive compound and its inactive precursor brings to light their mode of function.

Besides, the chemical diversity of secondary metabolites gives a hint at the metabolism of products or intermediates of primary metabolism. Since secondary metabolites are not generally included in standard biosynthetic pathways, the most effective way to analyze their structure and function, and investigate their ecological role, is by isolating them and carrying out biological tests.

Most described fungal secondary metabolites are isolated from easily accessible lab-grown fungal cultures. This can be explained by the seasonal accessibility and small amount of fruiting bodies often collected. The variety in the size, habitat, colour and mode of life of these fruiting bodies however, opens the possibility to a wide range of secondary metabolites. The aim of this work was therefore to isolate new secondary metabolites from fruiting bodies of higher fungi. In addition compounds isolated in an earlier work need to be fully characterized. After determining their structures, biological tests should be performed, so as to give information on their bactericidal, insecticidal and herbicidal activities. For this study, fungi of the genera *Mycena*, *Megacollybia* and *Tricholomopsis* were investigated.

V RESULTS AND DISCUSSION

1 *Mycena rosea*

1.1 Mushroom Description

The relatively small fungi *Mycena rosea* (Bull.) Gramberg, commonly known as rosy bonnet [54] (German name: Rosa Rettichhelmling), is a widespread mushroom in beech forests in Europe. It generally grows from August to November, displaying a pink cap ranging between 2 and 6 cm in diameter, occasionally with pale edges. The white or pale pink stipe is hollow, smooth with longitudinal fibres, and downy at the base. The broad gills are pale pink in colour, crowded and sinuate. [55] The fruiting bodies of the rosy bonnet has a characteristic radish odour.

Figure 4: *Mycena rosea* [56]

1.2 Previous Work

Earlier investigations on the flavour compounds in wild mushrooms revealed *Mycena rosea* to contain the volatile compounds hexanal and hexan-2-one, accounting for a green, fruity-ethereal odour. [57] Later, the pyrroloquinoline alkaloids mycenarubin A (**31**) and mycenarubin B (**32**) (Figure 5) were isolated and their structure elucidated.[58, 59] These red alkaloid pigments were determined as being responsible for the pink colour of the mushroom caps.

Furthermore, mycenarubin C (**33**) was also isolated from injured fruiting bodies and those infested with the bonnet mould *Spinellus fusiger*. Mycenarubin C was found to result from the reaction of mycenarubin A with formaldehyde, the latter being released after injury. [58]

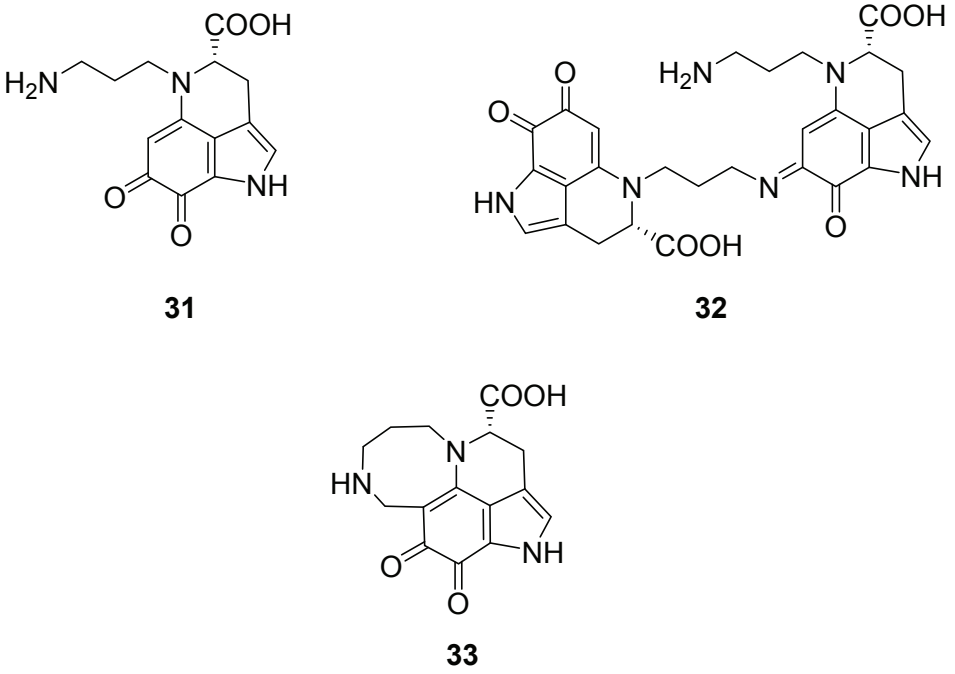

Figure 5: Structures of mycenarubin A (**31**), B (**32**) and C (**33**).

1.3 Other Known Red Pigments from the Genus *Mycena*

Besides **31**, **32** and **33**, a number of red pigments (Figure 6) have been identified from the fruiting bodies of the *Mycena* species. Haematopodin (**34**), the first pyrroloquinoline alkaloid identified in a terrestrial organism, was isolated from the fruiting bodies of the fungus *M. haematopus*.[60] Haematopodin (**34**) was determined as being a degradation product of the native unstable pigment praehaematopodin, which was later isolated and renamed haematopodin B (**35**).[61] Mycenarubin A (**31**) and haematopodin (**34**) showed positive bioactive activity against the mould fungus *Spinellus fusiger* and the mycoparasites of the *Hypomyces* species.[58] Mycenarubin C (**33**) also showed positive effect against the *Hypomyces* species, but not against spore formation in the mould fungus. *M. haematopus* also delivered the mycenarubins D (**36**), E (**37**) and F (**38**), which were formerly unknown compounds.[58, 61] The indolequinone alkaloid sanguinolentaquinone (**39**), another red pigment, was isolated from *M. sanguinolenta*, together with the blue pigments sanguinone A and B.[58, 62] The pelianthinarubins A (**40**) and B (**41**) on the other hand, were isolated and characterised

from the blackedge bonnet *M. pelianthina*.[58, 63] Even though the pelianthinarubins displayed no biological activity against tested organisms, it is assumed that they play an ecological role in the chemical defence of the fungus.[63]

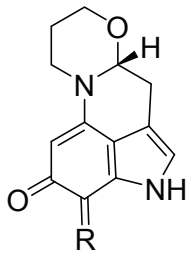

34: R = O
35: R = NH

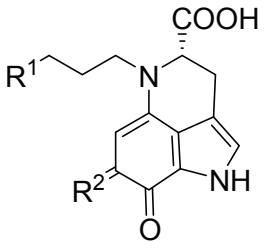

36: R^1 = NH_2, R^2 = NH
37: R^1 = OH, R^2 = NH
38: R^1 = OH, R^2 = O

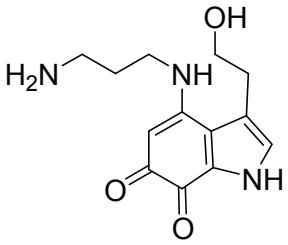

39

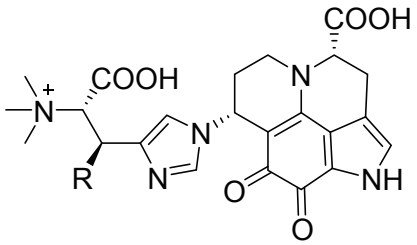

40: R = H
41: R = OH

Figure 6: Structures of red pigments from *Mycena* species: the haematopodins **34** and **35**, the mycenarubins **36** – **38**, sanguinolentaquinone **39**, and the pelianthinarubins **40** and **41**.

The structure of mycenarubin C (**33**) proposed by Peters in her doctoral thesis [59] was not fully resolved. The ^{1}H NMR experiment performed at 300 K exhibited broad signals and the protons at position C-10 were therefore hardly observed, rendering the interpretation of the spectrum difficult. The observed proton chemical shift, which is a sensitive parameter related to the conformation of a molecule, generally describes the average chemical shift of all conformations present. A change in temperature affects the observed chemical shift, since the available conformations are altered.

Hence 1D and 2D NMR experiments for the complete characterisation of **33** should be performed at a temperature higher than 300K, with the aim of improving the chemical shift

resolution, thereby reducing peak broadening. The new temperature should be chosen with care so that the compound does not decompose.

Since it is known that mycenarubin C (**33**) arises from the reaction of mycenarubin A (**31**) with formaldehyde, [58] this information can be used to optimise the amount of **33** to be isolated from the raw extract of *Mycena rosea*. The fungi raw extract should be treated with formaldehyde. This should convert mycenarubin A (**31**) in the extract to mycenarubin C (**33**).

1.4 Synthesis of Mycenarubin C from Mycenarubin A and its Isolation

In order to be sure to isolate as much mycenarubin C (**33**) as was necessary for full characterization, all the mycenarubin A (**31**) present in the fungi extract had to be converted to **33**. To ensure that the whole amount of **33** collected from the HPLC separation thereafter had as precursor **31** from the fungal source, the raw extract was directly treated with formaldehyde.

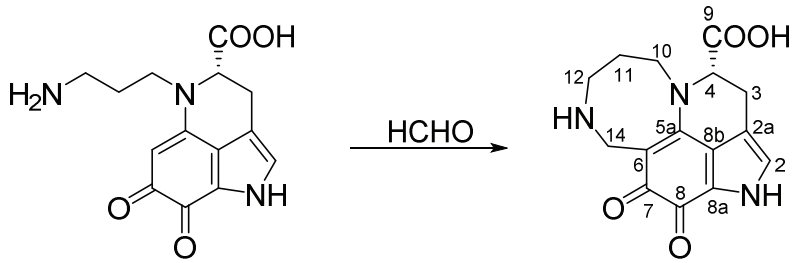

31 **33**

Scheme 5: Synthesis of mycenarubin C (**33**) from mycenarubin A (**31**).

After extracting frozen caps of *Mycena rosea* with MeOH and a H_2O-MeOH (50/50 v/v) solution at 25 °C, the raw extract was treated with a 37 % formaldehyde solution. The reaction solution was evaporated after two hours of reaction. After centrifuging to remove proteins extracted along with the desired compounds, the supernatant was further purified by SPE. The LC-UV chromatograms (Figure 7) of the raw extract before and after treatment with formaldehyde confirmed the formation of **33** after 2 hours of reaction. Mycenarubin A (**31**), which eluted after 14.8 minutes, was absent after the reaction with formaldehyde, being converted to **33**, which eluted after 16.6 minutes. The subsequent separation by preparative HPLC on an RP-18ec column yielded a maximum of 14 mg mycenarubin C (**33**) from 60 g of frozen caps, accounting for a 0.023 % yield.

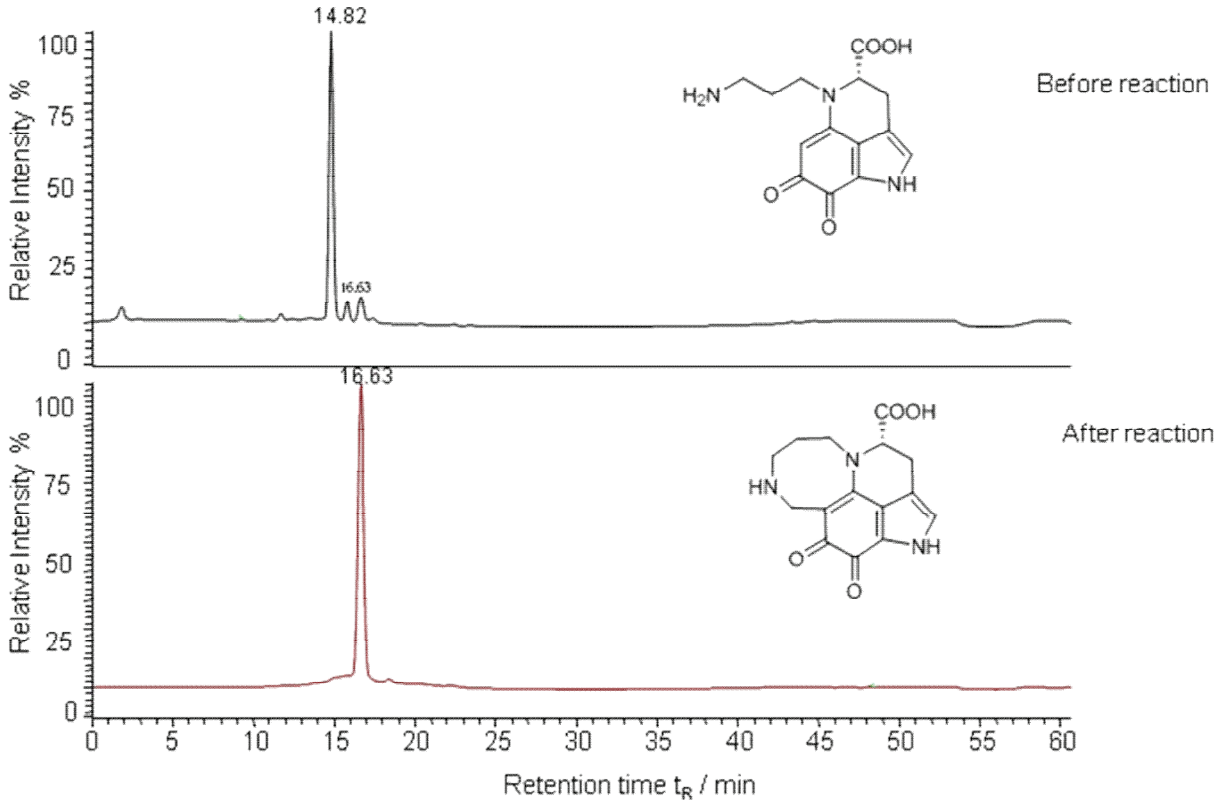

Figure 7: LC-UV chromatograms of raw extract of *M. rosea* at λ = 360 nm, before and after treatment with formaldehyde.

1.5 Structure Determination of Mycenarubin C

The UV/Vis spectrum exhibited three maxima at λ = 248, 360 and 530 nm, similar to the red pigment isolated by Peters. [58]

The ESI-MS showed an $[M+H]^+$ ion at *m/z* 302, with the characteristic MS/MS fragments at *m/z* 258 and 229. The fragment at *m/z* 258 represents the loss of a CO_2 unit, while the fragment at *m/z* 229 indicates the loss of CO_2 and CH_2NH units.

The ^{13}C NMR spectrum recorded at 330 K in D_2O exhibited fifteen carbon atoms. The ^1H NMR spectrum equally recorded at 330 K in D_2O showed twelve non-exchangeable protons. The HSQC correlations showed signals attributed to five CH_2 groups and two CH groups, implying the presence of eight quaternary carbon atoms. The COSY spectrum in combination with the ^1H NMR spectrum exhibited two spin systems. One spin system consisted of three successive CH_2 groups, each of which was split diastereotopically. From the HSQC assignments, this CH_2 chain ended with an amino group at both ends. The second spin system showed a single

proton coupling with two diastereotopically split protons. Two additional doublets of a diastereotopically split CH_2 group, not observed in mycenarubin A,[59] were exhibited in the ^1H NMR spectrum. According to the COSY spectrum, they coupled only with each other. In the HSQC spectrum they were directly connected to the carbon resonance at δ_C 40.63 ppm. These protons at δ_H 4.47 and 4.63 ppm exhibited HMBC correlations to four carbon atoms at δ_C 39.26, 95.80, 157.53 and 180.05 ppm, corresponding to positions C-12, C-6, C-5a and C-7 respectively. The carbon at position 6 had no hydrogen attached to it, indicating an additional substituent. This indicated that the carbon atom at δ_C 40.63 ppm was the link between the side chain and the indolequinone moiety. These findings led to the conclusion that the primary amino group in **31**[59] was bridged by a CH_2 group with the indolequinone, forming an eight-membered ring, matching to the compound isolated by Peters.[58]

NOESY and ROESY correlations gave information about the conformation of the diastereotopically split protons (Figure 8). The diastereotopic splitting of the protons in the CH_2 groups present in **33** probably occurs due to the absence of a plane of symmetry in the molecule that relates the protons. The protons are therefore chemically non-equivalent.

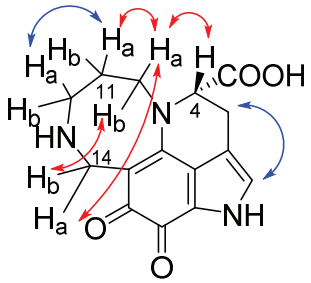

Figure 8: Selected NOESY (red) and ROESY (blue) correlations in mycenarubin C (**33**)

1.6 Biological Tests

Mycenarubin C (**33**) was tested for its antibacterial activity. For this purpose, 0.5 mg and 1 mg each of **33** was dissolved in 1 mL distilled and sterilized water. These solutions were dropped on paper discs of 6 mm in diameter and 0.5 mm thick, and allowed to dry under sterile conditions. They were then placed on agar plates inoculated with the test organisms *Escherichia coli*, *Bacillus subtilis* and *Staphylococus capitis*. These bacteria were chosen because they are easily accessible, easy to handle and fast-growing. This makes them ideal for lab investigations. Besides, they can also be found in the same environment where *M. rosea* settles. Hence the test results would give information on the chemical communication

between *Mycena rosea* and the tested organisms. The agar plates were incubated at 37 °C for 24 h.

Mycenarubin C (**33**) did not show any inhibitory activity against the tested organisms. This is in line with the observation that compounds with *ortho*-quinone core structures like mycenarubin C, such as the batzellines and the damirones isolated from marine sponges, show very little biological activity as compared to compounds with *para*-quinone core structures such as the isobatzellines.[64, 65]

However, bioactive natural products containing eight-membered ring structures like mycenarubin C have been isolated before. Compounds such as the manzamines, ircinals and nakadomarins have been isolated from marine sponges and found to exhibit antimalarial, antiviral and antitumor activities. [66–68] It is possible that mycenarubin C equally shows one or all of these characteristics.

1.7 Conclusions

Mycenarubin C (**33**) was isolated from the fungi *Mycena rosea* and its structure was completely characterized using 1D and 2D NMR spectroscopic methods. The amount of **33** isolated was optimised from 0.015 % to 0.023 % yield, by directly treating the fungal raw extract with formaldehyde, thereby converting mycenarubin A (**31**) to mycenarubin C (**33**). This reaction suggests that **33** arises in the fungi in an attempt to neutralize formaldehyde released enzymatically when the fruiting bodies are injured, so as to protect the fungi from its toxic effects. Even though **33** was inactive against the tested organisms *E. coli*, *B. subtilis* and *S. capitis*, it could have antimalarial, antiviral and/or antitumor activities, since secondary metabolites from marine sources containing an eight-membered ring structure like **33** have been found to exhibit these characteristics.

2 *Mycena epipterygia*

2.1 Mushroom Description

The commonly known yellowleg bonnet *Mycena epipterygia* (Scop.: Fr.) Gray (German Name: Dehnbarer Helmling) is a tiny mushroom that appears from September to November in deciduous and coniferous woodland in Europe. The cap is 1 to 3 cm in diameter, being initially bell-shaped and later expanding to become convex. The cap colour varies greatly from yellow-green to dark olive-brown, becoming paler at the edge. The translucent sticky cap skin which can easily be peeled off is a characteristic identification feature for this fungus. The long stipe, often flushed with the cap colour, ranges between 3 to 8 cm in height, and 1 to 3 mm in diameter. The gills are broad and creamy white in colour. *M. epipterygia* is usually found attached to wood residues by mycelia strands. [55]

Figure 9: *Mycena epipterygia*, Welle, October 2014.

2.2 Previous Work

Even though fruiting bodies of *Mycena epipterygia* bear an interesting feature with its sticky cap skin and elastic stipe, which probably deters possible predators, it seems not to have attracted enough curiosity. No scientific work about the secondary metabolites of *Mycena epipterygia* has been published so far.

2.3 Isolation of Yellow Pigments from *M. epipterygia*

Frozen fruiting bodies of *Mycena epipterygia* were extracted with MeOH, then with a H_2O-MeOH (50/50 v/v) solution on an orbital shaker at 25 °C. The raw extract was concentrated before being centrifuged, so as to precipitate potential proteins extracted along. Purification of the supernatant then followed by SPE on a C18 cartridge. The cartridge was first eluted with H_2O, followed by a H_2O-MeOH (50/50 v/v) solution and finally with MeOH. The H_2O-MeOH and MeOH fractions were reunited and concentrated since they were both coloured. The analytical HPLC of the yellow-brown extract (Figure 10) revealed three peaks denoted A, B and C, with characteristic UV maximum for yellow compounds at 224, 295, 394 and 412 nm for compound A; 295 and 395 nm for compound B; 289 and 388 for compound C.

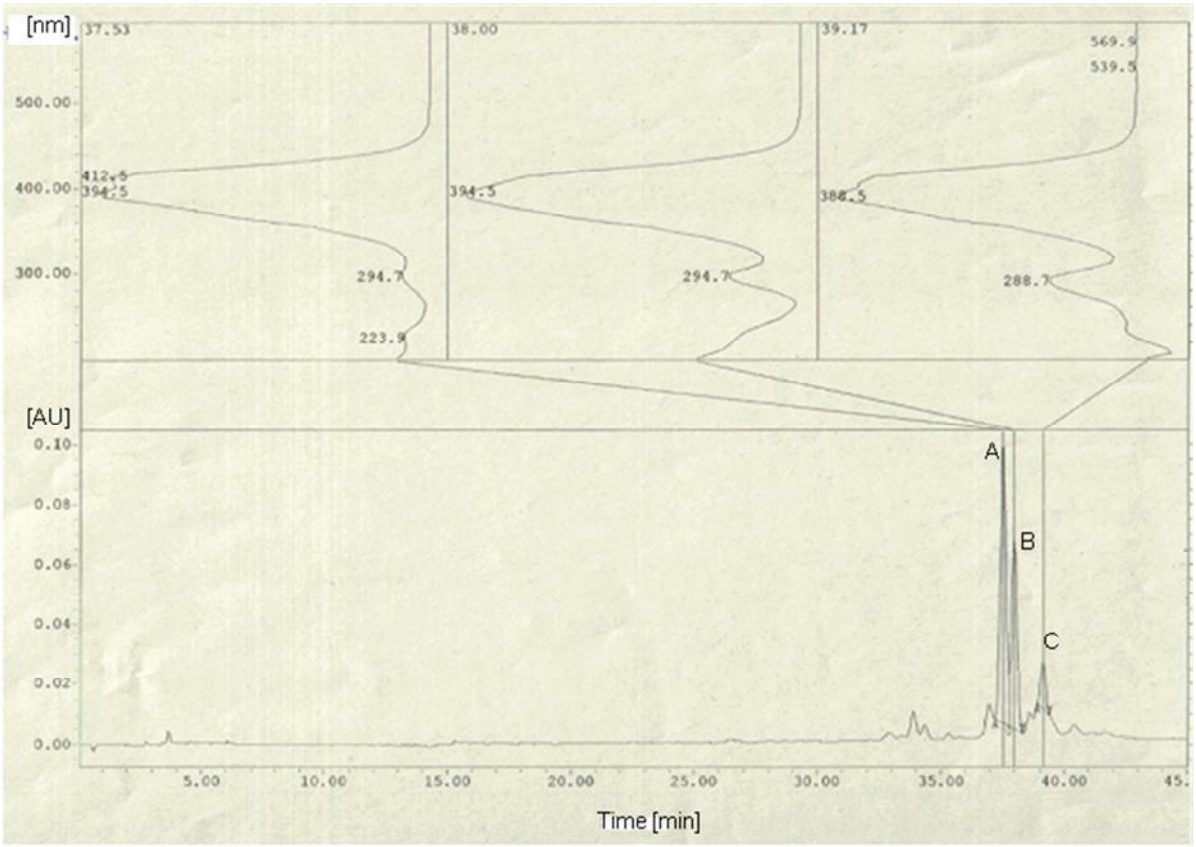

Figure 10: Analytical HPLC chromatogram of raw extract of *M. epipterygia* with UV spectra of peaks A, B and C at λ = 410 nm.

The metabolic pattern of fruiting bodies from different sites were analysed in order to determine if there were any differences between those collected in Bavaria and those

collected in Lower Saxony. No significant difference was observed as the chromatograms exhibited peaks similar in their retention times and absorption patterns.

Separation on a semi-preparative RP-18ec column at λ 410 nm confirmed the presence of three yellow pigments. The retention times of compounds A and B differed only by 0.5 min, both appearing as double peaks, which made a clean isolation difficult. Separation on RP-8, Phenylhexyl and RP-NH_2 columns did not achieve a better separation.

2.4 Structure Elucidation of Compound A

Compound A eluted first after 21.3 min. The HR-(+)-ESI-MS spectrum of A exhibited molecule ions $[M+NH_4]^+$ at *m/z* 334.1284 and $[M+H]^+$ at *m/z* 317.1019. The software Xcalibur used for MS data processing generated five possible molecular formulas matching with the $[M+H]^+$ ion. These formulas are shown in Table 1 with deviations from the theoretical value, expressed in ppm. Considering the HR-(+)-ESIMS/MS data, the molecular formulas number 2 and 3 (Table 1) came out as favourites. However, some MS/MS and MS^3 peaks did not generate formulas coinciding with the molecular formula number 3. This indicated that the molecular formula number 2 was the best option.

Table 1: Potential molecular formulas for compound A, with their respective deviations.

Nr.	Molecular formula $[M+H]^+$	Deviation [Δ ppm]
1	$C_{16}H_{11}N_7O$	– 0.19
2	$C_{17}H_{17}O_6$	– 0.20
3	$C_{15}H_{15}N_3O_5$	– 4.03
4	$C_{14}H_9N_{10}$	– 4.05
5	$C_{18}H_{13}N_4O_2$	– 4.42

The double bond equivalent was calculated to be ten, using equation (1). This gave the degree of unsaturation, thereby giving an idea about the number of double bonds or rings in the compound.

$$DBE = \#C - (\#H + \#N)/2 + 1 \quad (1)$$

Where: # C is the number of carbon atoms,

H is the number of hydrogen atoms,

N is the number of nitrogen atoms.

According to the HR-(+)-ESI-MS/MS data, fragments were formed by the mass losses of *m/z* 18.0106, 27.9949, and 42.0106. These mass losses correspond to the elimination of H_2O, CO and CH_2CO respectively. The fragmentation pattern is shown in Scheme 6 below.

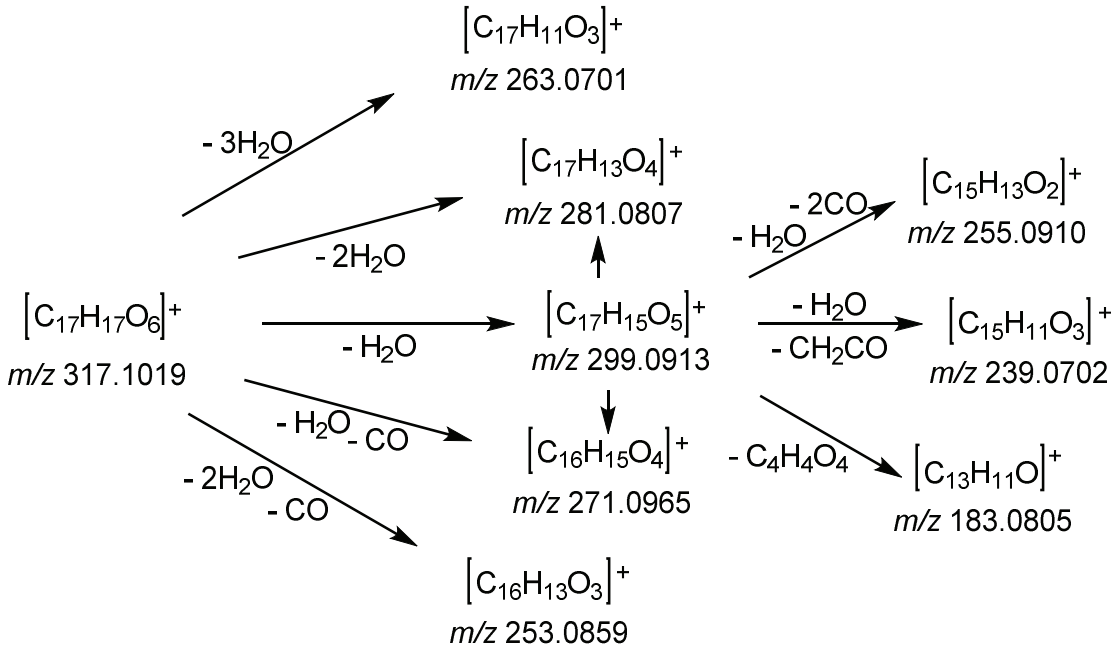

Scheme 6: Fragmentation pattern of compound A.

The further disintegration of the daughter ion with mass *m/z* 299.0913 yielded, in addition to the other ions observed by the disintegration of the molecule ion, an additional ion with mass *m/z* 183.0805, which seems to correspond to the core structure of the compound. From the fragmentation pattern, it can be assumed at this point that compound A could possess at least three OH, one CO and one CH_2CO entities. A comparison with the MS/MS pattern of pigments already isolated from the *Mycena* species revealed no similarities, not even with the yellow pigments mycenaflavin A, B and C isolated from *Mycena haematopus*. [58, 69]

The ^{1}H NMR spectrum recorded in CD_3OD at 300 K (Figure 11) exhibited protons clearly from more than one compound. The assignment of different correlations with the help of the COSY spectrum proved to be difficult due to the impurity. Correlations were observed between protons with unfitting integration, suggesting an overlap of proton signals of different molecules.

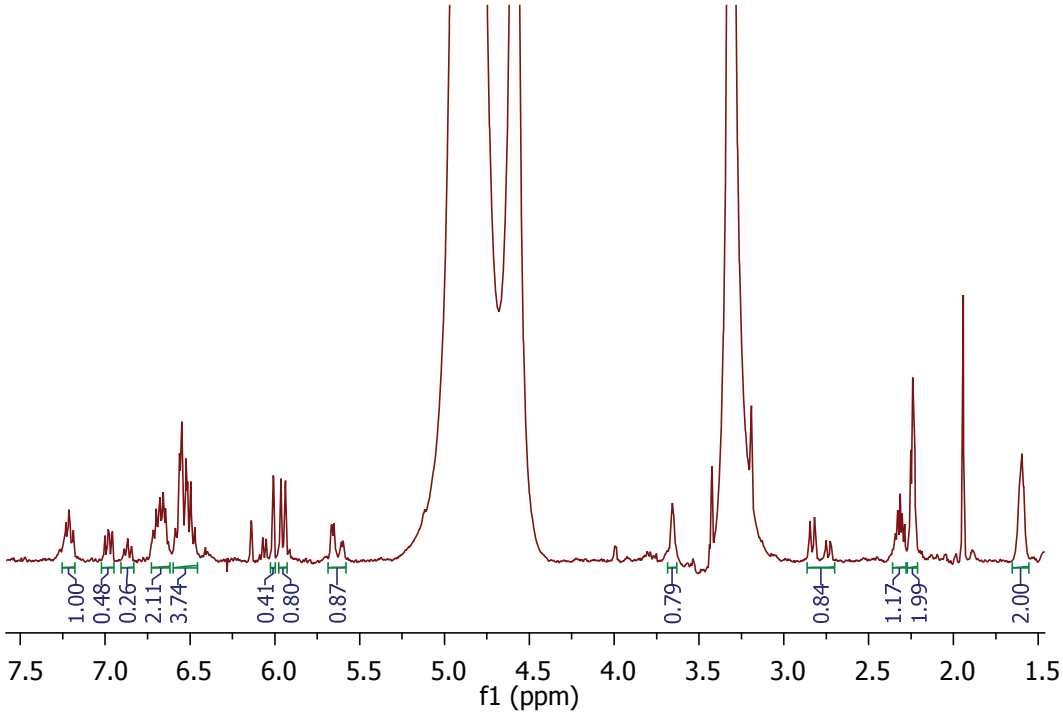

Figure 11: ^{1}H NMR spectrum (600 MHz, CD_3OD, 300 K) of compound A after HPLC separation.

In order to avoid further loss, the fraction was cleaned over Sephadex LH-20 instead of HPLC, which resulted in a more comprehensible ^{1}H NMR spectrum. However, the number of non-exchangeable hydrogen atoms displayed on the ^{1}H NMR spectrum still gave evidence of the presence of more than one compound. From the MS/MS data, at least three exchangeable hydrogen atoms are expected; adding to the fifteen observed on the ^{1}H NMR spectrum (Figure 12) would result to eighteen, exceeding the amount seventeen generated by the molecular formula.

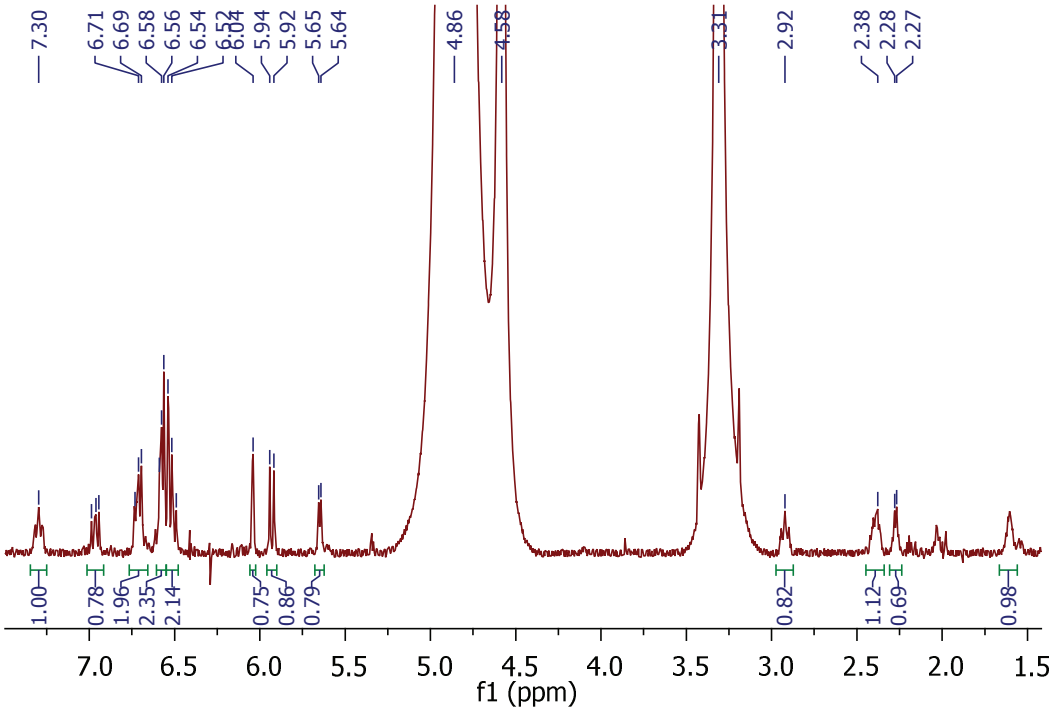

Figure 12: ^{1}H NMR spectrum (600 MHz, CD_3OD, 300 K) of compound A after size exclusion chromatography over Sephadex LH-20.

Nevertheless, the COSY spectrum (Figure 13) revealed well interpretable correlations. A spin system could be observed between some protons occurring downfield in the aromatic region, leading to the fragment represented in Figure 14.

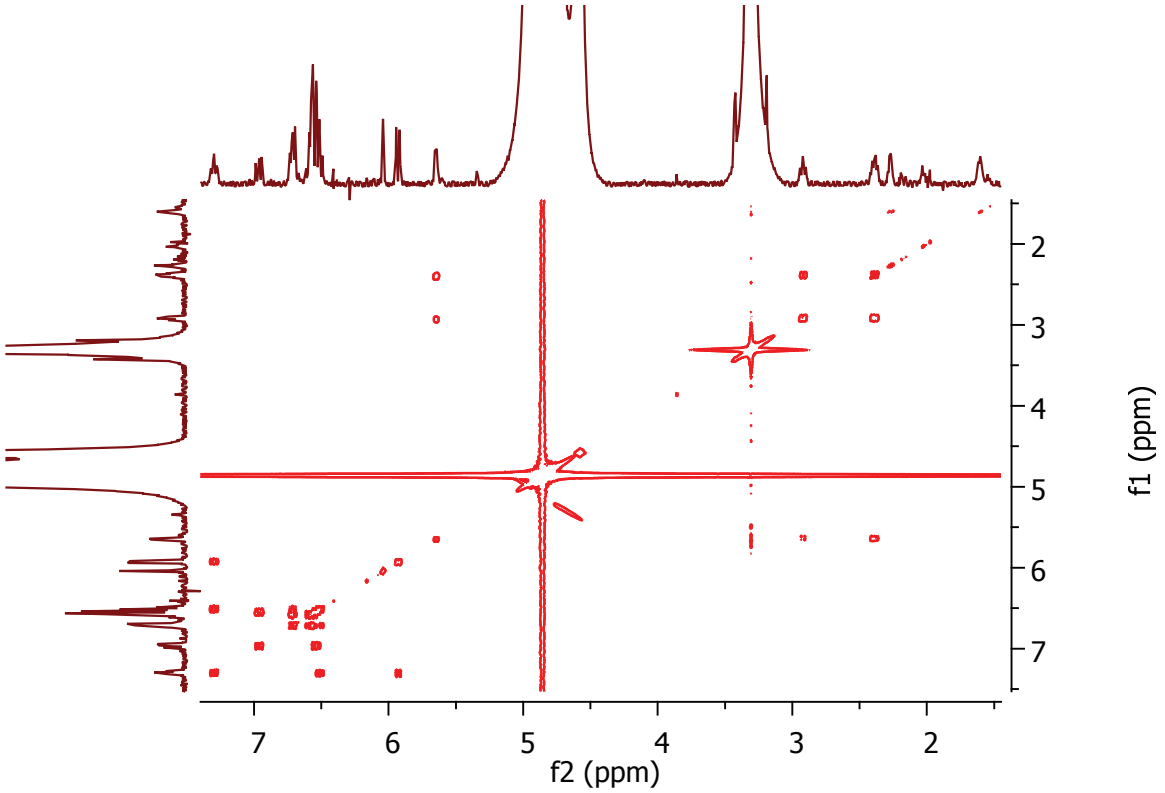

Figure 13: COSY spectrum (600 MHz, CD_3OD, 300 K) of compound A.

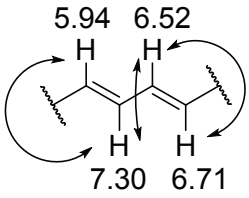

Figure 14: Fragment of compound A assigned by COSY correlations.

Another spin system (Figure 15) was observed independently of the one already described, still between protons appearing downfield. The assumption here is that this fragment belongs to the other compound present in the sample. The proton at δ_H 6.71 ppm in this spin system, which should belong to a π-system, exhibited ^3J correlations to protons at δ_H 6.58 and 6.54 ppm, different from the neighbouring protons in the first spin system presented in Figure 14.

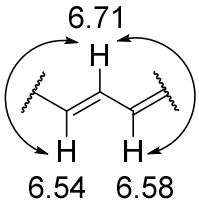

Figure 15: COSY correlations of second fragment.

Recording the ^{13}C NMR proved very challenging due to the fact that the sample was dilute. The carbon chemical shifts were therefore read from the HSQC spectrum (Figure 16). This again confirmed the presence of at least two compounds in the sample with very similar proton chemical shifts, since for the proton signal at δ_H 6.71 ppm for example, two carbon chemical shifts were observed, at δ_C 140.00 and 141.07 ppm. This indicated the presence of two protons under this proton peak, bonded to different carbon atoms. Table 2 shows the NMR data gathered so far, with the ^{13}C chemical shifts assigned from HSQC measurements.

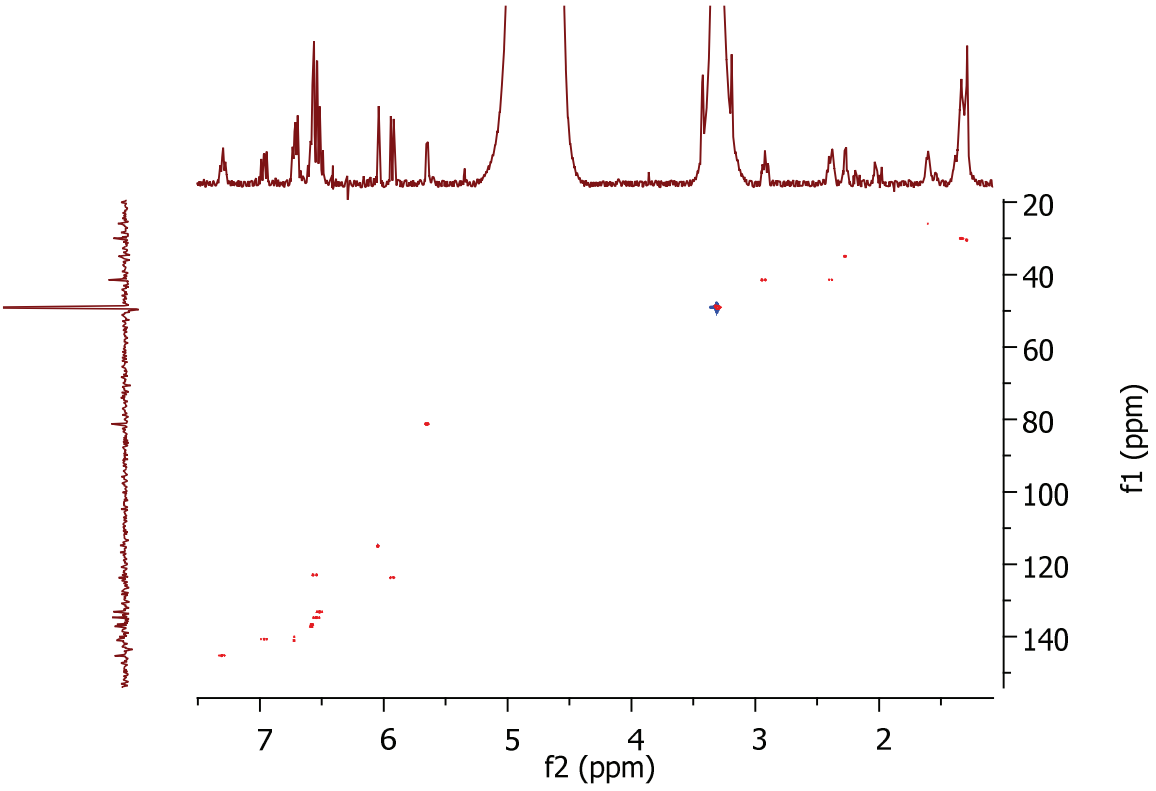

Figure 16: HSQC spectrum (600 MHz, CD_3OD, 300 K) of compound A.

HMBC measurements just like the ^{13}C NMR, did not achieve useful results. The recording of the HSQC spectrum took over 24 h, since the sample was dilute. This made the recording of the HMBC and ^{13}C NMR spectra unrealizable. Quaternary carbon atoms which might be present in the compound therefore could not be determined. Further extraction was needed for further experimentation. Unfortunately, there were no more fruiting bodies of *M. epipterygia* in reserve for further extraction. Hence compound A could not be fully characterized.

Table 2: ^{1}H NMR chemical shifts with attached ^{13}C chemical shifts (assigned from HSQC) of compound A (measured in CD_3OD).

Nr.	**δ_C** (from HSQC spectrum) **[ppm]**	**δ_H [ppm]**	**COSY**
1	145.21	7.30	H-8, H-9
2	141.07	6.71	H-8, H-5 / 6, H-7
3	140.66	6.96	H-7, H-8
4	140.00	6.71	H-8, H-5 / 6, H-7
5	137.21	6.58	H-2 / 4,
6	136.65	6.58	H-2
7	134.72	6.54	H-2 / 4, H-3,
8	133.14	6.52	H-1, H-2 / 4, H-3
9	123.68	5.93	H-1
10	122.93	6.55	-
11	114.97	6.04	-
12	81.24	5.65	H-13
13	41.46	2.92 / 2.38	H-12

2.5 Compounds B and C

In HR-(+)-ESI-MS compound B revealed the same molecule ion $[M+H]^+$ at *m/z* 317.1019 as compound A, with a similar fragmentation pattern in the HR-(+)-ESI-MS/MS data.

Considering the difficulty of getting a distinct separation of compound A from compound B by HPLC even after cleaning the separated fraction over Sephadex LH-20, and the identical mass and fragmentation pattern by the HR-(+)-ESI-MS/MS measurements, it was assumed that compounds A and B might present an *E*/*Z* isomerism. Literature research on how to separate *E*/*Z* isomers by HPLC remained unsuccessful. However, a similar situation was encountered by Peters while separating benzoxepin fatty acid esters extracted from *Mycena galopus*.[58] The *E*/*Z* isomers were purified by a two-step HPLC separation, first on an RP-18 column, followed by a normal phase column. More fungal extract was needed to attempt this method. Unfortunately, new extract could not be produced due to shortage of fruiting bodies of *Mycena epipterygia*.

Compound C was not further investigated because the amount collected from the HPLC separation was much too low to undertake any characterisation.

2.6 Conclusions

The yellow compounds A, B and C were isolated from the yellowleg bonnet *Mycena epipterygia*. The molecular formulas of compounds A and B were resolved with the help of HRMS to be $C_{17}H_{17}O_6$. Some fragments of compound A were revealed by COSY experiments. However the complete structure of A could not be determined due to impurity in the sample which made the interpretation of the different spectra difficult. In addition, the low yield after HPLC separation rendered the measurement of ^{13}C and HMBC NMR improbable, since for these experiments concentrated samples are often required. Compounds A and B are assumed to be *E*/*Z* isomers, since both eluted almost simultaneously from the HPLC column and have the same molecular formula and fragmentation patterns. Further investigation of compound C was not possible due to the very low yield obtained after the HPLC separation.

In order to fully characterise compounds A, B and C, at least three to four times the amount of *M. epipterygia* used for this study would be needed to isolate enough compounds for further investigation. Biological tests should then be performed to examine their ecological role.

3 *Megacollybia platyphylla*

3.1 Mushroom Description

The whitelaced shank *Megacollybia platyphylla* (Pers.: Fr.) Kotl. & Pouz. (German name: Breitblättriger Rübling), also known as *Collybia platyphylla* (Pers.:Fr.) Mos., is a large mushroom generally found on rotten deciduous woodland. The cap is 5 to 15 cm in diameter, hemispherical in shape, later becoming outspread. The grey-brown cap has a surface striped by radial fibres, often with lacerated edge when dry. The gills are very broad and creamy white in colour. The tough fibrous stipe is 5 to 15 cm in height and 10 to 20 mm in diameter, with long whitish mycelial strands at the base which attach the mushroom to wood residues from Mai to October. [70]

Figure 17: *Megacollybia platyphylla*, Bad Fallingbostel, October 2015.

3.2 Previous Work

No report was found on secondary metabolites isolated from *Megacollybia platyphylla*. However, mycelia extracts were found to exhibit inhibitory activity against bacteria such as *Micrococcus luteus*, *Staphylococcus aureus* and *Staphylococcus epidermidis*, as well as against fungi such as *Candida albicans*, *Cladosporium herbarum* and *Aspergillus niger*. [71, 72]

3.3 Extraction and Isolation of Compounds 42 and 43

Fruiting bodies of *Megacollybia platyphylla* were extracted with MeOH at 25 °C. After concentrating the extract, it was purified by SPE over a C18 cartridge. In doing so, the cartridge was eluted first with water, followed by a H_2O-MeOH solution (50/50 v/v) and finally with methanol. The water-methanol and methanol fractions were reunited and separated by HPLC on a semi-preparative RP-18ec column. Two broadened peaks could be observed towards the end of the HPLC chromatogram as seen in Figure 18, the first (**43**) after 25.5 min and the second (**42**) after 29.2 min.

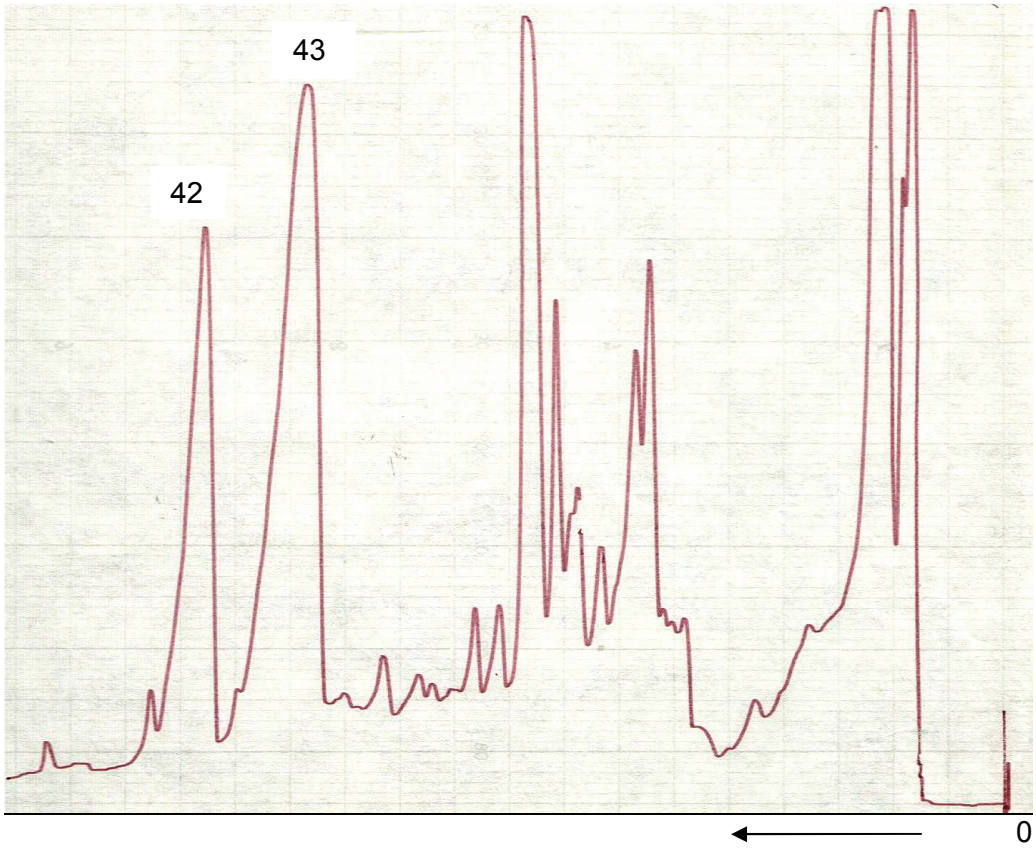

Figure 18: Semi-preparative HPLC chromatogram of *Megacollybia platyphylla* with UV detection at λ = 270 nm.

3.4 Structure Elucidation of 3-(1-Carboxyvinyloxy)-5-hydroxy-4-methoxybenzoic acid (42)

Compound **42** eluted after 29.2 min, displaying a UV/Vis spectrum with absorption maxima at λ = 220, 252 and 294 nm. The absorption band at 220 and 252 nm indicated the presence of double bonds.

The HR-(+)-ESI-MS revealed molecule ions $[M+Na]^+$ at *m/z* 277.0318, $[M+NH_4]^+$ at *m/z* 272.0766 and $[M+H]^+$ ion at *m/z* 255.0499. The $[M+H]^+$ ion was consistent with the molecular formula $C_{11}H_{11}O_7$. The DBE was then calculated to be seven (1). The HR-(+)-ESI-MS/MS data delivered fragments formed by the mass losses of *m/z* 18.0106 and 36.0212, corresponding to the elimination of two H_2O units.

The ^{13}C NMR confirmed the presence of eleven carbon atoms, which according to HSQC correlations accounted for one CH_3 group, two CH groups, one CH_2 group with diastereotopically split protons, and seven quaternary carbon atoms. The ^1H NMR spectrum of compound **42** measured in DMSO (Figure 19) exhibited one exchangeable and seven non-exchangeable protons. The broad peak displayed at δ_H 9.91 ppm was attributed to an OH group belonging to a carboxylic group or a phenol. Two doublets were observed downfield at δ_H 7.24 and 6.93 ppm, each with coupling constants of 2.02 Hz. This indicated a $^4J_{HH}$ coupling, which together with their ^1H-NMR chemical shifts are typical to aromatic systems. This was confirmed by the COSY spectrum (Figure 20), where these two protons constituted one spin system, as well as by their HSQC correlations (Figure 21) with aromatic carbon resonances at δ_C 113.27 and 110.47 ppm respectively.

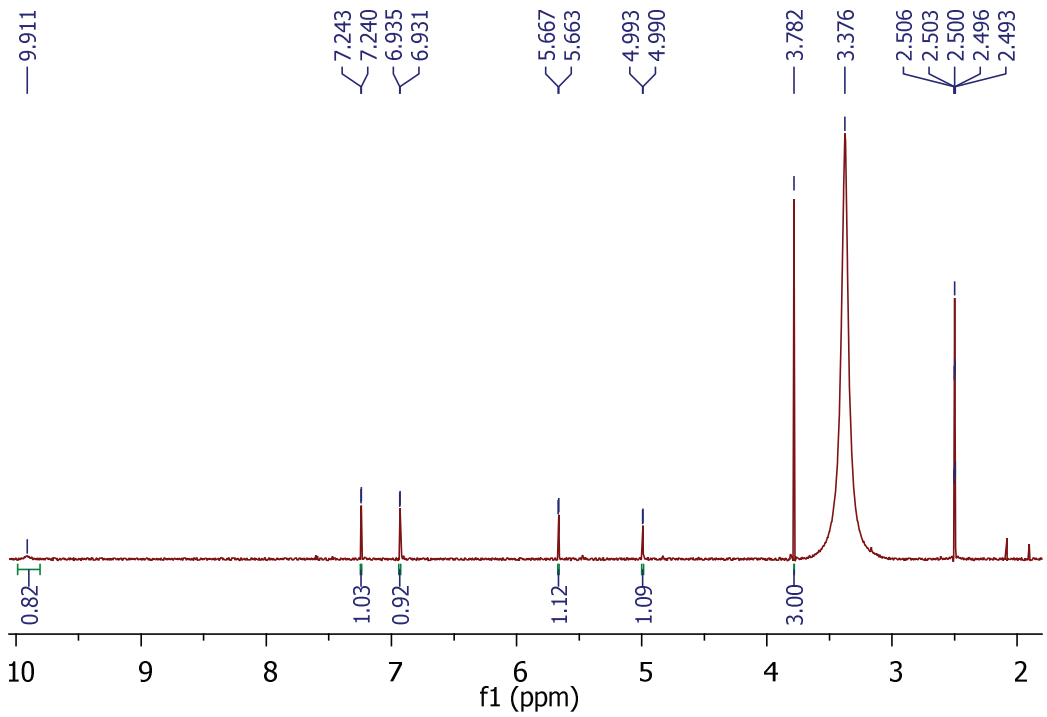

Figure 19: ^{1}H NMR spectrum (600 MHz, d_6-DMSO, 300 K) of **42**.

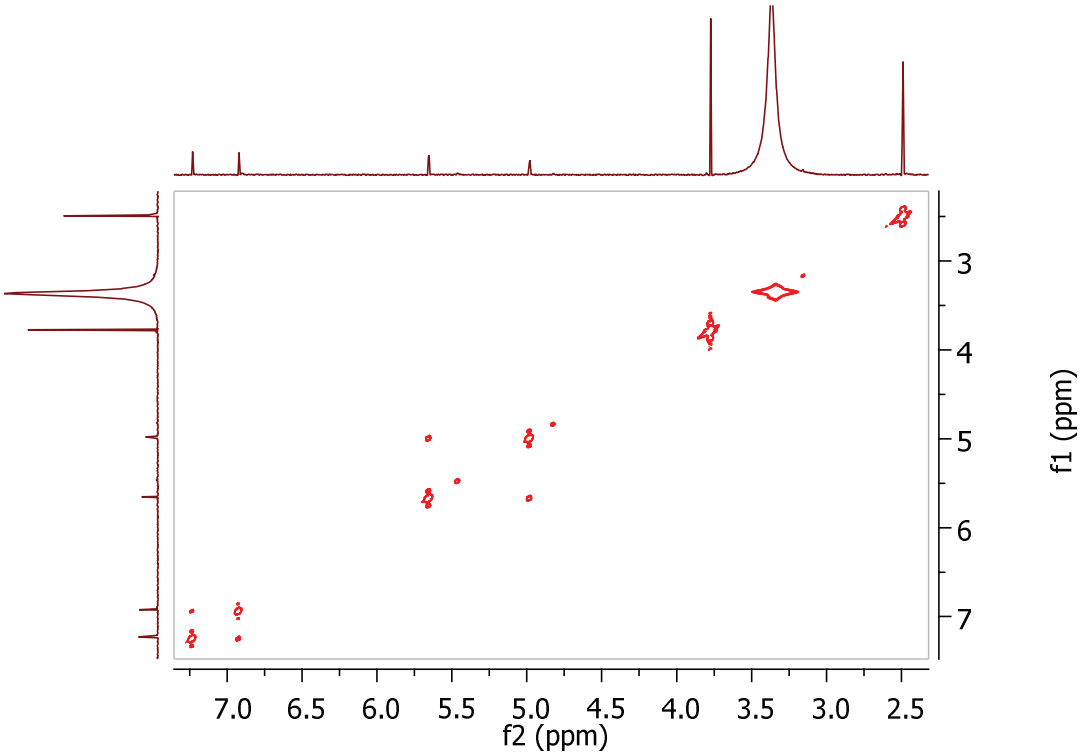

Figure 20: COSY spectrum (600 MHz, d_6-DMSO, 300 K) of **42**.

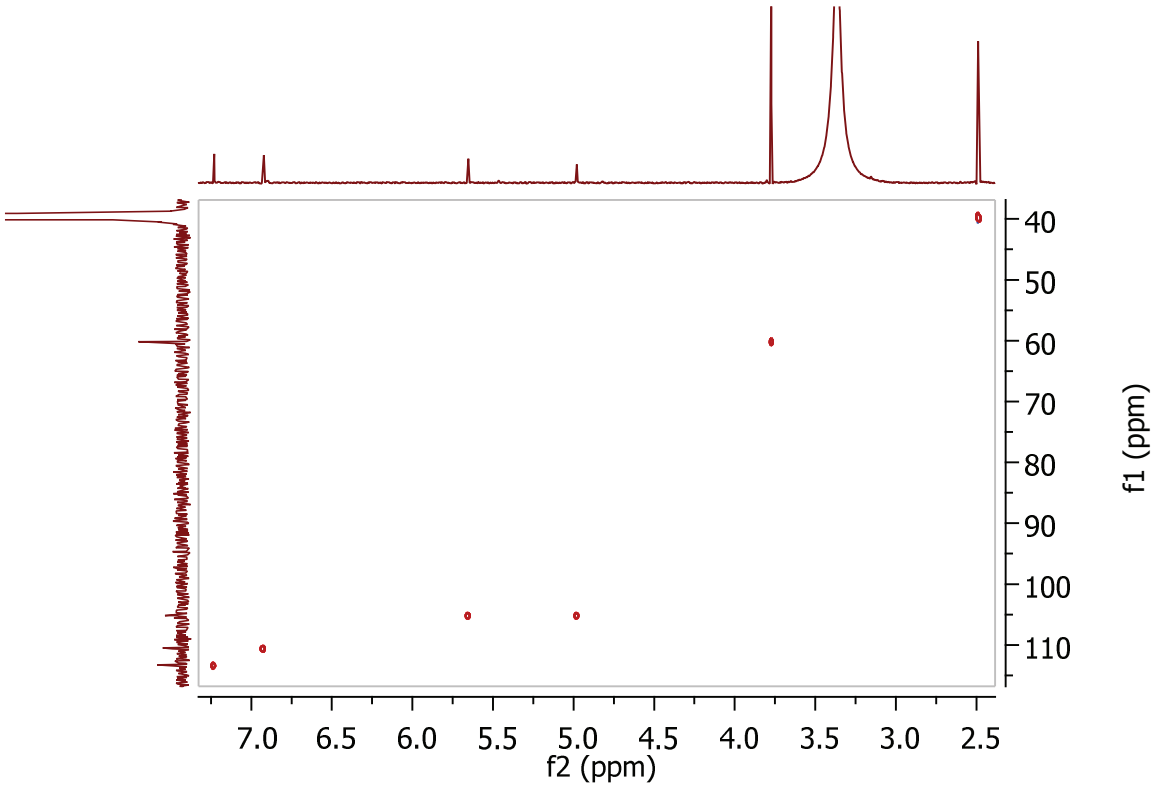

Figure 21: HSQC spectrum (600 MHz, d_6-DMSO, 300 K) of **42**.

In the HMBC spectrum (Figure 22), the proton at δ_H 7.24 ppm featured strong correlations to three carbons at δ_C 166.54, 142.02 and 110.47 ppm. Weaker correlations were observed to carbons at δ_C 151.23 and 125.92 ppm. Likewise, the proton at δ_H 6.94 ppm exhibited strong HMBC correlations to carbons at δ_C 166.54, 142.02 and 113.27 ppm, and weaker correlations to δ_C 148.68 and 125.92 ppm. Considering the fact that strong correlations in HMBC are attributed to $^3J_{CH}$ coupling and weaker correlations to $^2J_{CH}$ or $^4J_{CH}$ coupling, the two protons at δ_H 7.24 and 6.94 ppm were assigned to be at equal distances to the carbons at δ_C 166.54, 142.02 and 125.92 ppm (Figure 23). The ^{13}C chemical shift at δ_C 166.54 ppm, being typical to carbonyl groups and in this case being attached to no hydrogen atom, was attributed to a carboxyl group.

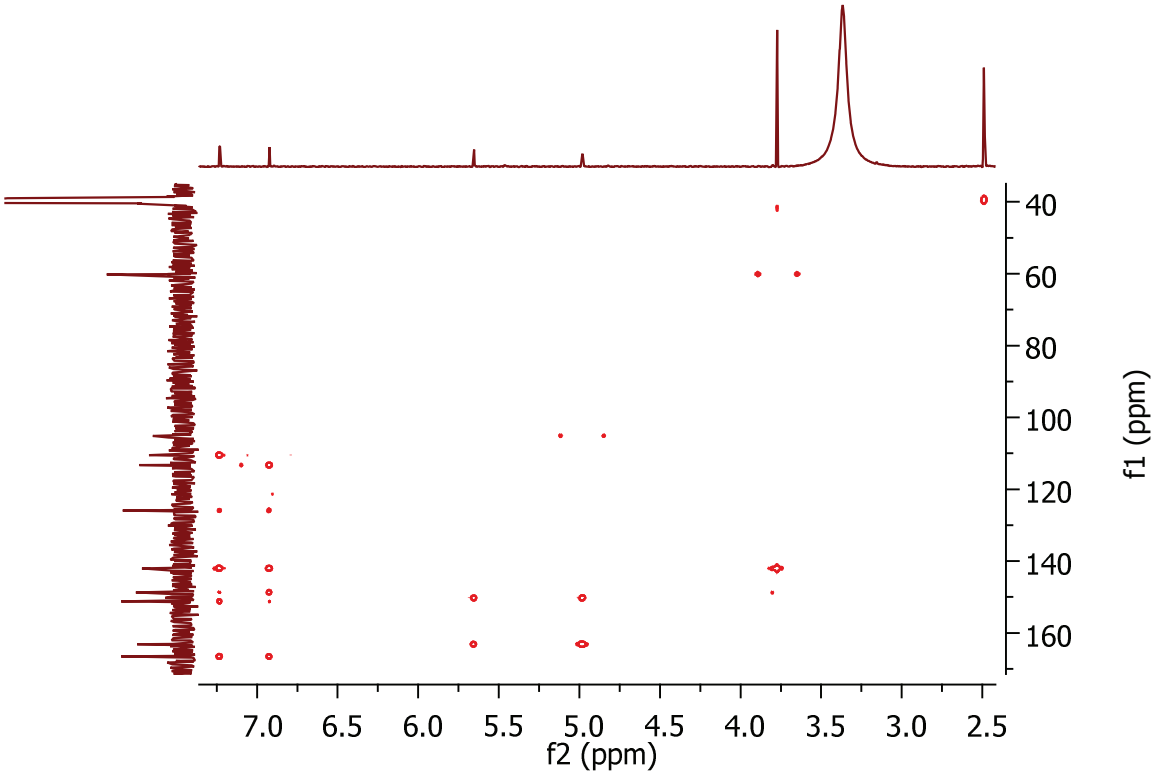

Figure 22: HMBC spectrum (600 MHz, d_6-DMSO, 300 K) of **42**.

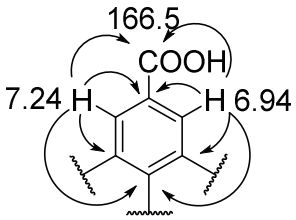

Figure 23: Selected HMBC correlations of the aromatic fragment of **42**.

The second spin system exhibited on the COSY spectrum showed correlation between two doublets at δ_H 5.66 and 4.99 ppm. These two protons showed correlation to one and the same carbon resonance at δ_C 105.16 ppm in the HSQC spectrum, accounting for the diastereotopically split protons of the CH_2 group. In the HMBC spectrum both protons coupled with two carbons with chemical shifts δ_C 163.12 and 150.23 ppm (Figure 24). The carbon resonance at δ_C 163.12 ppm was attributed to a carboxyl group, since it was a quaternary carbon and had a characteristic carbonyl chemical shift. Compound 42 thus has two carboxyl groups.

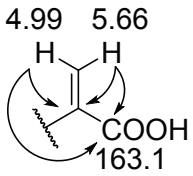

Figure 24: HMBC correlations of the side chain of **42**.

From the integral of the ^{1}H NMR chemical shift at δ_H 3.78 ppm, the peak was attributed to a CH_3 group directly bond to an oxygen atom since it exhibited a characteristic OCH_3 chemical shift. In the HMBC spectrum these protons exhibited $^{3}J_{CH}$ correlation only to the carbon at δ_C 142.02 ppm, which was part of the aromatic system. The carbon resonance at δ_C 148.68 ppm on the aromatic fragment as well as δ_C 150.23 ppm on the side chain supposed in both cases a link to an oxygen atom. This gave the link between the two fragments. The enolpyruvic acid side chain was linked to the aromatic system at position C-3. The NOE correlation between the protons at δ_H 6.94 and 5.66 ppm supported this attribution.

From the molecular formula generated from the HR-(+)-ESIMS and the different NMR correlations, compound **42** could be completely characterised (Figure 25).

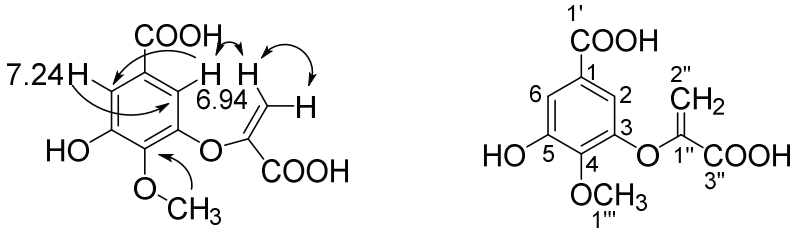

Figure 25: Selected HMBC (→) and NOE (↔) correlations for full characterisation of **42**.

This structure is in line with the double bond equivalent calculated from the molecular formula to be seven. Table 3 summarises all the NMR data of compound **42**.

In the HR-(+)-ESI-MS/MS of compound **42** (Scheme 7), besides the commonly known splits of H_2O and CO, a fragment was also observed due to the unusual loss of a $C_3H_4O_3$ unit arising from the $C_{11}H_9O_6$ fragment.

Table 3: NMR data (600 MHz, DMSO, 300 K) of compound **42**.

Nr.	δ_C [ppm]	δ_H [ppm]	Type	Multiplicity (J_{HH} [Hz])	COSY	HMBC
1	125.92	-	C_q	-	-	-
2	110.47	6.94	CH	d (2.0)	H-6	C-1, C-3, C-4, C-6, C-1’
3	148.68	-	C_q	-	-	-
4	142.02	-	C_q	-	-	-
5	151.23	-	C_q	-	-	-
6	113.27	7.24	CH	d (2.0)	H-2	C-1, C-2, C-4, C-5, C-1’
1’	166.54	-	C_q	-	-	-
1”	150.23	-	C_q	-	-	-
2”	105.16	5.66 / 4.99	CH_2	d / d (1.9)	H-2”a / b	C-1”, C-3”
3”	163.12	-	C_q	-	-	-
1”’	60.19	3.78	CH_3	s	-	C-4

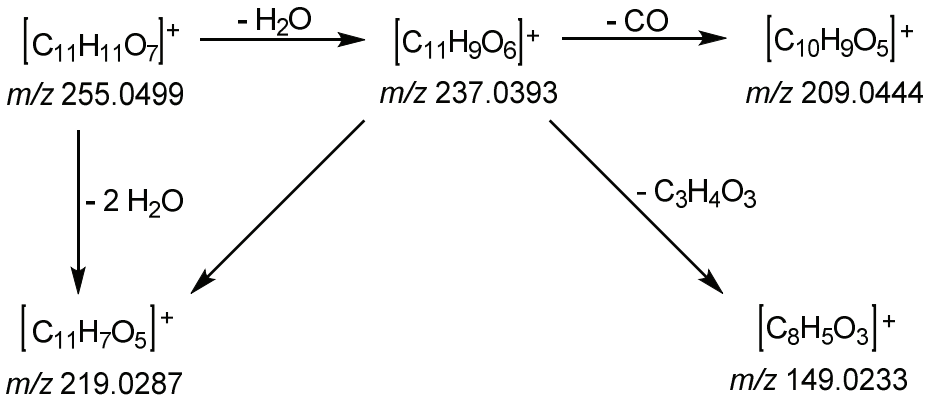

Scheme 7: Fragmentation of **42** based on HR-(+)-ESI-MS/MS measurement.

Compound **42**, which from its structure can be derived from chorismic acid (**11**) or gallic acid (Figure 26), has not been described before. This is therefore the first description of **42** as a secondary metabolite isolated from the fruiting bodies of a higher fungus. Chorismic acid derivatives have been isolated from cultures of higher fungi and will be discussed later in section 3.6.

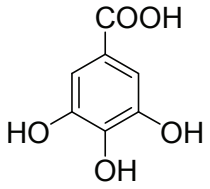

Figure 26: Structure of gallic acid (**44**).

3.5 Structure Elucidation of 3-(1-Carboxyvinyloxy)-4, 5-dihydroxybenzoic acid (43)

Compound **43** eluted first from the HPLC column after 25.5 min and is therefore more polar than **42**. The UV/Vis spectrum was similar to that of **42**, with absorption maxima at λ = 222 and 265 nm. The maximum at 222 nm just like by **42**, indicated the presence of double bonds.

The ESI-MS measured in negative mode, revealed an $[M–H]^-$ ion at *m/z* 239, implying a mass unit difference of 14 u from **42**. The MS/MS spectrum delivered fragments at *m/z* 195 and 151, corresponding to a two-time loss of the mass unit 44 u. This suggested the presence of two carboxylic groups or twice a C_2H_4O unit. In addition, weak signals at *m/z* 169 and 125 were observed at a mass unit difference of 26 u each from the fragments at *m/z* 195 and 151 respectively. This suggested the loss of a C_2H_2 unit.

The ^1H NMR of **43** (Figure 27) when compared with that of **42** (Figure 19) showed the absence of the methyl group. The rest of the signals were consistent, even though the doublets of the aromatic protons were slightly shifted downfield. This gave indication of the presence of an additional OH group on the aromatic fragment of **43**, which deshielded the protons. Measured in DMSO (Appendix A.11), the presence of two OH groups was supported by the presence of a broadened peak at δ_H 8.86 ppm which revealed two protons on integration.

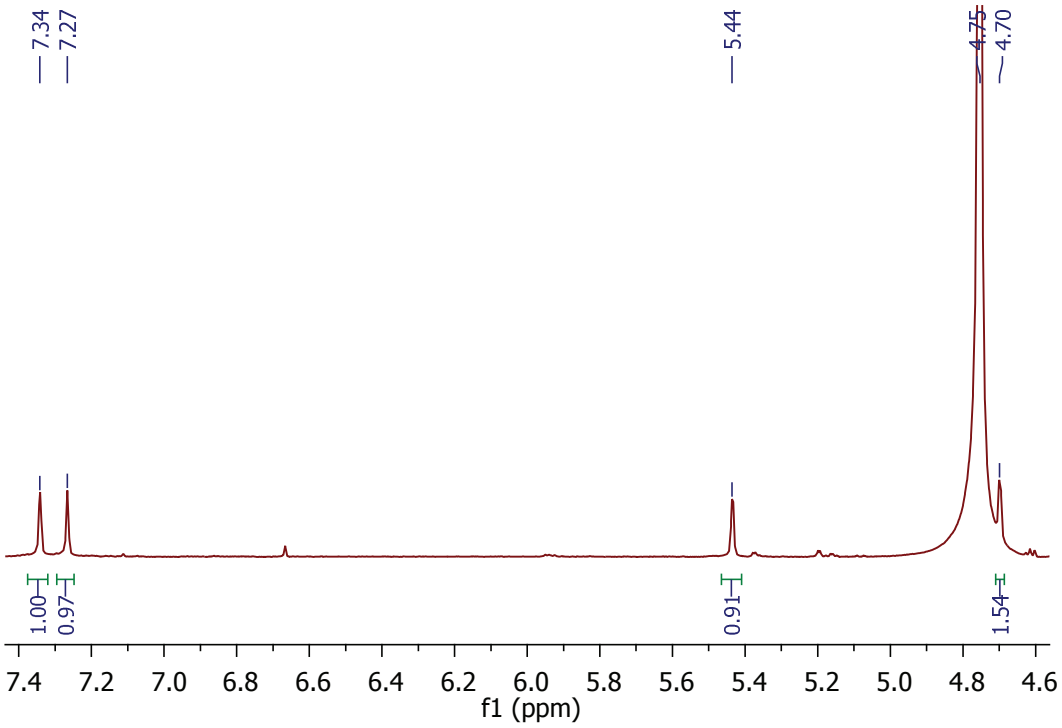

Figure 27:[1]H NMR spectrum (600 MHz, D_2O, 300 K) of compound **43**.

In the HMBC spectrum (Figure 28) two correlations were observed to C-4 from the aromatic protons at δ_H 7.27 and 7.34 ppm, as was the case in **42**. The third correlation which came from the methyl group was absent. From this observation and considering the ^{13}C chemical shift, the additional OH group was assigned to be attached to C-4. Figure 29 shows the HMBC correlations for the confirmation of the structure of compound **43**, as well as the NOE correlations form the NOESY spectrum (Figure 30).

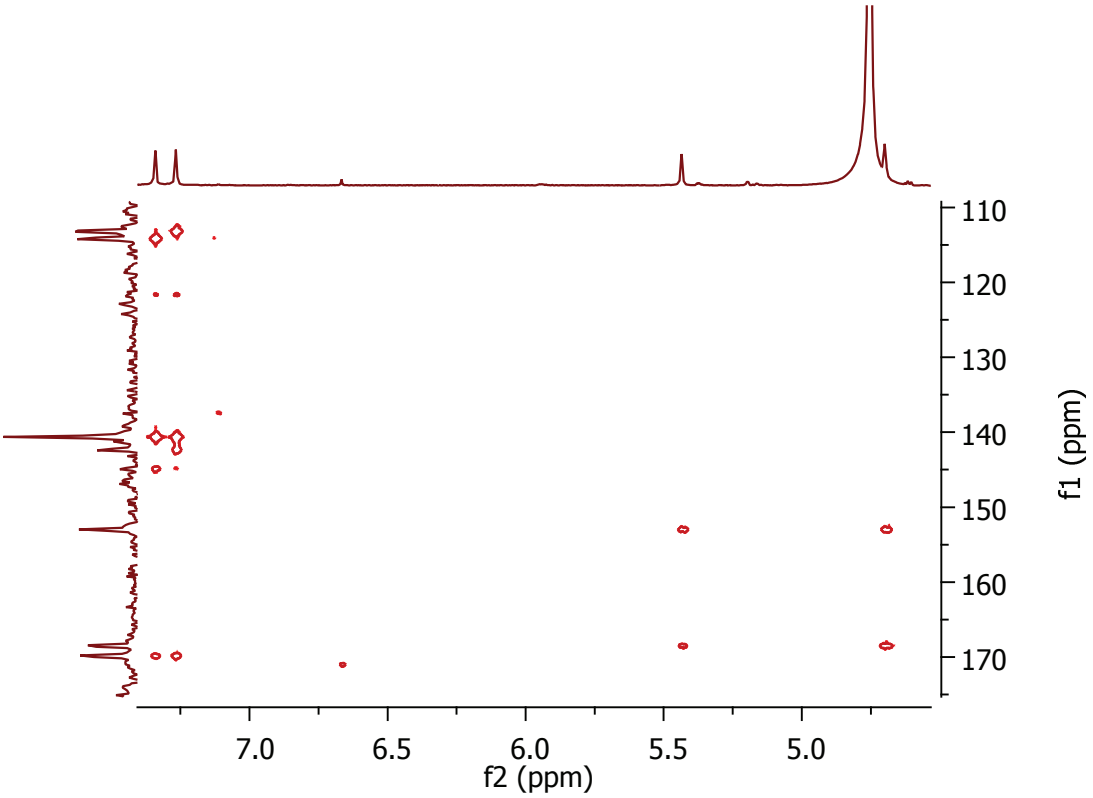

Figure 28: HMBC spectrum (D_2O, 300 K) of compound **43**.

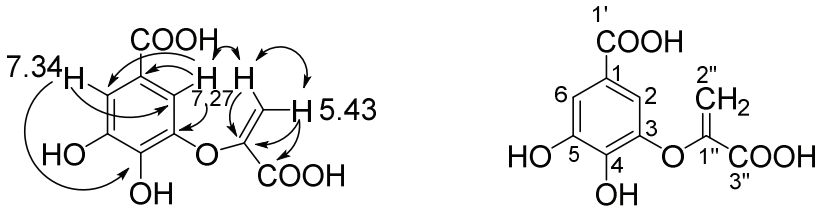

Figure 29: Selected HMBC (→) and NOE (↔) correlations for confirmation of the structure of compound **43**.

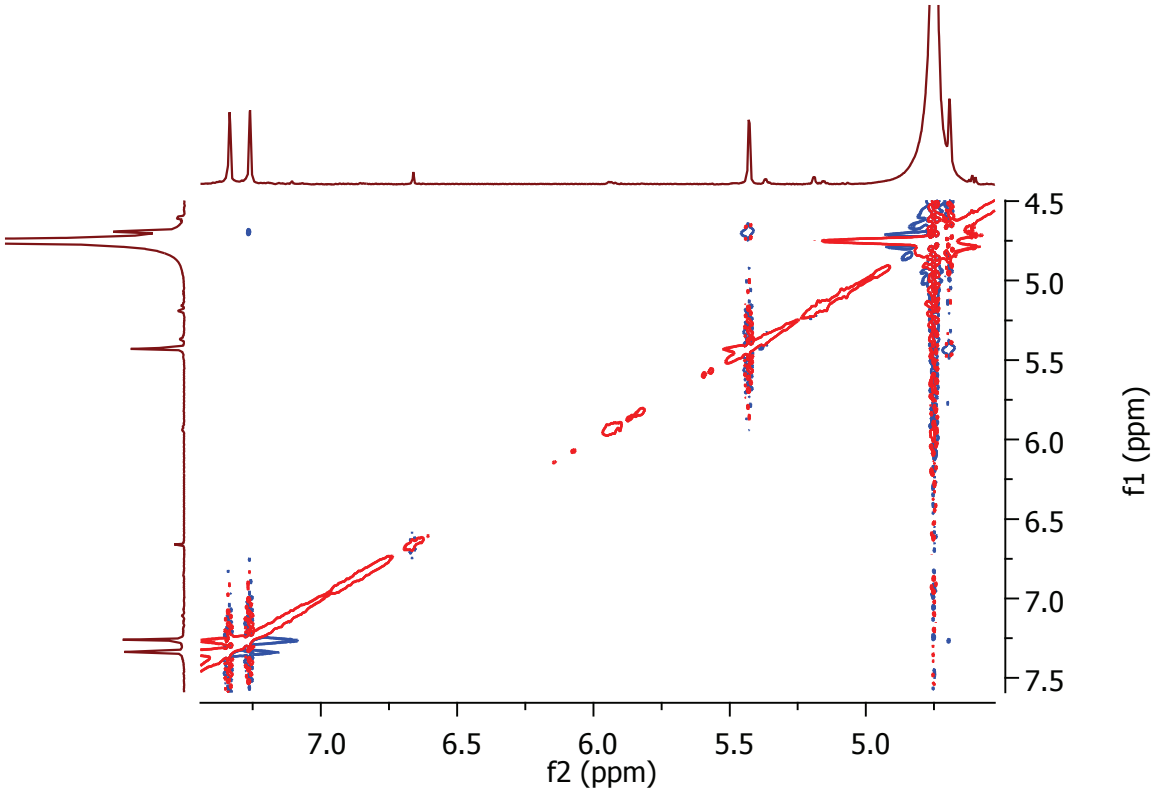

Figure 30: NOE spectrum (600MHz, D_2O, 300 K) of compound **43**.

Table 4 summarises once more all the NMR data of compound **43**.

Table 4: NMR data (600 MHZ, D_2O, 300 K) of compound **43**.

Nr.	δ_C [ppm]	δ_H [ppm]	Type	Multiplicity (J_{HH} [Hz])	COSY	HMBC
1	121.64	-	C_q	-	-	-
2	114.18	7.27	CH	d (1.9)	H-6	C-1, C-3, C-4, C-6, C-1’
3	142.38	-	C_q	-	-	-
4	140.63	-	C_q	-	-	-
5	144.89	-	C_q	-	-	-
6	113.18	7.34	CH	d (1.9)	H-2	C-1, C-2, C-4, C-5, C-1’
1’	169.83	-	C_q	-	-	-
1”	152.98	-	C_q	-	-	-
2”	99.89	5.44 / 4.70	CH_2	d / d (1.9)	H-2”a / b	C-1”, C-3”
3”	168.48	-	C_q	-	-	-

The structure of compound **43** obtained from NMR experiments matches with the ESI-MS/MS data and the fragmentation can be assigned as shown in Scheme 8.

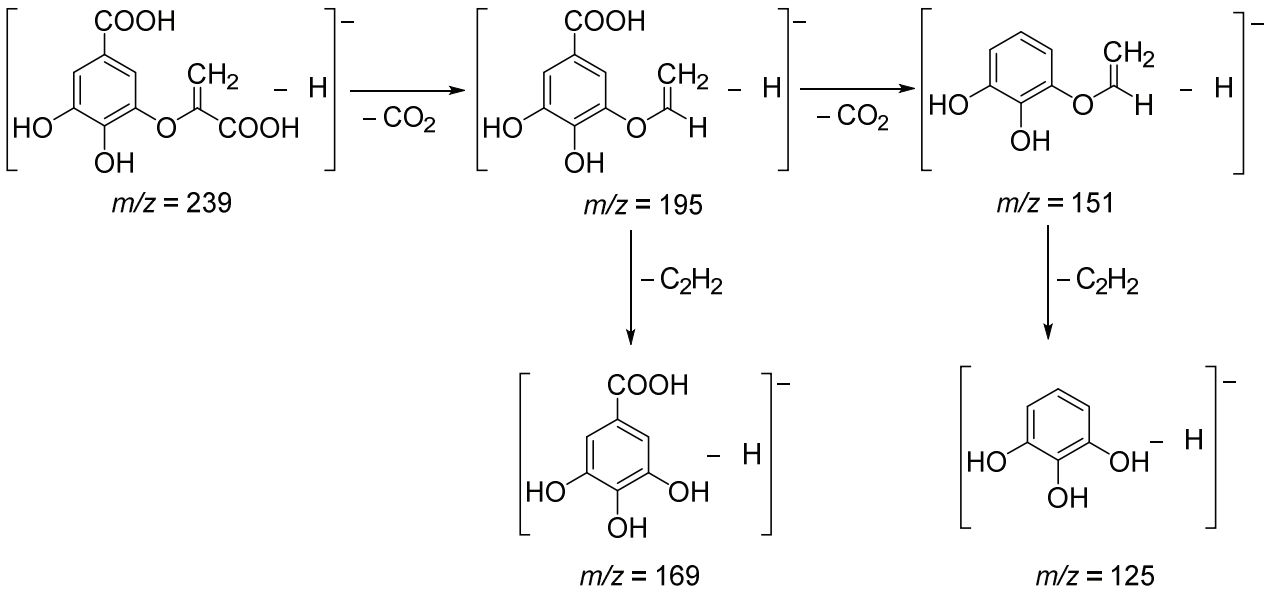

Scheme 8: Fragmentation of **43** based on ESI-MS/MS experiments.

Compound **43** has been described as a synthetic product, to mimic the substrate chorismic acid (**11**), in the inhibition studies of the enzyme *Mycobacterium tuberculosis* salicylate synthase (MbtI).[73] MbtI catalyses the first step in the biosynthesis of the siderophore mycobactin T, which is essential for both the virulence and survival of the agent of tuberculosis *Mycobacterium tuberculosis*.

Compound **43** was synthesized, as shown in Scheme 9, from the commercially available ethyl gallate (**45**).[73] The OH groups at position C-4 and C-5 were first protected before the insertion of diazophosphonoacetate at position C-3 to obtain the phosphonate **46**. The side chain was then converted to an enol-pyruvate ester derivate. Compound **43** was finally obtained by saponificaton of the ester moieties and removal of acetonide.

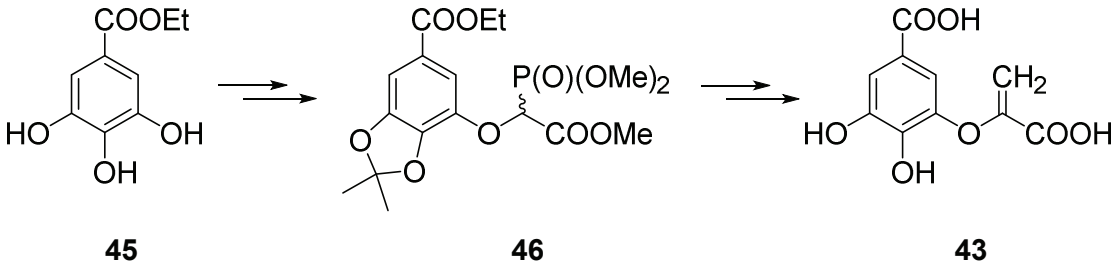

45 **46** **43**

Scheme 9: Synthesis of **43** from commercially available ethyl gallate (**45**).[73]

Compound **43** was found to be a poor inhibitor of MbtI, due to the presence of the hydroxyl substituent at position C-5, which caused steric hindrance at the active site of the enzyme.[73] However, **43** was a potent inhibitor of the enzyme *Serratia marcescens* anthranilate synthase.[73] *Serratia marcescens* is an opportunistic human pathogen commonly found in the respiratory and urinary tracts, and in damp environments.

Compound **43** was therefore described as a synthetic product, not as a natural product. This is the first isolation of **43** from the fruiting bodies of a higher fungus. Table 5 compares the ^{13}C- and ^{1}H NMR chemical shifts of the natural occurring and synthesized[73] compound **43**. The data are consistent with one another.

Table 5: Comparison of ^{13}C- and ^{1}H-NMR chemical shifts of the natural and synthesized **43**.

	Naturally occurring (in D_2O)		**Synthesized**[73] (in MeOD)	
Nr.	**δ_C [ppm]**	**δ_H [ppm]**	**δ_C [ppm]**	**δ_H [ppm]**
1	121.6	-	122.4	-
2	114.2	7.27	115.0	7.19
3	142.4	-	143.5	-
4	140.6	-	143.2	-
5	144.9	-	147.8	-
6	113.2	7.34	114.5	7.34
1’	169.8	-	169.4	-
1”	152.9	-	152.0	-
2”	99.9	5.44 / 4.70	102.1	5.62 / 4.77
3”	168.5	-	165.8	-

3.6 Occurrence of Chorismic acid Derivatives in Higher Fungi

Chorismic acid derivatives have been isolated from higher fungi. The cyathiformines A – D[74] (**46**–**49**) (Figure 26) were isolated from the ethyl acetate extracts of solid cultures of *Clitocybe cyathiformis*. They were considered to be derived from chorismic acid (**11**), the last common

intermediate in the shikimate pathway, and thought to be synthesized as defensive substances or as potential sources of hydroxy or aromatic amino acids. [74]

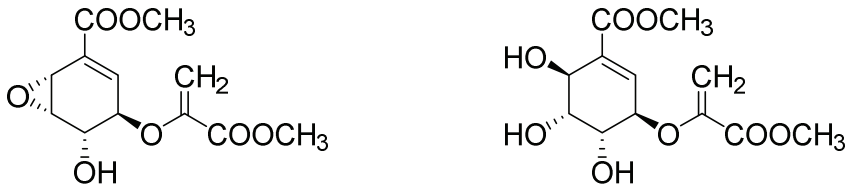

47

48

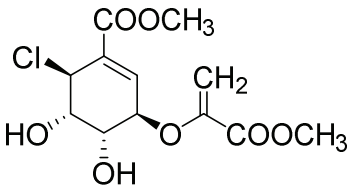

49

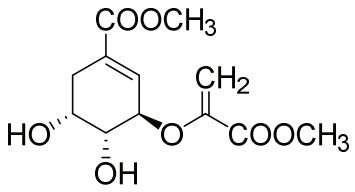

50

Figure 26: Structure of cyathiformines A – D (**47** – **50**) isolated from *Clitocybe cyathiformis*.

3.7 Hypothetical Biosynthetic Pathway of Compounds 42 and 43

Compounds **42** and **43** can be regarded as having either a chorismic acid (**11**) or a gallic acid (**44**) basic structure. For this reason, two possible biosynthetic pathways can be considered starting from shikimic acid (**8**) as precursor.

In the first route (Scheme 10), shikimic acid (**8**) would be converted to **11** as seen in the chorismate biosynthesis pathway (Scheme 1). Subsequent aromatization and hydroxylation at position C-5 would yield **43**, where the replacement of the hydrogen atom of the hydroxyl group at position C-4 by a methyl group would yield **42**.

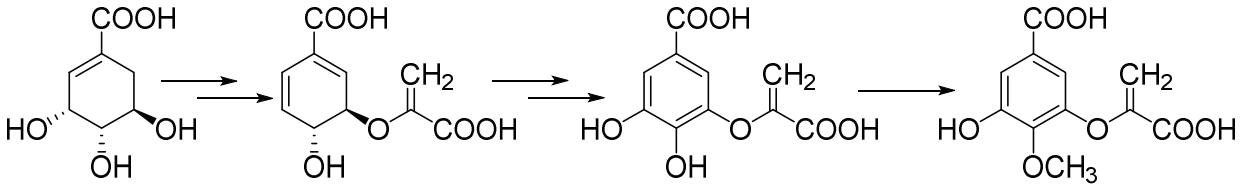

8 **11** **43** **42**

Scheme 10: Hypothetical biosynthetic pathway of compounds **42** and **43** via chorismic acid (**11**).

The second route (Scheme 11) would rather proceed via gallic acid (**44**). The introduction of the pyruvate side chain would yield **43**, before the introduction of the methyl group at position C-4 to replace hydrogen, thus yielding **42**.

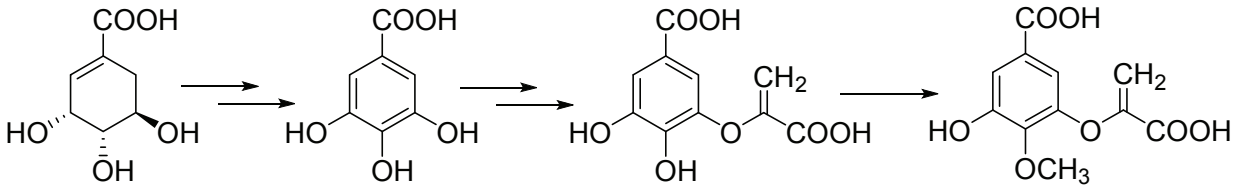

8 **44** **43** **42**

Scheme 11: Hypothetical biosynthetic pathway of compounds **42** and **43** via gallic acid (**44**).

The occurrence of the structurally related cyathiformines (Figure 26) in higher fungi supports the first route which proceeds through chorismic acid (**11**). Although the cyathiformines were isolated from cultures and not from fruiting bodies, it is very likely that compounds **42** and **43** are also derived from **11**, due to their structural similarity.

3.8 Biological Tests

Many shikimate derivatives, such as salicylic acid, vanillic acid, 4-hydroxybenzoic acid and ferulic acid were found to be allelopathic, thereby inhibiting the growth or germination of a wide range of plant species.[74] Likewise, dehydrochorismic acid (**51**) (Figure 31) showed inhibitory activity towards pollen tube elongation in *Camellia japonica*, but did not inhibit growth.[75]

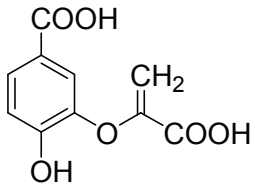

Figure 31: Dehydrochorismic acid (**51**)

Compounds **42** and **43** were tested for their antibacterial and herbicidal effect. For each compound, 0.5 mg and 1 mg were separately dissolved in 1 mL sterilized water and the solutions were dropped on paper discs (ø 6 mm, thickness 0.5 mm). After the paper discs had dried under sterile conditions, they were placed on agar plates charged with the test organisms *Escherichia coli*, *Bacillus subtilis* and *Staphylococus capitis*. The plates were then incubated for 24 h at 37 °C.

For the herbicidal test, the 1 mg/mL concentrated solutions of compounds **42** and **43** were dropped on sterilized cotton balls in glass containers. Seeds of the fast growing garden cress *Lepidium sativum* were placed on the cotton balls and allowed to grow at 25 °C for seven days.

Compounds **42** and **43** exhibited no inhibitory activity against *Escherichia coli*, *Bacillus subtilis* und *Staphylococcus capitis*. No growth inhibition was observed as well against *Lepidium sativum*.

Nevertheless, the chorismic acid derivatives **42** and **43** probably play an important role in protecting the fungus against bacteria such as *Serratia marcescens*, since **42** was found to be a potent inhibitor of the anthranilate synthase enzyme of this bacteria.

3.8 Conclusions

Two new chorismic acid derivatives were isolated from the fungus *Megacollybia platyphylla* and their structures determined with the help of MS, as well as 1D and 2D NMR experiments. Their biological activity was investigated by testing their antibacterial and herbicidal effects. In spite of the fact that they neither showed antibacterial nor herbicidal activities against the tested organisms, they likely defend the fungus against other species of bacteria such as *Serratia marcescens*.

4 *Tricholomopsis decora*

4.1 Mushroom Description

Tricholomopsis decora (Fr.) Sing. commonly known as prunes and custard (German name: Olivgelber Holzritterling) is a yellow mushroom found on decayed wood of conifers between June and November. The cap is 3 to 9 cm in diameter, convex, later becoming broadly flattened or centrally depressed. The yellow surface is covered especially over the centre with brownish to greyish scales. The yellow gills are crowded and attached to the sulphur-yellow, fibrous stipe, which is 3 to 7 cm long and up to 10 mm in diameter. [70]

Figure 32: *Tricholomopsis decora*. [76]

4.2 Previous Work

No report has been published about secondary metabolites isolated from *Tricholomopsis decora*.

4.3 Isolation and Structure Elucidation of Compound D

Fruiting bodies of *Tricholomopsis decora* were extracted with a H_2O-MeOH (50/50 v/v) solution at 25 °C. The orange extract was purified by SPE over a C18 cartridge by eluting with water,

then H_2O-MeOH (50/50 v/v) and finally MeOH. The H_2O-MeOH and MeOH fractions were reunited before being separated by HPLC on an RP-18ec column. The analytical HPLC (Figure 29) revealed a compound which eluted after 23.7 min denoted D, with UV maximum at λ = 424 nm.

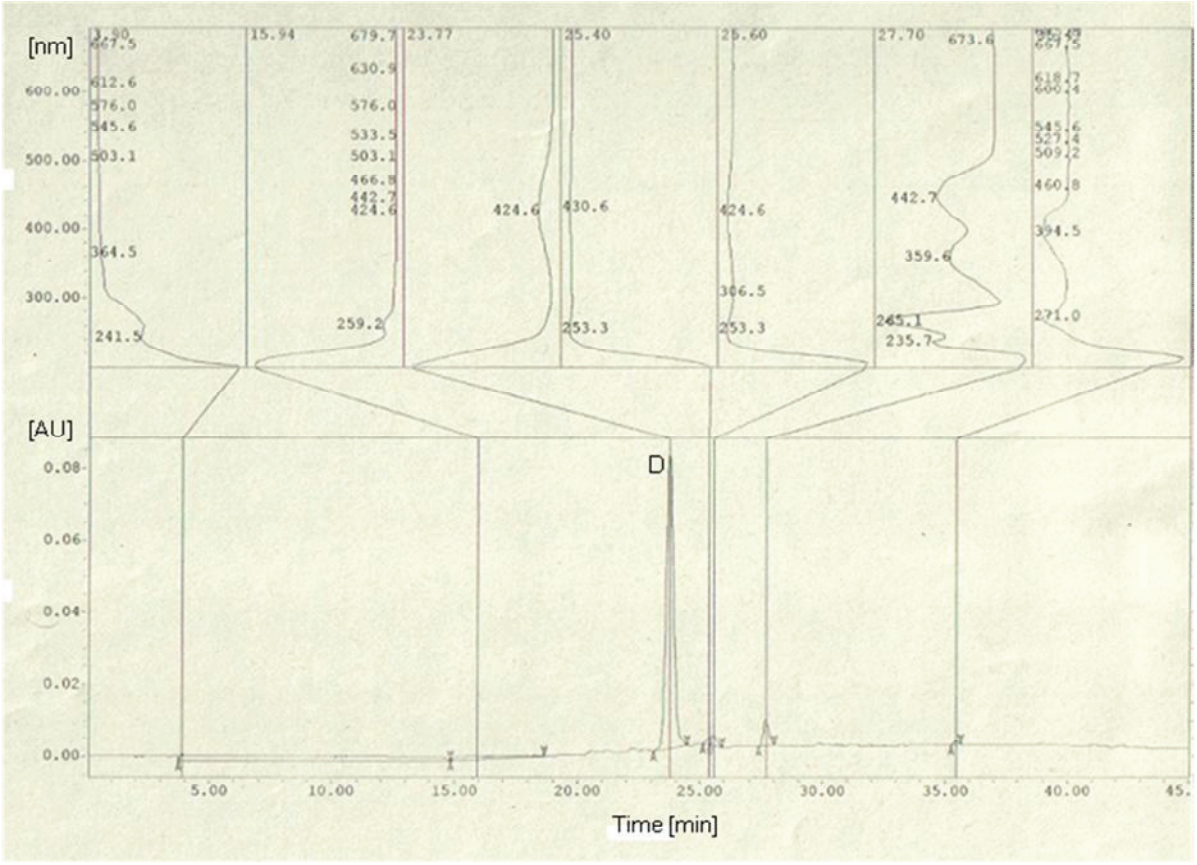

Figure 33: Analytical HPLC chromatogram of raw extract of *Tricholomopsis decora* with UV spectrum of peak D at λ = 425 nm.

In an attempt to separate the extract on a semi-preparative RP-18ec column, a small amount of an orange fraction was collected. This fraction when analysed by ^{1}H NMR was highly contaminated and had to be further purified. Purification over Sephadex LH-20 yielded no satisfactory results. An HPLC separation was then carried out at two different wavelengths at a time, 280 and 420 nm (Figure 34), so as to be able to exclude impurities occurring at a lower wavelength. Enough amount of compound D was thereby collected for MS measurements but not for NMR experiments. An attempt to record a ^{1}H NMR spectrum (Appendix A17) showed a compound with resonances in the aromatic region, present in too small quantity for any

characterization as compared to other impurities. For this reason, further NMR spectra were not recorded.

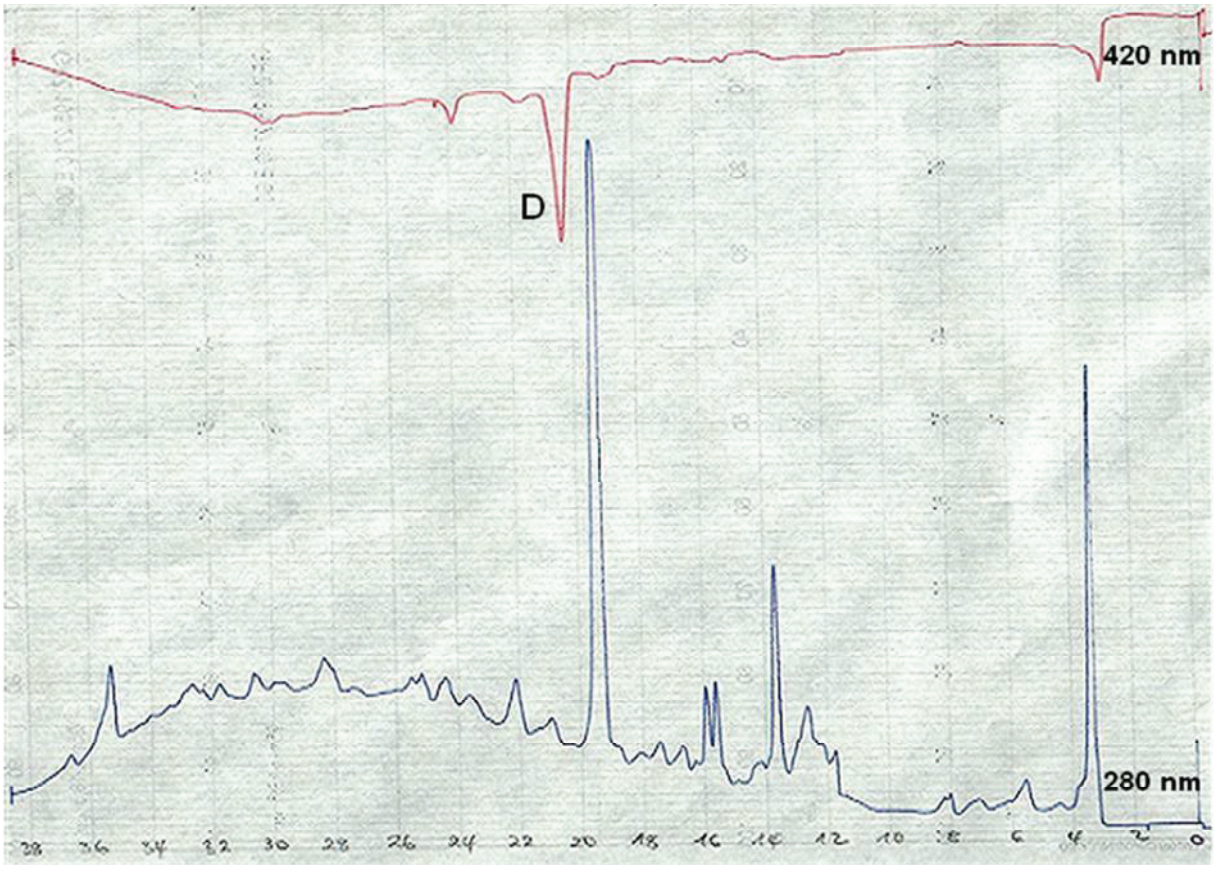

Figure 34: Semi-preparative HPLC chromatogram of raw extract of *Tricholomopsis decora* at λ = 280 and 420 nm.

The HR-(+)-ESI-MS exhibited an $[M+H]^+$ ion at *m/z* 804.3579. Generating the molecular formula from the obtained *m/z* value proved to be very challenging. The high molecular mass obtained for compound D highly increases the number of potential molecular formulas. More than 5000 possibilities were proposed by the molecular formula finder tool ChemCalc.[77] From the list proposed by the molecular formula generating software Xcalibur used for analysing the HR-(+)-ESI-MS measurements, six potential molecular formulas (Table 6) were retained for further consideration. In order to pick out the correct formula, the "seven golden rules for heuristic filtering of molecular formulas" [78] were applied.

Table 6: Potential molecular formulas for compound D

Nr.	Molecular formula $[M+H]^+$	*m/z*	Deviation (Δ) $[ppm]^+$
1	$C_{32}H_{56}N_9O_{11}P_2$	804.3569	1.1
2	$C_{35}H_{47}N_{15}O_6P$	804.3566	1.5
3	$C_{36}H_{60}N_3O_{13}P_2$	804.3596	– 2.3
4	$C_{37}H_{59}NO_{16}P$	804.3566	1.4
5	$C_{38}H_{55}N_5O_{12}P$	804.3579	– 0.2
6	$C_{40}H_{50}N_7O_{11}$	804.3563	1.8

These rules are summarized below for non-charged molecules:

i – restrict number of elements during formula generation,

ii – perform Lewis and Senior check,

iii – perform isotopic pattern filter,

iv – perform H / C ratio check,

v – perform N, O, P, S / C ratios check,

vi – perform H, N, O, P, S / C high probability ratios check,

vii – perform –TMS check for GC-MS if a silylation step is involved.

The number of carbon atoms was restricted by dividing the nominal mass of the neutral molecule 803 by 12. This gave the maximum number of carbon atoms to be expected. The number of nitrogen, sulphur, phosphorus and oxygen were all set at a maximum of 30. The isotopic pattern filter permitted the elimination of sulphur, since sulphur isotopic pattern was not observed. This was equally the case with halogens, whose isotopic patterns were not present. Applying the isotopic abundance patterns reduced the number of potential candidates. The H/C element ratio check applied to the various formulas gave results that were all good in the range of 0.5 to 2.0 typical for natural compounds. The heteroatom ratio check resulted to values mostly in the common regions of 0 – 1.3 for N/C, 0 – 1.2 for O/C and 0 – 0.3 for P/C. Rule number 7 (vii) was not taken into consideration since GC-MS experiments were not performed.

Taking into account these rules, molecular formula number 5 was picked out to be the most probable for compound D. The simulated *m/z* values of the formula number 5 and the measure values for compound D were most similar. Moreover, their isotopic patterns shown in Table 7 had the best match.

Table 7: Comparison of isotopic patterns of compound D with the generated molecular formula number 5.

Ion	Compound D		$C_{38}H_{55}N_5O_{12}P$	
	m/z	Relative abundance (%)	*m/z*	Relative abundance (%)
$[M+H]^+$	804.3579	100	804.3579	100
M+1	805.3599	41.18	805.3611	41.10
M+2	806.3621	10.50	806.3638	8.20

The HR-(+)-ESI-MS/MS (Figure 35) delivered fragments at *m/z* 786.3304, 690.2751, 542.1937 and 514.1991. The first and second fragments corresponds to the loss of the mass units 18.0275 and 114.0827, suggesting the dissociation of a water molecule and the amino acid ornithine respectively. It was then difficult to ascertain these suggestions, since the various formulas generated were not conclusive. The other fragments were too large and unspecific.

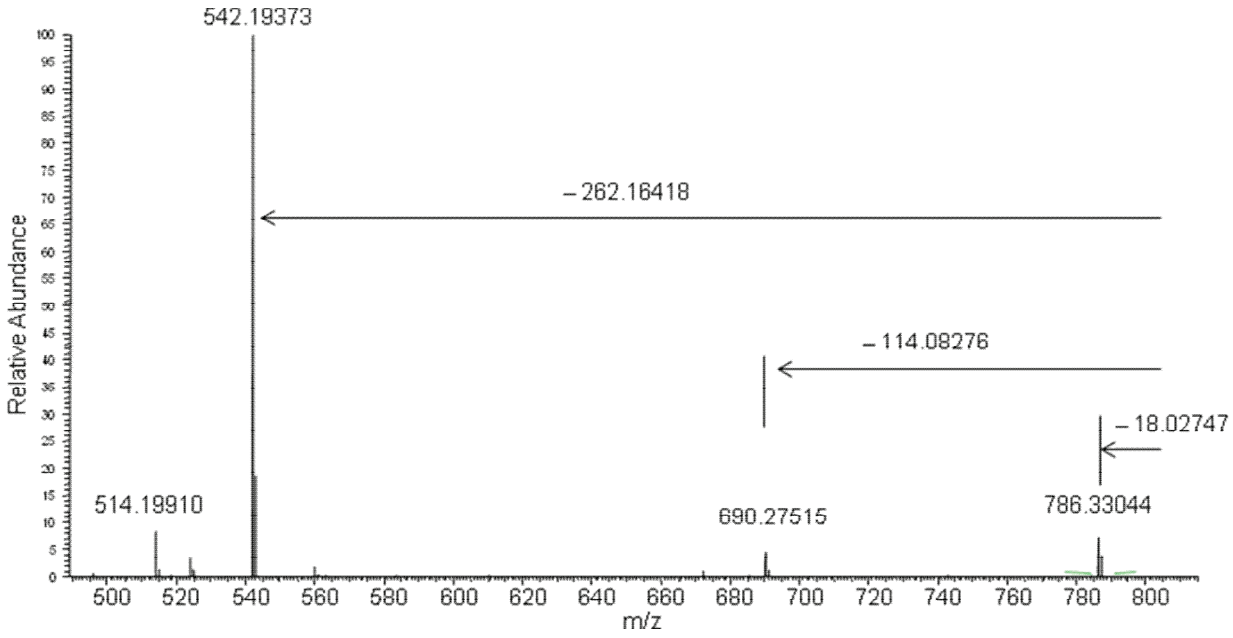

Figure 35: HR-(+)-ESI-MS/MS of compound D, parent ion *m/z* = 804.

Even though a well pronounced orange colour was observed, it should be noted that compound D is present in very small amount. This can be witnessed by observing the absorption band in the chromatogram (Figure 33), which is quite low. More of *Tricholomopsis decora* could unfortunately not be collected, as it was not found in the different excursions in the forest for mushroom harvesting. The isolation of enough amount of compound D for further characterisation entails extracting from much more than 50 g of fruiting bodies.

4.4 Conclusions

The orange pigment isolated from *Tricholomopsis decora* exhibited an $[M+H]^+$ ion at *m/z* 804.3579. This high molecular mass rendered the determination of the molecular formula difficult, since the number of potential formulas generally increases with the increase in molecular mass. Applying the "seven golden rules for heuristic filtering of molecular formulas" permitted the postulation of the molecular formula $C_{38}H_{55}N_5O_{12}P$. The very low yield obtained after the HPLC separation made the recording of NMR spectra unsuccessful. Further extraction was not possible due to lack of mushroom material. For further investigation, at least four to five times the amount of fungi used in this work would be needed.

VI OUTLOOK

Fungal secondary metabolites were mostly isolated from cultures in the past decades. Recently, the interest in the fruiting bodies of higher fungi is equally increasing, partly due to their successful mode of living.

In the scope of this work, new secondary metabolites were isolated from the fruiting bodies of higher fungi (Basidiomycetes) and in some cases, their structure was fully characterised. The structure of mycenarubin C, formerly isolated from *Mycena rosea* by Peters, was fully characterised after optimising the amount isolated from the fungi. Mycenarubin C, though inactive against the tested organisms, could exhibit antimalarial, antiviral or antitumor activity as other secondary metabolites with an eight-membered ring structure, isolated from marine sponges. Therefore, further tests should determine if mycenarubin C has any of these characteristics.

The chorismic acid derivatives **42** and **43**, isolated for the first time from the fruiting bodies of the higher fungus *Megacollybia platyphylla*, probably serve as potential sources for aromatic amino acids or protect the fungus from other species of bacteria than the tested organisms. Since compound **43** had been found to inhibit the enzyme *Serratia marcescens* anthranilate synthase, biological tests on bacteria of the *Serratia* genus would give more information on the activity of compounds **42** and **43**.

Compounds isolated from *Mycena epipterygia* and *Tricholomopsis decora* could not be characterised completely. In the case of *Mycena epipterygia*, compounds A and B could not be distinctly separated by HPLC, and the quantity of fruiting bodies for further trials was insufficient. The fruiting bodies of fungi are short-lived and cannot be cultivated. The quantity collected every season depends solely on nature. It is therefore possible to harvest a good quantity in a season, and find none the next season, even at the same spots. This creates the first difficulty in the screening of fruiting bodies of higher fungi. In order to obtain sufficient amounts of the compounds A and B for further experiments and full characterisation, large quantities of fruiting bodies would be required, since *Mycena epipterygia* is a small fungus. The extract was separated on an RP-18 column. Separation on RP-8, phenylhexyl and RP-NH_2 columns were equally non satisfactory. For further investigations, a two stage separation should be considered, first on an RP-18 column followed by a normal phase column. This method was used to separate *E*/*Z* isomers of benzoxepin fatty acid esters and could function as well to separate compounds A and B. Moreover, biological tests should determine any bactericidal, herbicidal or fungicidal activity, as fruiting bodies of *Mycena epipterygia* are hardly attacked by potential enemies. This would also give information about the interaction between the mushroom and its environment.

The orange pigment, compound D, was isolated from *Tricholomopsis decora* in so low yield that NMR experiments could not be run. With the help of HR-(+)-ESI-MS measurements and applying the golden rules for heuristic filtering of molecular formula, a molecular formula could be determined. Large quantities of fruiting bodies would be required to isolate enough of compound D for characterisation. When this is achieved, biological tests should give information about the ecological role of compound D.

VII EXPERIMENTAL SECTION

1 General

1.1 Chemicals

Methanol, HPLC grade, from VWR International GmbH.

Acetonitril, HPLC grade, from VWR International GmbH.

Acetic acid, Rotipuran 100 % *p.a*, from VWR International GmbH.

Deionised H_2O, from corresponding water supply.

Deuterated solvents

CD_3OD, 99.80 % atom D, from ABCR GmbH.

D_2O, 99.90 % atom D, from EURISO-Top.

DMSO, 99.80 % atom D, from EURISO-Top.

1.2 Equipment and Material

HPLC Analytical measurements were carried out on a unit consisting of two Waters 510 pumps equipped with an automated gradient controller and a Waters 996 photodiode array detector.

LC-MS experiments were performed on an Agilent 1100 HPLC system, equipped with a G1322A membrane degasser, a G1312A binary pump, a G1313A column oven and a G1315A photodiode array detector, coupled to a Thermo Fischer Scientific LCQ DecaXP Plus ESIMS spectrometer. Electrospray ionisation was carried out at atmospheric pressure. Detection of ions occurred in positive or negative mode. Nitrogen was used as sheath gas and Helium as collision gas for fragmentation in CID experiments.

Preparative and semi-preparative HPLC were performed on a unit consisting of two Waters 510 pumps equipped with an automated gradient controller and a Knauer Variable Wavelength UV/Vis detector.

HPLC separation columns

HPLC separations were performed on columns from Macherey-Nagel as follows:

Analytical:	Nucleodur C_{18} ec, 100 Å, 5 µm, 4.6 x 250 mm.
LC-MS:	Nucleodur C_{18} ec, 100 Å, 5 µm, 3 x 250 mm columns.
Semi-preparative:	Nucleodur C_{18} ec, 100 Å, 5 µm, 10 x 250 mm.
Preparative:	Nucleodur C_{18} ec, 100 Å, 5 µm, 21 x 250 mm.

Size Exclusion Chromatography (SEC)

SEC was performed on Sephadex LH-20 from Pharmacia Biotech. The separating material was allowed to swell in the eluent for at least 30 min prior to separation.

Centrifugation

Two different centrifuges were used depending on the volume of the extract to be centrifuged, Hettich Universal 16R cooling centrifuge and Heraus Biofuge 15.

Lyophilisation

Freeze-drying of aqueous samples was carried out on the lyophilisers Christalpha 1-2 and Christalpha 1-4, equipped with rotary vane pumps from Pfeiffer.

EI-MS EI-MS spectra were recorded on a double focusing sector mass spectrometer MAT 95 from Finnigan MAT.

HR-ESI-MS HR-ESI-MS and HR-ESI-MS/MS spectra were recorded on a Thermo Fisher Scientific LTQ Orbitrap mass spectrometer, coupled with an Ultimate type HPLC system from DIONEX. The spectra were recorded in positive mode (1 spectrum / s, mass range 50 – 1000) with a nominal mass resolving power of 60000 at *m/z* 400, with a scan rate of 1 Hz. Through automatic gain control high-accuracy mass measurements were achieved within 2 ppm deviation, using polydimethylcyclosiloxane ($[(CH_3)_2SiO]_6$, *m/z* 445.120025) as internal lock mass. Nitrogen served as sheath gas (6 arbitrary units), for fragmentation in CID experiments helium served as collision gas.

NMR

All spectra were recorded on a BRUKER Avance DRX-600 spectrometer, equipped with a HCN-5mm inverse probe head (^{1}H-measurements) or CH-5mm dual probe head (^{13}C-measurements) (^{1}H resonance frequency at 600.22 MHz, ^{13}C resonance frequency at 151 MHz). The residual proton chemical shift of the solvents (Table 6) was used to reference the spectra, the reference signal for samples measured in D_2O being calculated from equation 2 for measurements at 330 K, and equation 3 for measurements at 300 K. [79]

$$\delta = 5.060 - 0.0122T + (2.11 \times 10^{-5})T^2 \quad (2)$$

$$\delta = 5.051 - 0.0111 \times T \quad (3)$$

where T = temperature in °C.

Referencing ^{13}C spectra in D_2O was achieved using carbon resonance from the HSQC spectrum. All chemical shifts are expressed in ppm.

Table 6: Reference signals of NMR solvents.

Solvent	δ_H	δ_C
D_2O	4.43 ppm (330 K)	-
	4.75 ppm (300 K)	-
CD_3OD	3.31 ppm	49.00 ppm
d_6-DMSO	2.50 ppm	39.52 ppm

Solid Phase Extraction (SPE)

Ready-made polypropylene columns with C_{18} or C_{18}ec phases from AGILENT (Varian Bond Elut) and MACHEREY-NAGEL (Chromabond) were used. The cartridges were conditioned before use with three column volumes each of H_2O, followed by a H_2O–MeOH (50:50) solution, then MeOH and reversed till finally H_2O again.

1.3 Medium for Biological Evaluation

Two different media were used for the cultivation of bacteria. The media were sterilized at 121 °C for 15 min, immediately after which 25 – 35 mL were transferred into Petri dishes (90 mm diameter, SARSTET) under sterile conditions and allowed to cool.

Malt Peptone Agar

Malt extract	30 g
Peptone	3 g
Agar	15 g
Distilled water	1000 mL

LB Broth

Tryptone	10 g
Yeast extract	5 g
Sodium chloride	5 g
Agar	15 g
Distilled water	1000 mL

Herbicidal Activity

To test herbicidal activity, ca. 0.4 g of cotton balls were placed in glass containers before being sterilized together with the lids at 121 °C for 15 min. After cooling, the glass containers were closed and kept under sterile conditions.

2 Experimental Data of Compounds Isolated from *Mycena rosea*

2.1 Mushroom Material

Fruiting bodies of *M. rosea* were collected in September and October 2011, 2012 and 2015 from Mühltal near Starnberg in Bavaria, and Bad Fallingbostel near Walsrode in Lower Saxony. After quick-freezing with liquid nitrogen, they were stored at – 35 °C.

2.2 Extraction and Isolation

60 g of frozen caps were extracted first with 200 mL MeOH for 10 min, then with 50 mL of a H_2O-MeOH solution (50/50) for 5 min. After filtration, the filtrate was concentrated in vacuo at room temperature. The raw extract was dissolved in 3 mL H_2O-MeOH (50/50) and centrifuged at 15000 rpm and 25 °C for 5 min. The supernatant was prepurified on a C_{18}ec cartridge, first with water as eluent, followed by H_2O-MeOH (50/50), and finally MeOH. The water-methanol and methanol fractions were reunited, concentrated and separated by preparative HPLC on an RP-18ec column, at a flow rate of 10 mL/min, with UV detection at 360 nm. The extract of ca. 14 g of mushroom caps was separated per run.

Gradient:

LC-MS (0.55 mL/min)

Time	% H_2O	% MeOH
0	100	0
5	100	0
45	0	100

Preparative HPLC

Time	% H_2O	% MeOH
0	100	0
5	100	0
35	50	50
40	0	100

2.3 Evidence of Mycenarubin A

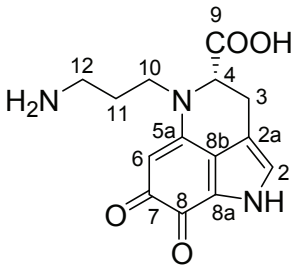

31

Yield not determined

HPLC t_R = 14.8 min (analytical),

t_R = 21.8 min (preparative)

UV/Vis λ_{max} = 242, 356, 536 nm

LCESIMS *m/z* = 290 $[M + H]^+$

LCESIMS/MS (parent ion *m/z* = 290, 35 eV): *m/z* = 246 $[M + H - CO_2]^+$, 217 $[M + H - CO_2 - (CH_2{=}NH)]^+$, 203 $[M + H - CO_2 - (C_2H_5N)]^+$, 189 $[M + H - CO_2 - (C_3H_7N)]^+$

2.4 Mycenarubin C

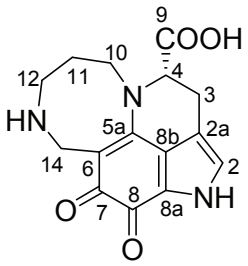

33

Yield 14 mg (0.023 % from 60 g) red solid

HPLC t_R = 16.6 min (analytical)
t_R = 23.6 min (preparative)

UV/Vis λ_{max} = 248, 362, 530 nm

^{1}H NMR (600 MHz, D_2O, 330 K): δ_H = 7.12 (s, 1 H, H-2), 4.63 (d, 1 H, *J* = 15.3 Hz, H_a-14), 4.47 (d, 1 H, *J* = 15.3 Hz, H_b-14), 4.31 (dd, 1 H, *J* = 2.9, 5.7 Hz, H-4), 4.18 (br, 1 H, H_b-10), 3.99 (br, 1 H, H_a-10), 3.58 (m, 1 H, H_a-12), 3.22 (dd, 1 H, *J* = 3.7, 6.9 Hz, H_b-12), 3.20 (m, 1 H, H-3), 2.28 (m, 1 H, H_a-11), 2.23 (m, 1 H, H_b-11)

^{13}C NMR (151 MHz, D_2O, 330 K): δ_C = 181.9 (C-7), 178.7 (C-9), 171.4 (C-8), 159.4 (C-5a), 128.7 (C-2), 127.8 (C-8b), 126.5 (C-8a), 119.6 (C-2a), 97.7 (C-6), 72.8 (C-4), 54.0 (C-10), 42.5 (C-14), 41.2 (C-12), 27.5 (C-11), 26.2 (C-3)

ESIMS *m/z* = 302 $[M + H]^+$, 603 $[2M + H]^+$

ESIMS/MS (parent ion *m/z* = 302, 35 eV): *m/z* = 273 $[M + H - (CH_2NH)]^+$, 258 $[M + H - CO_2]^+$, 229 $[M + H - CO_2 - (CH_2NH)]^+$, 215 $[M + H - CO_2 - (C_2H_5N)]^+$

2.5 Synthesis of Mycenarubin C from Mycenarubin A

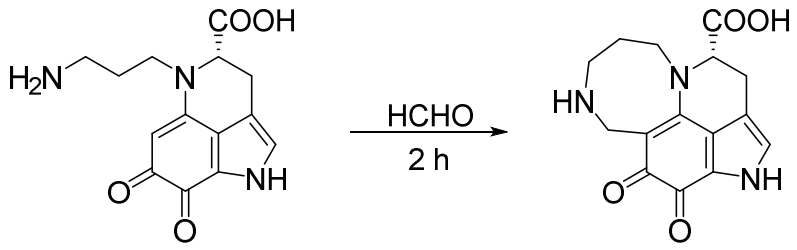

31 **33**

60 g of frozen caps were extracted first with 200 mL MeOH for 10 min, then with 50 mL of a H_2O-MeOH solution (50/50) for 5 min. After filtration and concentration in vacuo at room temperature, 0.5 mL of a 37 % formaldehyde solution was added to the raw extract and stirred for 2 h. The solution was again concentrated in vacuo and prepurified with a C_{18} cartridge. The preparative HPLC separation then followed on an RP-18ec column with UV detection at 360 nm.

2.6 Biological Tests

For plate diffusion assays, 0.5 mg (1.66 µmol) and 1 mg (3.32 µmol) each of **33** was dissolved in distilled and sterilized water, and dropped on paper discs (ø 6 mm, thickness 0.5 mm). The paper discs, after drying under sterile conditions, were placed on agar plates inoculated with test organisms (*Escherichia coli*, *Bacillus subtilis* and *Staphylococus capitis*) and incubated at 37 °C for 24 h. These plates were then compared with those having no other substance on the paper discs but water (negative test), and those with Gentamicin (positive test).

3 Experimental Data of Compounds Isolated from *Mycena epipterygia*

3.1 Mushroom Material

Fruiting bodies of *M. epipterygia* were collected in September and October 2013, 2014 and 2015 from Mühltal near Starnberg in Bavaria, Welle and Holm-Seppensen in Lower Saxony. They were quick-frozen using liquid nitrogen and stored at – 35 °C.

3.2 Extraction and Isolation

50 g fruiting bodies were extracted with 200 mL MeOH for 20 min, then with 50 mL of a H_2O-MeOH solution (50/50) for 10 min. After filtration and concentration under vacuo at 25 °C, the yellow-brown raw extract was dissolved in 2 mL H_2O-MeOH (50/50), before being prepurified on a C_{18} cartridge. It was eluted first with water, followed by H_2O-MeOH (50/50) and finally MeOH. The water-methanol and methanol fractions were reunited since they were both coloured yellow. The subsequent HPLC separation was carried out on an RP-18ec column, at a flow rate of 1 mL/min for analytical and 5 mL/min for semi-preparative separation. UV detection was set at 410 nm.

Gradient:

Analytical HPLC

Time	% H_2O (+0.1 % HOAc)	% MeOH
0	100	0
5	100	0
45	0	100

Semi-preparative HPLC

Time	% H_2O (+0.1 % HOAc)	% MeOH
0	100	0
10	50	50
40	0	100

3.3 Compound A

Yield not determined

HPLC t_R = 37.5 min (analytical)
t_R = 21.3 min (semi-preparative)

UV/Vis λ_{max} = 295, 395, 412 nm

HRESIMS *m/z* = 317.1019 $[M + H]^+$ (calculated for $C_{17}H_{17}O_6$ 317.1025, Δ = – 0.20 ppm), 334.1284 $[M + NH_4]^+$ (calculated for $C_{17}H_{20}O_6N$ 317.1291)

HRESIMS/MS (parent ion *m/z* = 317, 35 eV): *m/z* (%) = 299.0913 (100) $[M + H – H_2O]^+$ (calculated for $C_{17}H_{15}O_5$ 299.0919, Δ = – 0.30 ppm), 281.0807 (50) $[M + H – 2H_2O]^+$ (calculated for $C_{17}H_{13}O_4$ 281.0814, Δ = – 0.30 ppm), 271.0964 (10) $[M + H – H_2O – CO]^+$ (calculated for $C_{16}H_{15}O_4$ 271.0970, Δ = – 0.43 ppm), 263.0702 (11) $[M + H – 3H_2O]^+$ (calculated for $C_{17}H_{11}O_3$ 263.0708, Δ = – 0.31 ppm), 253.0859 (37) $[M + H – 2H_2O – CO]^+$ (calculated for $C_{16}H_{13}O_3$ 253.0865, Δ = – 0.12 ppm), 239.0703 (75) $[M + H – 2H_2O – CH_2CO]^+$ (calculated for $C_{15}H_{11}O_3$ 239.0708, Δ = – 0.21 ppm), 211.0753 (9) (calculated for $C_{14}H_{11}O_2$ 211.0759, Δ = 0.16 ppm), 195.0806 (12) (calculated for $C_{14}H_{11}O$ 195.0809), 183.0805 (2) (calculated for $C_{13}H_{11}O$ 183.0809).

^{1}H NMR (600 MHz, CD_3OD, 300 K): δ_H = 7.30 (t), 6.96 (m), 6.71 (m), 6.58, 6.58, 6.55, 6.54, 6.52, 6.04 (s), 5.93 (d, *J* = 15.1 Hz), 5.65 (d, *J* = 8.1 Hz), 2.92 (t), 2.38 (m).

^{13}C NMR (151 MHz, CD_3OD, 300 K): δ_C = 145.21, 141.07, 140.66, 140.00, 137.21, 136.65, 134.72, 133.14, 123.68, 122.93, 114.97, 81.24, 41.46.

3.4 Compound B

Yield not determined

HPLC t_R = 38.0 min (analytical)
t_R = 25.9 min (semi-preparative)

UV/Vis λ_{max} = 295, 395 nm

HRESIMS *m/z* = 317.1019 $[M + H]^+$ (calculated for $C_{17}H_{17}O_6$ 317.1025, Δ = – 0.20 ppm)

HRESIMS/MS (parent ion *m/z* = 317, 35 eV): *m/z* (%) = 299.0913 (100) $[M + H – H_2O]^+$ (calculated for $C_{17}H_{15}O_5$ 299.0919, Δ = – 0.30 ppm), 281.0807 (50) $[M + H – 2H_2O]^+$ (calculated for $C_{17}H_{13}O_4$ 281.0814, Δ = – 0.30 ppm), 271.0964 (10) $[M + H – H_2O – CO]^+$ (calculated for $C_{16}H_{15}O_4$ 271.0970, Δ = – 0.43 ppm), 263.0702 (11) $[M + H – 3H_2O]^+$ (calculated for $C_{17}H_{11}O_3$ 263.0708, Δ = – 0.31 ppm), 253.0859 (37) $[M + H – 2H_2O – CO]^+$ (calculated for $C_{16}H_{13}O_3$ 253.0865, Δ = – 0.12 ppm), 239.0703 (75) $[M + H – 2H_2O – CH_2CO]^+$ (calculated for $C_{15}H_{11}O_3$ 239.0708, Δ = – 0.21 ppm), 211.0753 (9) (calculated for $C_{14}H_{11}O_2$ 211.0759, Δ = 0.16 ppm), 195.0806 (12) (calculated for $C_{14}H_{11}O$ 195.0809), 183.0805 (2) (calculated for $C_{13}H_{11}O$ 183.0809).

4 Experimental Data of Compounds Isolated from *Megacollybia platyphylla*

4.1 Mushroom Material

Fruiting bodies of *M. platyphylla* were collected in September and October 2011, 2012 and 2015 from Mühltal near Starnberg in Bavaria, and Bad Fallingbostel near Walsrode in Lower Saxony. They were quick-frozen using liquid nitrogen before being stored at – 35 °C.

4.2 Extraction and Isolation

50 g of fresh fruiting bodies were extracted with 200 mL H_2O-MeOH (50/50) for 30 min. After filtration and concentration in vacuo at 25 °C, the raw extract was dissolved in 5 mL H_2O-MeOH (50/50) and centrifuged at 4000 rpm for 5 min. The supernatant was concentrated and then prepurified over a C_{18} cartridge. The analytical HPLC was run at a flow rate of 1 mL/min and the semi-preparative separation followed on an RP-18ec column with UV detection at 270 nm, at a flow rate of 5 mL/min. The extract of 12.5 g of mushrooms was separated per run.
Gradient:
Analytical HPLC

Time	% H_2O (+0.1 % HOAc)	% MeOH
0	100	0
5	100	0
55	0	100

Semi-preparative HPLC

Time	% H_2O (+0.1 % HOAc)	% MeOH
0	100	0
5	100	0
45	0	100

4.3 3-(1-Carboxyvinyloxy)-5-hydroxy-4-methoxybenzoic acid

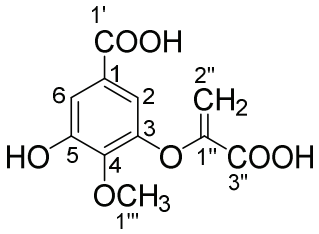

42

Yield 4.1 mg (0.0082 %) from 50 g fresh mushrooms, off-white solid

HPLC t_R = 47.9 min (analytical)
t_R = 29.2 min (semi-preparative)

UV/Vis λ_{max} = 220, 252, 294 nm

^{1}H NMR (600 MHz, DMSO, 300 K): δ_H = 9.90 (br, 1 H, OH), 7.24 (d, 1 H, *J* = 2.1 Hz, H-6), 6.94 (d, 1 H, *J* = 2.1 Hz, H-2), 4.99 (d, 1 H, *J* = 2.0 Hz, H_a-2''), 5.67 (d, 1 H, *J* = 2.0 Hz, H_b-2''), 3.78 (s, 3 H, H-1''').

^{13}C NMR (151 MHz, DMSO, 300 K) δ_C = 166.4 (C-1'), 163.1 (C-3''), 151.2 (C-5), 150.2 (C-1''), 148.6 (C-3), 142.0 (C-4), 125.9 (C-1), 113.0 (C-6), 110.2 (C-2), 104.8 (C-2''), 59.9 (C-1''')

HRESIMS *m/z* = 255.0499 $[M + H]^+$ (calculated for $C_{11}H_{11}O_7$ 255.0505, Δ = 0.08 ppm), 272.0766 $[M + NH_4]^+$ (calculated for $C_{11}H_{14}O_7N$ 272.0770, Δ = 0.28 ppm), 277.0318 $[M + Na]^+$ (calculated for $C_{11}H_{10}O_7Na$ 277.0324, Δ = – 0.10 ppm)

HRESIMSMS (parent ion *m/z* = 255, 35 eV) *m/z* (%) = 237.0393 (80) $[M + H – H_2O]^+$ (calculated for $C_{11}H_9O_6$ 237.0399, Δ = – 0.43 ppm), 219.0287 (100) $[M + H – 2H_2O]^+$ (calculated for $C_{11}H_7O_5$ 219.0293, Δ = – 0.36 ppm), 209.0444 $[M + H – H_2O – CO]^+$ (calculated for $C_{10}H_9O_5$ 209.0450, Δ = – 0.452 ppm), 149.0233 (calculated for $C_8H_5O_3$ 149.0238, Δ = – 0.36 ppm)

4.4 3-(1-Carboxyvinyloxy)-4, 5-dihydroxybenzoic acid

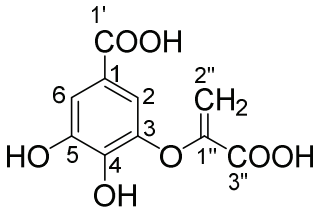

43

Yield 14.4 mg (0.0288 %) from 50 g fresh mushrooms, off-white solid

HPLC t_R = 43.9 min (analytical)
t_R = 25.5 min (semi-preparative)

UV/Vis λ_{max} = 220, 265 nm

^{1}H NMR (600 MHz, D_2O, 300 K): δ_H = 7.34 (d, 1 H *J* = 1.9 Hz, H-6), 7.26 (d, 1 H, *J* = 1.9 Hz, H-2), 5.43 (d, 1 H, *J* = 1.9 Hz, H_b-2''), 4.70 (d, 1 H, *J* = 1.9 Hz, H_a-2'')

^{13}C NMR (151 MHz, D_2O, 300 K): δ_C = 169.9 (C-1'), 168.4 (C-3''), 152.9 (C-1''), 144.9 (C-5), 142.4 (C-3), 140.6 (C-4), 121.6 (C-1), 114.2 (C-2), 113.2 (C-6), 99.9 (C-2'')

ESIMS *m/z* = 239. $[M - H]^-$

ESIMS/MS (parent ion *m/z* = 239, 35 eV) *m/z* (%) = 211 (5) $[M - H - CO]^-$, 195 (100) $[M - H - CO_2]^-$, 169 (10), 151 (15) $[M - H - 2CO_2]^-$

4.5 Biological Tests

For plate diffusion assays, 0.5 mg and 1 mg of **42** and **43** was dissolved in 1 mL distilled and sterilized water each, and dropped on paper discs (ø 6 mm, thickness 0.5 mm). The paper discs, after drying under sterile conditions, were placed on agar plates inoculated with test organisms (*Escherichia coli*, *Bacillus subtilis* and *Staphylococus capitis*) and incubated at 37 °C for 24 h. The plates were then compared with other plates having no other substance on the paper discs but water (negative test) and those having Gentamicin (positive test).

In order to test herbicidal activity, 1 mg of **42** and **43** was dissolved in 1 mL of distilled and sterilized water each, and the solution was used to moisturize cotton balls in glass containers.

Five seeds of *Lepidium sativum* were then placed on each cotton ball in a glass container closed with a lid, and their growth was monitored for seven days at 25 °C. The weight of the seedlings was then measured as well as their length, and compared to seeds grown on cotton balls moisturized only with water.

5 Experimental Data of Compounds Isolated from *Tricholomopsis decora*

5.1 Mushroom Material

Fruiting bodies were collected in September 2012 and 2013 from the mushroom exhibition in Munich, Bavaria and stored at – 35 °C after quick-freezing with liquid nitrogen.

5.2 Extraction and Isolation

50 g of frozen fruiting bodies were extracted with a H_2O-MeOH solution (50/50) untill no more colouration was observed. The combined extract was then concentrated in vacuo at room temperature. The resulting orange-brown residue was dissolved in 5 mL water and prepurified on a C_{18} cartridge, with water as eluent, followed by a H_2O-MeOH solution (50/50), then MeOH. The H_2O-MeOH and MeOH fractions were reunited and concentrated. The subsequent HPLC separation on an RP-18ec analytical column showed a compound with absorbance at λ_{max} = 424 nm. The semi-preparative separation was carried out at flow rate 4 mL/min with double UV detection at 280 and 425 nm.

Gradient:

Time	% MeOH
0	0
5	0
45	100

5.3 Compound D

Yield not determined

HPLC t_R = 23.8 min (analytical)
t_R = 20.5 min (semi-preparative)

UV/Vis λ_{max} = 424 nm

HRESIMS *m/z* = 804.3579 $[M + H]^+$ (calculated for $C_{38}H_{54}N_5O_6P$ 804.3585, Δ = – 0.20 ppm)

HRESIMS/MS (parent ion *m/z* = 804, 35 eV): *m/z* (%) = 786.3304 (7 %), 690.2751 (5 %), 542.1937 (100 %), 514.1991 (8 %)

VIII REFERENCES

[1] D. A. Dias, S. Urban, U. Roessner, *Metabolites* **2012**, *2*, 303–336.

[2] D. J. Newman, G. M. Cragg, *J. Nat. Prod.* **2007**, *70*, 461–477.

[3] D. J. Newman, G. M. Cragg, K. M. Snader, *J. Nat. Prod.* **2003**, *66*, 1022–1037.

[4] K. C. Nicolaou, T. Montagnon, *Molecules that changed the world*, Wiley-VCh Verlag GmbH, **2008**.

[5] H. Sauter, W. Steglich, T. Anke, *Angew. Chem.* **1999**, *111*, 1416–1438.

[6] T. Anke, F. Oberwinkler, W. Steglich, G. Schramm, *J. Antibiot*. **1977**, *30*, 806–810.

[7] P. Spiteller, *Higher Fungi – A Treasure Trove of Highly Diverse Natural Products and New Chemical Defence Mechanisms.*

[8] E. Thines, R. Weber, *Vorbild Natur* **2007**, 59–63.

[9] N. P. O. Green, G. W. Stout, D. J. Taylor, *Biological Science* (Ed.: R. Soper), Cambridge University Press, **1995**.

[10] J. Velíšek, K. Cejpek, *Czech J. Food Sci*. **2011**, *29*, 87–102.

[11] V. Tzin, G. Galili, *ASPB*: *The Arabidopsis Book,* **2010**, 1–18.

[12] A. R. Knaggs, *Nat. Prod. Rep*. **2000**, *17*, 269–292.

[13] F. Lingens, *Angew. Chem. Int. Ed*. **1968**, *7*, 350–360.

[14] P. M. Dewick, *Medicinal Natural Products: A Biosynthetic Approach*, John Wiley and Son, West Sussex, UK, **2002**.

[15] T. Pusztahelyi, I. J. Holb, I. Pócsi, *Front. Plant Sci.* **2015**, *6*, 1–23.

[16] E. Perez-Nadales et al., *Fungal Genet. Biol.* **2014***, 70*, 42–67.

[17] D. H. Scharf, T. Heinekamp, A. A. Brakhage, *PloS Pathog.* **2014**, *10*, 1–3.

[18] A. A. L. Gunatilaka, “Fungal secondary metabolites” in a*ccess-science.com*, *Research Review*, **2010**.

[19] N. P. Keller, G. Turner, J. W. Bennet, *Nat. Rev. Microbiol.* **2005**, *3*, 937–947.

[20] A. A. L. Gunatilaka, E. M. K. Wijeratne, “Natural Products from Bacteria and Fungi” in *UNESCO Encyclopedia of Life Support Systems, Phytochemistry & Pharmocognosy* (Eds.: J. M. Pezutto, M. J. Kato), UNESCO Press, **2012**.

[21] S. M. Colegate, R. J. Molyneux, *Bioactive Natural Products: Detection, Isolation and Structural Determination*, CRC Press, Taylor & Francis Group, **2008**.

[22] M. Lucker, *Secondary Metabolism in Microorganisms, Plants, and Animals*, Springer-Verlag, Berlin Heidelberg GmbH, **1990**.

[23] T. Hartmann, *Proc. Natl. Acad. Sci.* **2008**, *105*, 4541–4546.

[24] J. Mann, *Murder, Magic, and Medicine,* Oxford University Press, New York, **1994**.

[25] S. A. S. Mapari, K. F. Nielsen, T. O. Larsen, J. C. Frisvad, A. S. Meyer, U. Thrane, *Curr. Opin. Biotechnol.* **2005**, *16*, 231–238.

[26] F. A. Nagia, R. S. R. EL-Mohamedy, *Dyes Pigments* **2007**, *75*, 550–555.

[27] P. Velmurugan, S. Kamala-Kannan, V. Balachandar, P. Lakshmanaperumalsamy, J.-C. Chae, B.-T. Oh, *Carbohyd. Polym.* **2010**, *79*, 262–268.

[28] J. Marqua, S. Formánek, *Der Tintling* **2010**, *65*, 24–30.

[29] P. Feeny, *Herbivores: Their Interactions with Secondary Metabolites,* Academic, San Diego, **1992**.

[30] D. Spiteller, “Chemical Defense Strategies of Plants” in *Encyclopedia of Ecology* (Eds.: S. E. Jorgensen, B. Fath), Elsevier, **2008**.

[31] M. Wink, “Occurrence and Function of Natural Products in Plants” in *UNESCO EOLSS, Phytochemistry & Pharmocognosy* (Eds. J. M. Pezutto, M. J. Kato), UNESCO Press, **2012**.

[32] J. B. Harborne, “Plant Chemical Ecology” in *Comprehensive Natural Products Chemistry* (Eds. D. Barton, K. Nakanishi, O. Meth-Cohn; Vol. Ed.: K. Mori), Elsevier, **1999**.

[33] U. Wittstock, J. Gershenzon, *Curr. Opin. Plant Biol.* **2002**, *5*, 1–8.

[34] N. Theis, M. Lerdau, *Int. J. Plant Sci.* **2003,** *164*, S93–S103.

[35] M. Kettering, D. Weber, O. Sterner, T. Anke, *Biospektrum* **2004**, *2*, 147–149.

[36] P. Spiteller, *Chem. Eur. J*. **2008**, *14*, 9100–9110.

[37] T. Anke, *Can. J. Bot*. **1995**, *73 (S1)*, 940–945.

[38] L. Ryan, “Plants and Their Defense Mechanisms” in *Landscapes*, summer **2004**.

[39] D. Michelot, L. M. Melendez-Howell, *Mycol. Res*. **2003**, *107*, 131–146.

[40] W. Steglich, L. Kopanski, M. Wolf, M. Moser, G. Tegtmeyer, *Tetrahedron Lett*. **1984**, *25*, 2341–2344.

[41] O. Sterner, B. Stefan, W. Steglich, *Tetrahedron* **1987**, *43*, 1075–1082.

[42] D. Hamprecht, J. Josten, W. Steglich, *Tetrahedron* **1996**, *53*, 10883–10902.

[43] P. Spiteller, D. Hamprecht, W. Steglich, *J. Am. Chem. Soc.* **2001**, *123,* 4837–4838.

[44] S. Peters, R. J. R. Jaeger, P. Spiteller, *Eur. J. Org. Chem*. **2008**, 1187–1194.

[45] B. L. J. Kindler, P. Spiteller, *Angew. Chem*. **2007**, *119*, 8222–8224; *Angew. Chem*. *Int. Ed*. **2007**, *46*, 8076–8078.

[46] J. Caspar, P. Spiteller, *ChemBioChem*. **2015**, *16*, 570–573.

[47] O. Sterner, R. Bergman, J. Kihlberg, B. Wickberg, *J. Nat. Prod*. **1985**, *48*, 279–288.

[48] P. Spiteller, *Nat. Prod. Rep.* **2015**, *32*, 971–993.

[49] K. L.-C. Wang, H. Li, J. R. Ecker, *Plant Cell* **2002**, S131–S151.

[50] B. Schulze, C. Kost, G.-I. Arimura, W. Boland, *ChiuZ.* **2006**, *40*, 366–377.

[51] V. A. Halim, A. Vess, D. Scheel, S. Rosahl, *Plant. Biol*. **2006**, *8*, 307–313.

[52] H. Grisebach, J. Ebel, *Angew. Chem*. **1978**, *90*, 668–681; *Angew. Chem. Int. Ed*. **1978**, *17*, 635–647.

[53] M. Kettering, O. Sterner, T. Anke, *Z. Naturforsch.* **2004**, *59C*, 816–823.

[54] “Recommended English Names for Fungi in the UK”, *British Mycological Society*.

[55] G. Robich, *Mycena d'Europa*, Associazione Micologica Bresadola,Trento, **2003**.

[56] www.pilz-baden.ch/galerie/deutsch/helmling-90/rosa_rettich-helmling-265, as at: 26.10.2017

[57] S. Breheret, T. Talou, S. Rapior, J. – M. Bessiere, *Cryptogamie, Mycol.* **1997**, *18*, 111–114.

[58] S. Peters, *Dissertation*, Technische Universität München, **2007**.

[59] S. Peters, P. Spiteller, *Eur. J. Org. Chem.* **2007**, 1571–1576.

[60] C. Baumann, M. Bröckelmann, B. Fugmann, B. Steffan, W. Steglich, W. S. Sheldrick, *Angew. Chem*. **1993**, *105*, 1120–1121, *Angew. Chem. Int. Ed.* **1993**, *32*, 1087–1089.

[61] S. Peters, R. J. R. Jaeger, P. Spiteller, *Eur. J.Org. Chem.* **2008**, 319–323.

[62] S. Peters, P. Spiteller, *J. Nat. Prod.* **2007**, *70*, 1274–1277.

[63] A. Pulte, S. Wagner, H. Kogler, P. Spiteller, *J. Nat. Prod*. **2016**, *79*, 873–878.

[64] E. M. Antunes, B. R. Copp, M. T. Davies-Coleman, T. Samaai, *Nat. Prod. Rep.* **2005**, *22*, 62–72.

[65] M. El-Naggar, R. J. Capon, *J. Nat. Prod.* **2009**, *72*, 460–464.

[66] E. Fattorusso, O. Taglialatela-Scafoti, *Mar. Drugs* **2009**, *7*, 130–152.

[67] K. V. Rao, M. S. Donia, J. Peng, E. Garcia-Palomero, D. Alonso, A. Martinez, M. Medina, S. G. Franzblau, B. L. Tekwani, S. I. Khan, S. Wahyuono, K. L. Willett, M. T. Hamann, *J. Nat. Prod.* **2006**, *69*, 1034–1040.

[68] J. Kobayashi, D. Watanabe, N. Kawasaki, M. Tsuda, *J. Org. Chem.* **1997**, *62*, 9236–9239.

[69] J. Lohmann, *Masterarbeit*, Universität Bremen, **2014**.

[70] H. E. Laux, *Der große Kosmos Pilzführer*, Franckh-Kosmos Verlags-GmbH & Co., Stuttgart, **2010**.

[71] H. Vahidi, F. Namjoyan, *IJPR* **2004**, *2*, 115–117.

[72] V. Pujol, V. Seux, J. Villard, *Ann*. *Pharm*. *Fr*. **1990**, *48*, 17–22.

[73] A. Manos-Turvey, E. M. M. Bulloch, P. J. Rutledge, E. N. Baker, J. S. Lott, R. J. Payne, *ChemMedChem* **2010**, *5*, 1067–1079.

[74] A. Arnone, R. Cardillo, G. Nasini, O. V. De Pava, *Tetrahedron* **1993**, *49*, 7251–7258.

[75] S. Kobayashi, T. Ozawa, H. Imagawa, *Agric. Biol. Chem*. **1982**, *46*, 845–847.

[76] www.norwegen-freunde.com/sopp/gfx/kalender/holzritterling_oliv2.jpg, stand: 26.10.2017.

[77] www.chemcalc.org/mf_finder

[78] T. Kind, O. Fiehn, *BMC Bioinformatics* **2007**, *8*, 105.

[79] H. E. Gottlieb, V. Kotlyar, A. Nudelman, *J. Org. Chem.* **1997**, *62,* 7512–7515.

IX APPENDIX

Mycenarubin C (33)

A1 Preparative HPLC chromatogram of raw extract of *Mycena rosea* at detection λ = 360 nm.

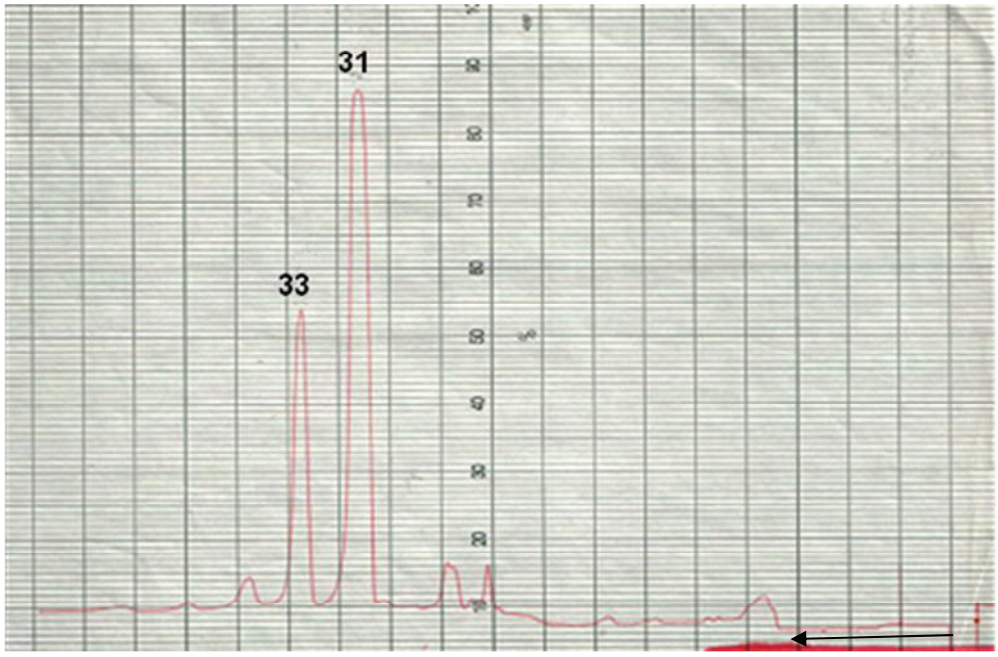

A2 ^{1}H NMR spectrum (600 MHz, D_2O, 330 K) of mycenarubin C.

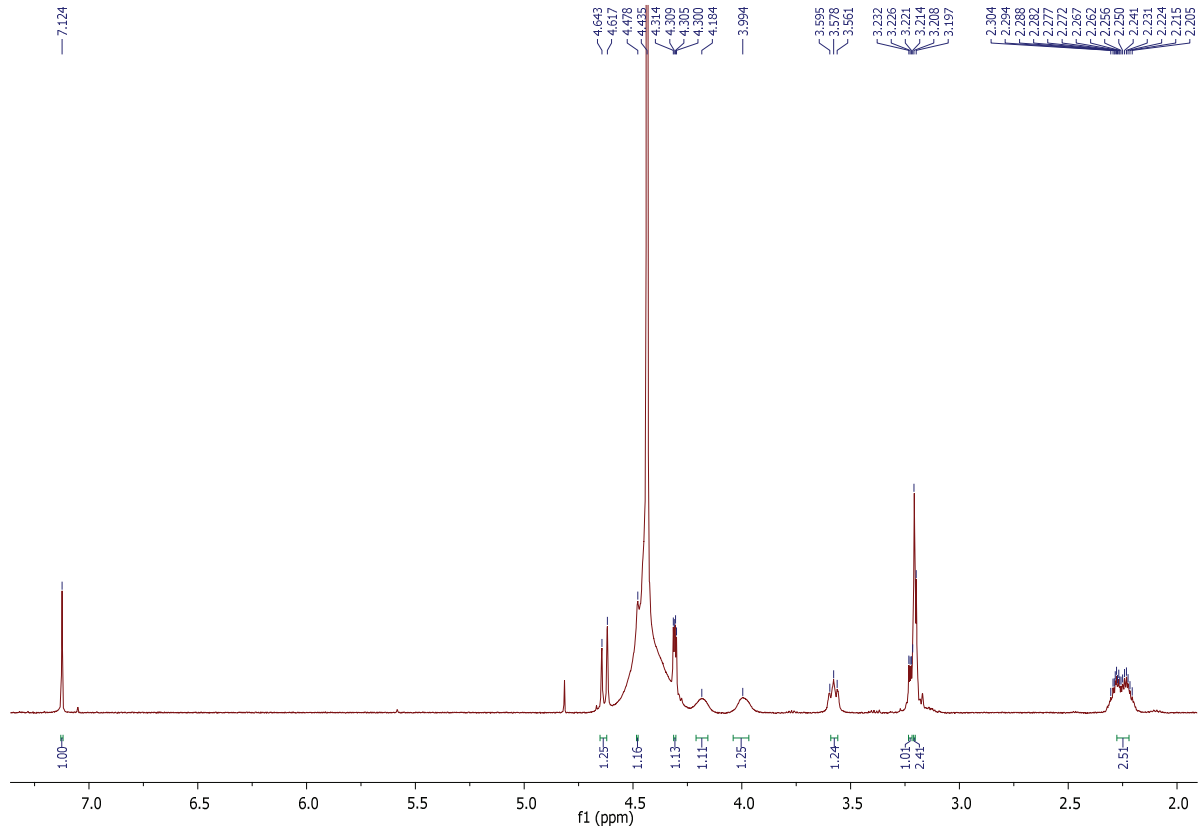

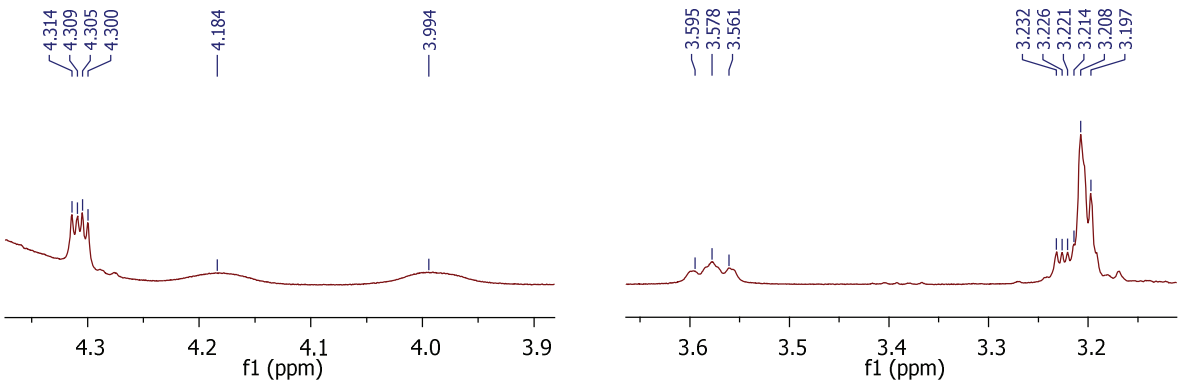

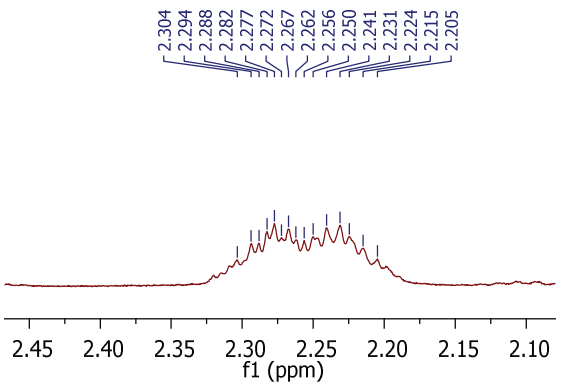

A3 ^{13}C NMR spectrum (151 MHz, D_2O, 330 K) of mycenarubin C.

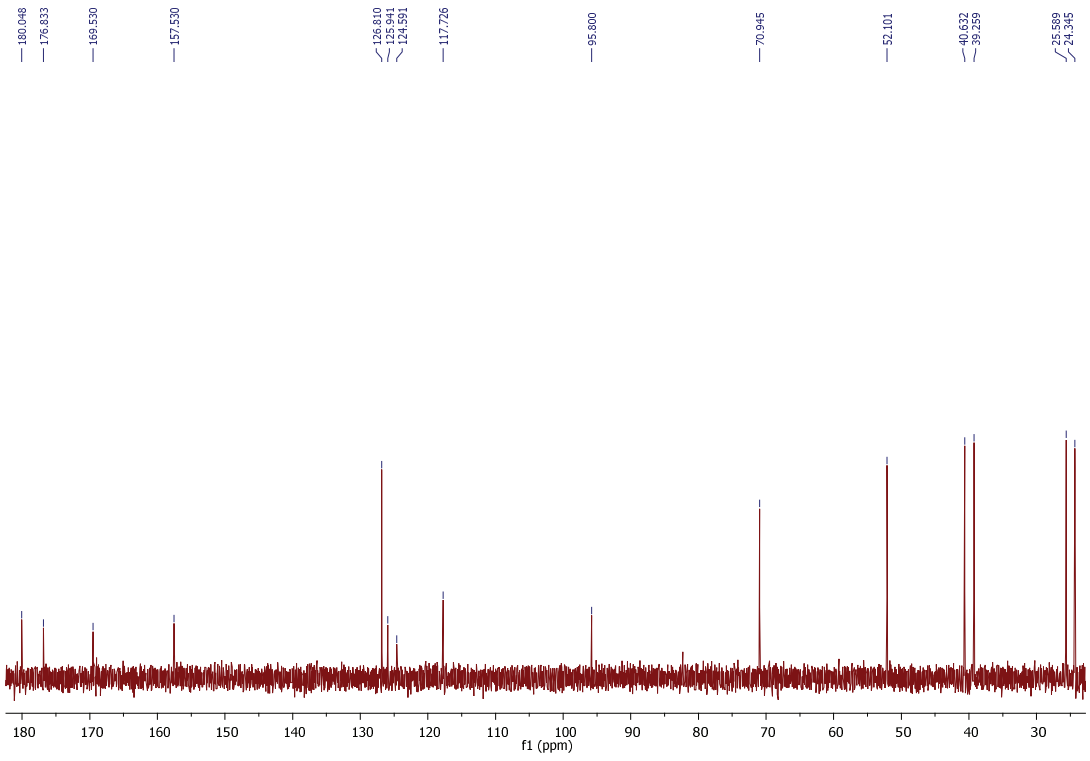

A4 COSY spectrum (600 MHz, D_2O, 330 K) of mycenarubin C.

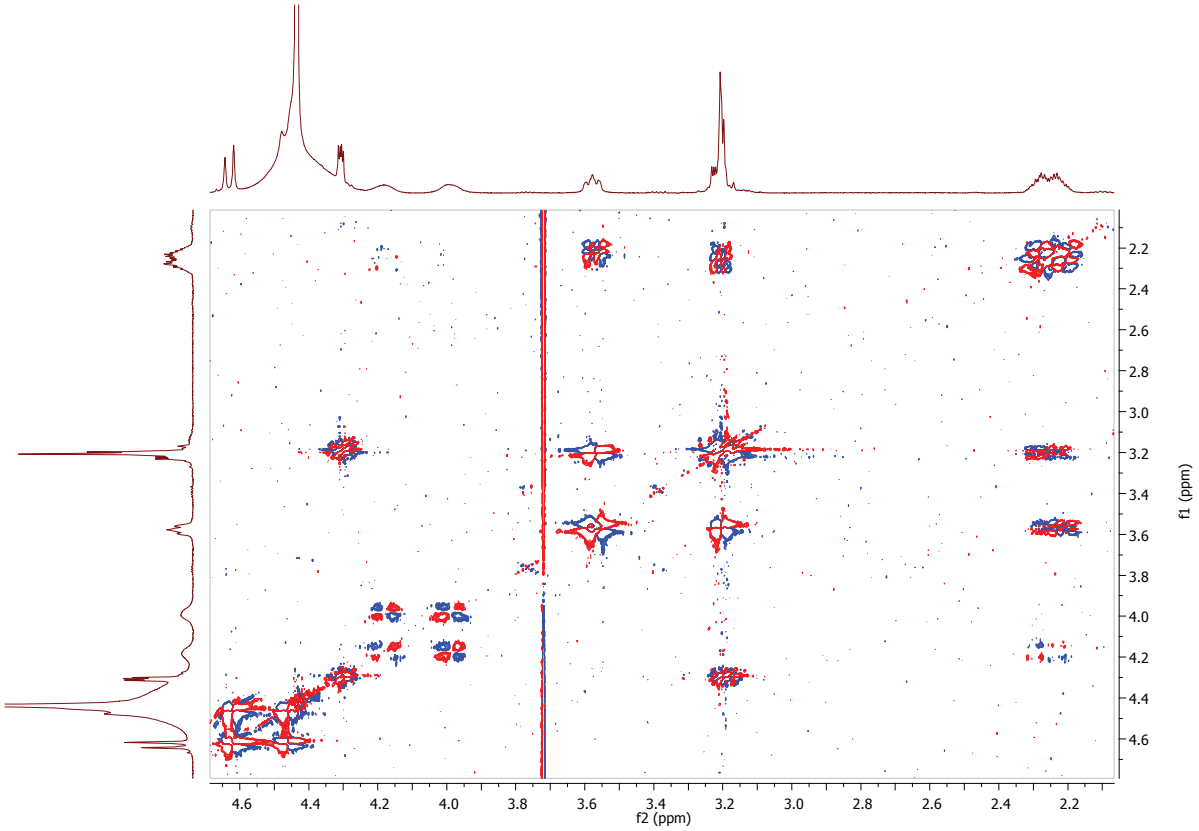

A5 HSQC spectrum (600 MHz, D_2O, 330 K) of mycenarubin C.

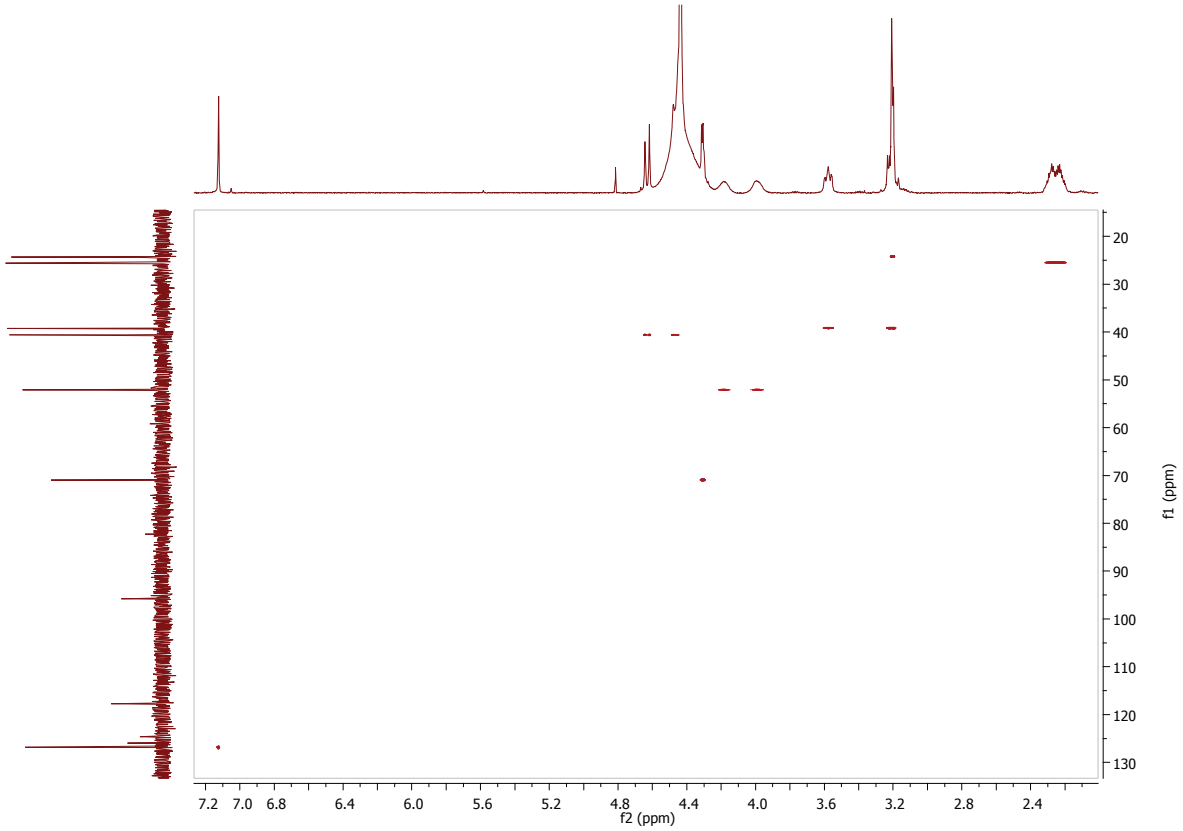

A6 HMBC spectrum (600 MHz, D_2O, 330 K) of mycenarubin C.

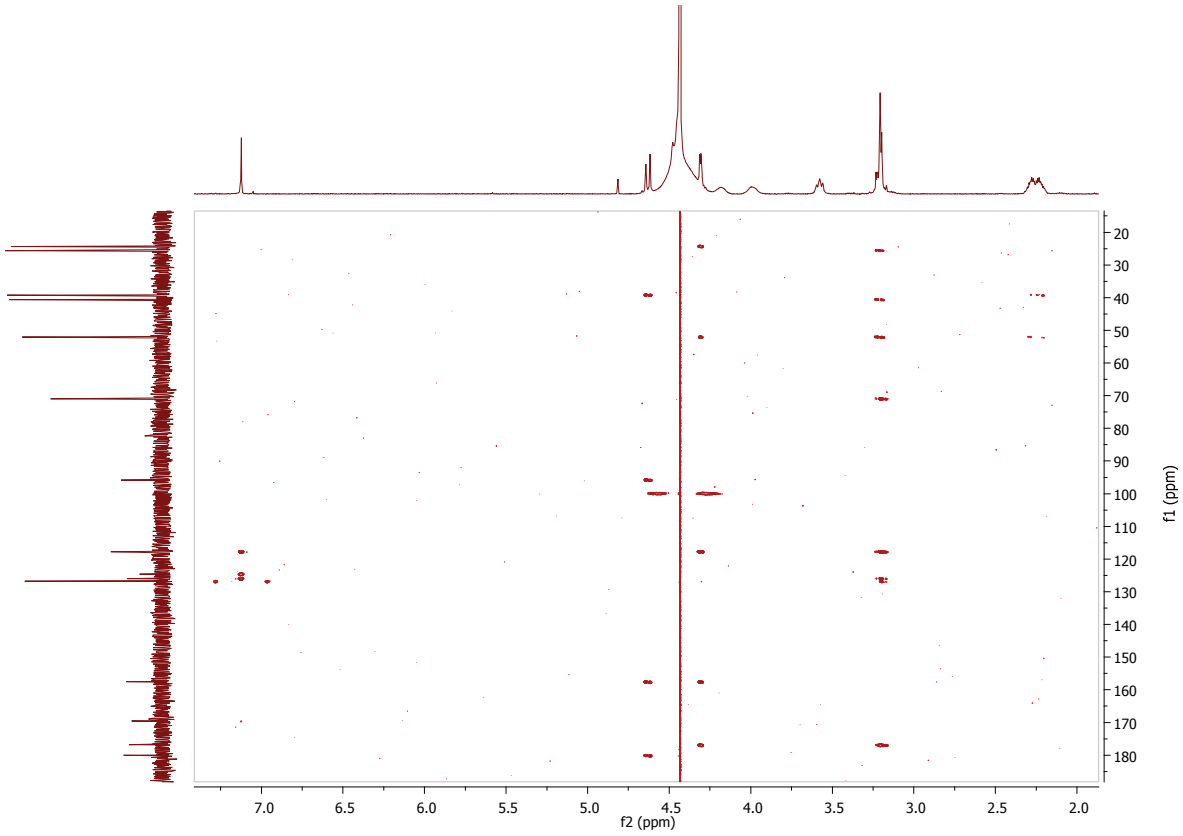

A7 NOESY spectrum (600 MHz, D_2O, 330 K) of mycenarubin C.

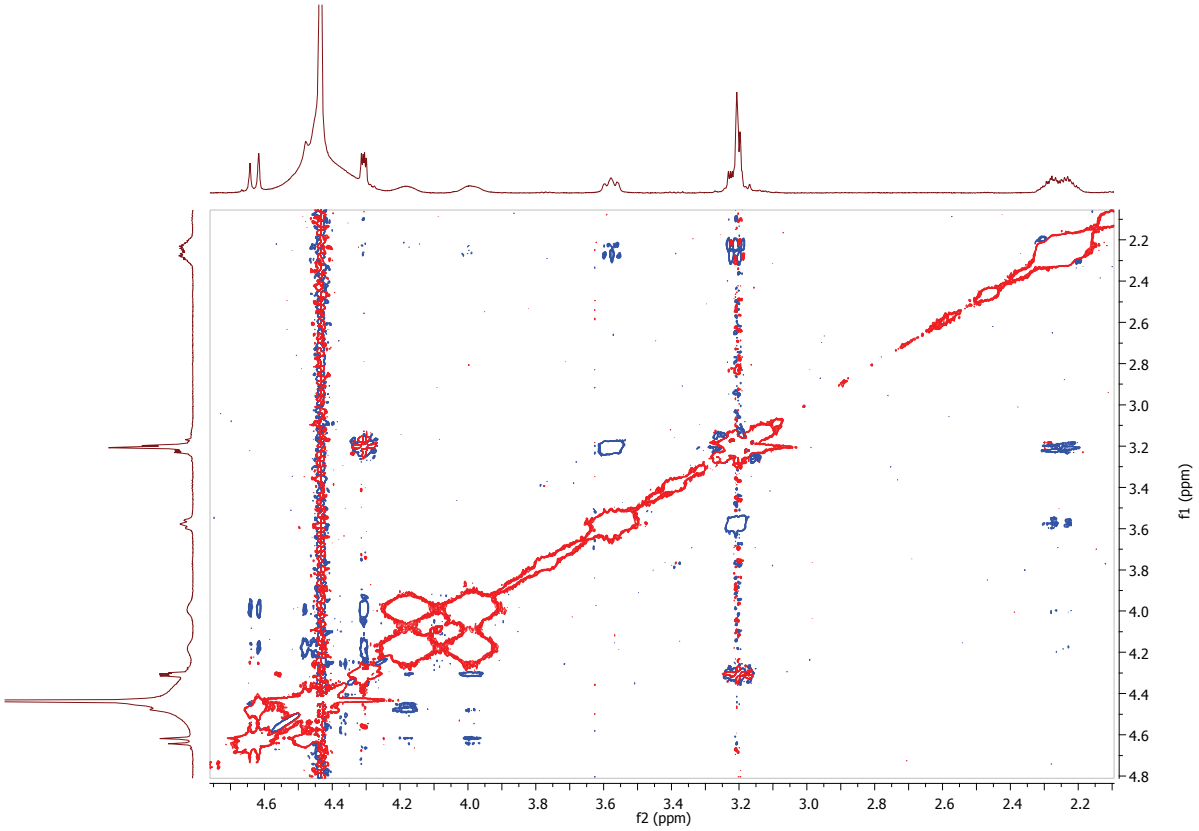

A8 ROESY spectrum (600 MHz, D_2O, 330 K) of mycenarubin C.

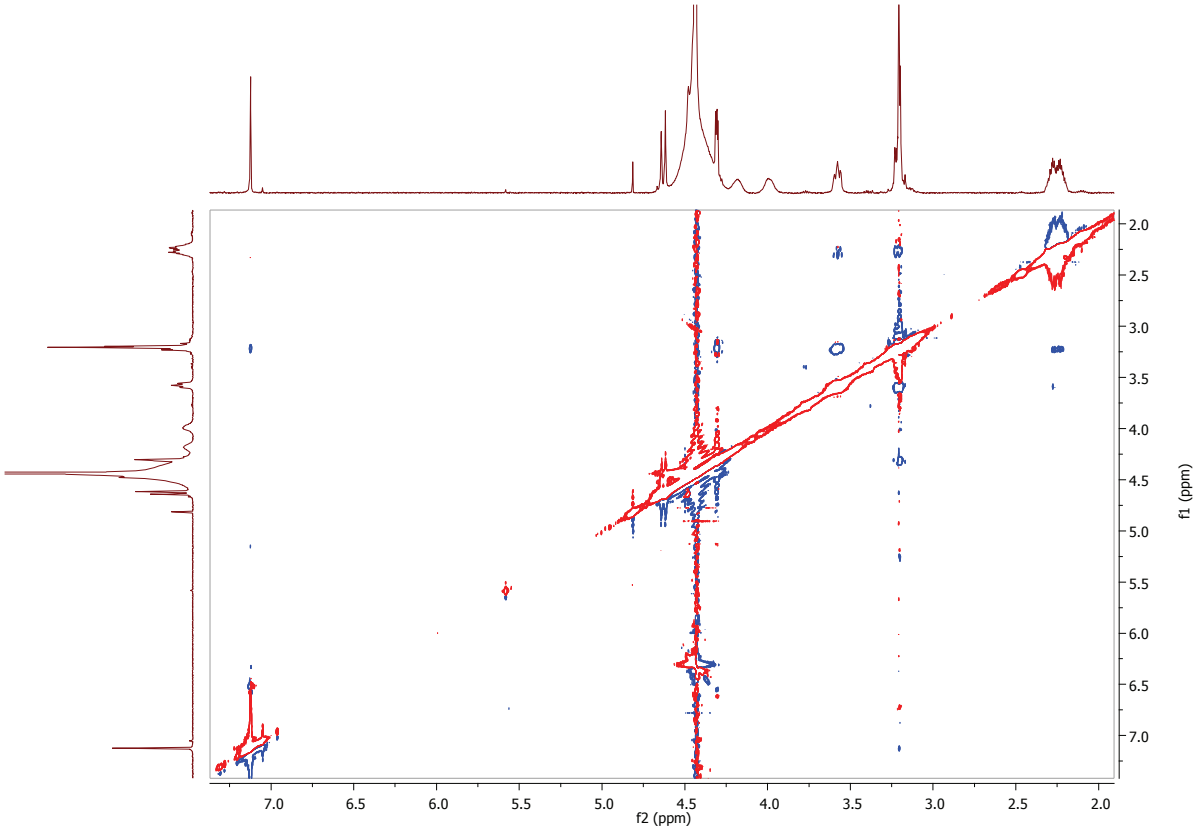

Mycena epipterygia

A9 Semi-preparative HPLC chromatogram of raw extract of *Mycena epipterygia* at λ = 410 nm.

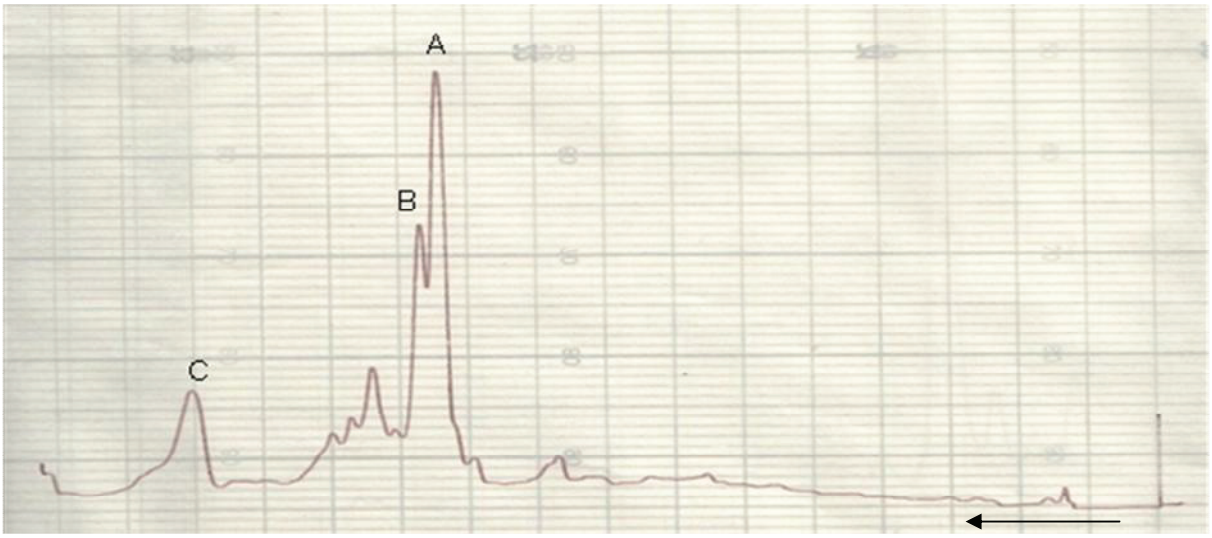

3-(1-Carboxylvinyloxy)-4-methoxy-5-hydroxybenzoic acid (**42**)

A10 ^{13}C NMR spectrum (151 MHz, d_6-DMSO, 300 K) of **42**.

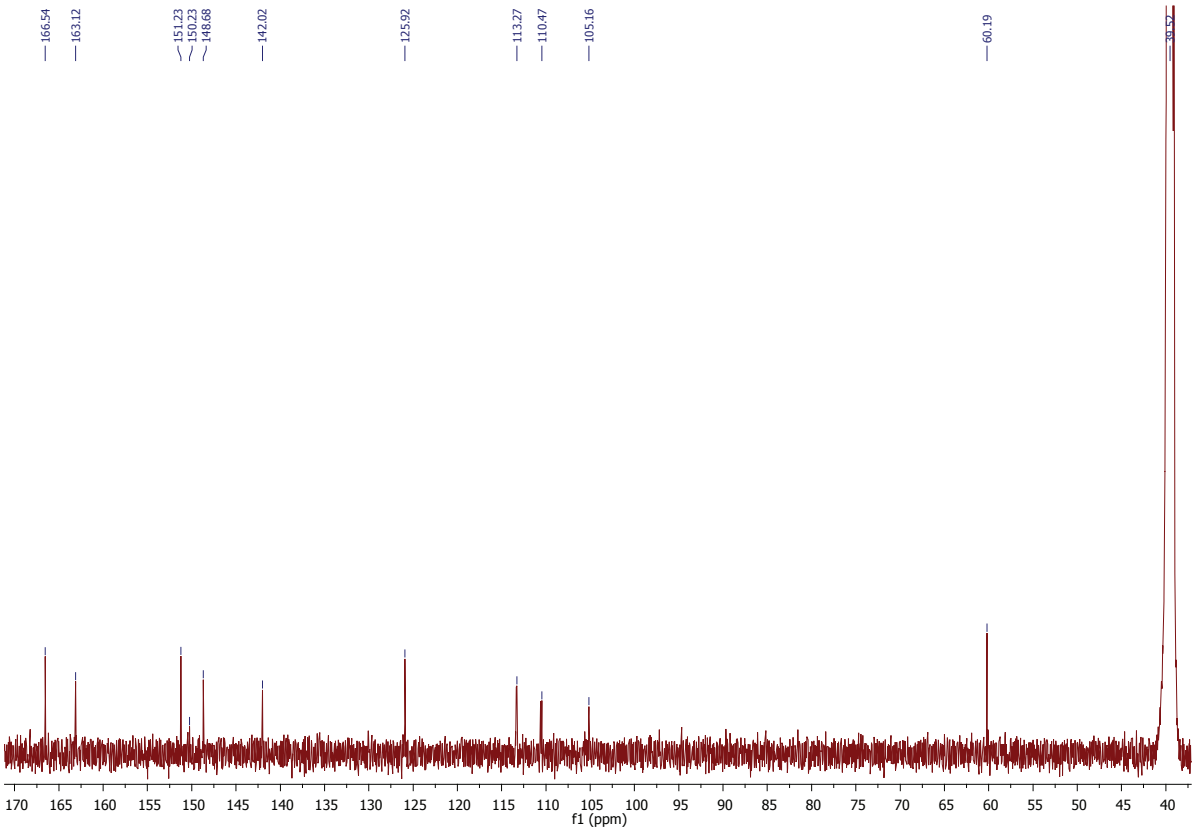

3-(1-Carboxylvinyloxy)-4, 5-dihydroxybenzoic acid (**43**)

A11 ^{1}H NMR spectrum (600 MHz, d_6-DMSO, 300 K) of **43**.

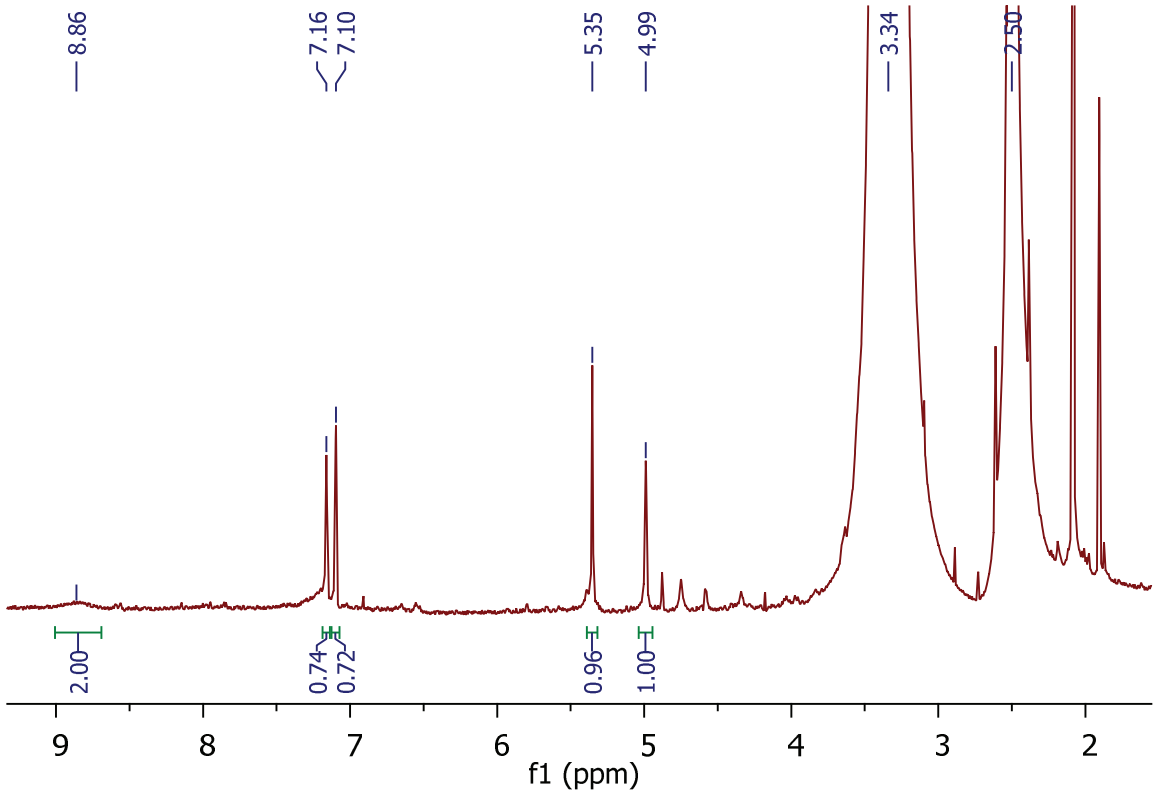

A12 COSY spectrum (600 MHz, D_2O, 300 K) of **43**.

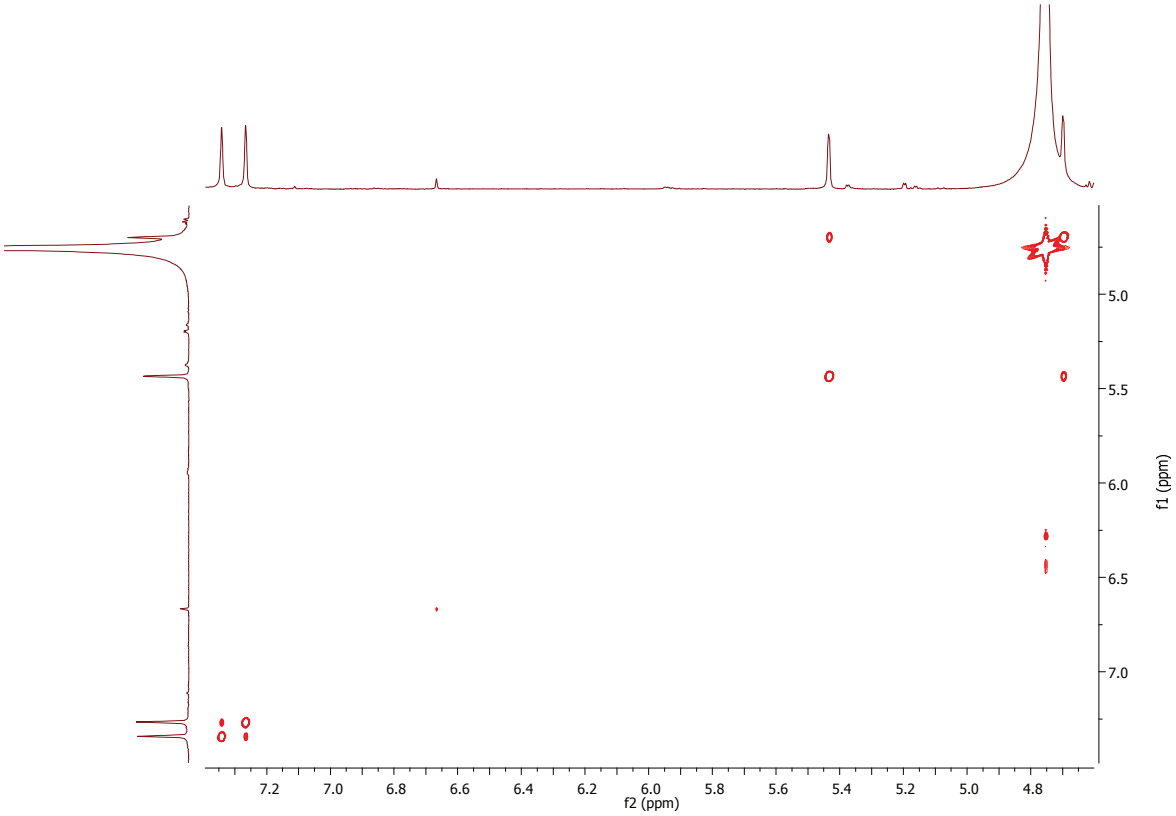

A13 HSQC spectrum (600 MHz, D_2O, 300 K) of **43**.

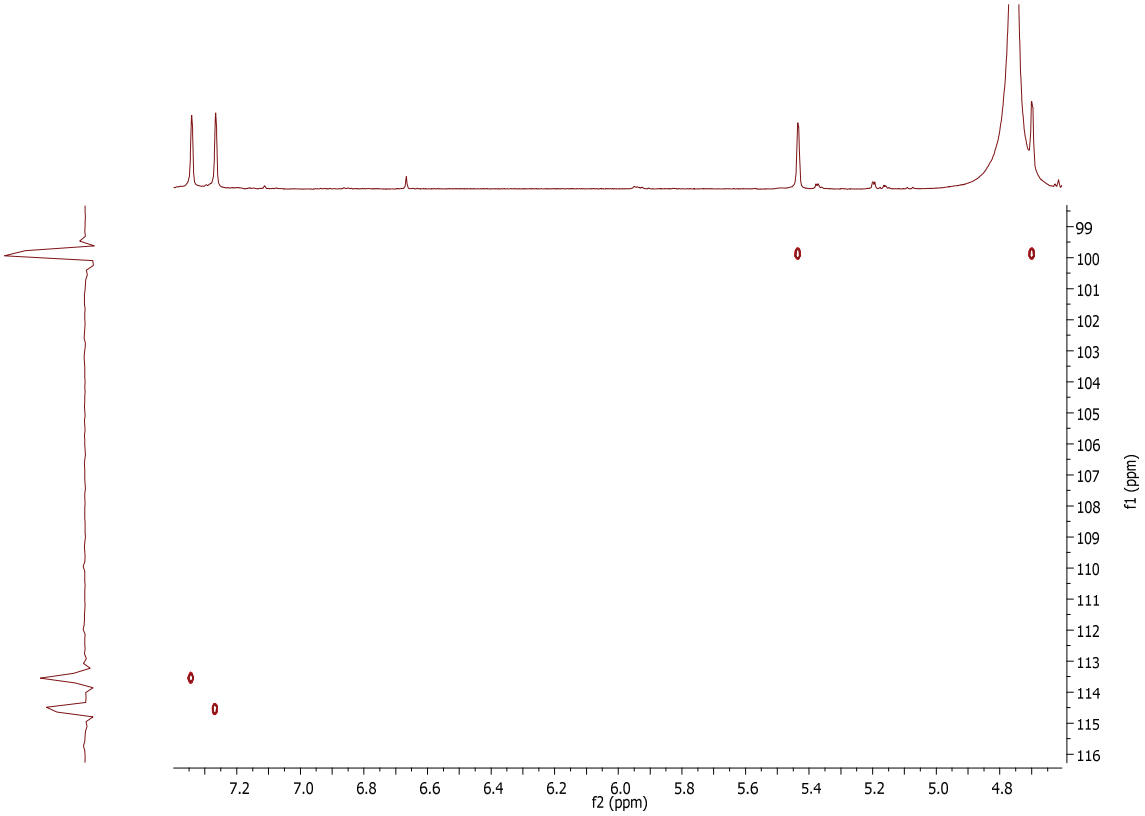

A14 (-)-ESI-MS/MS spectrum of compound **43**.

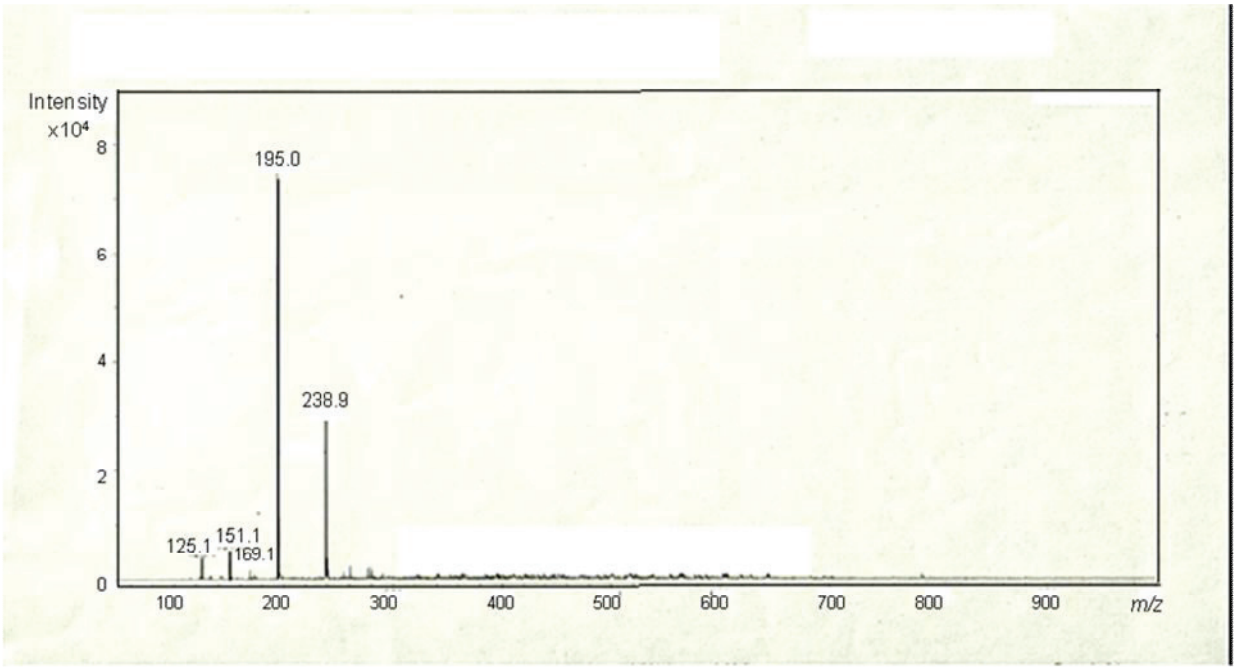

Compound D

A15 HR-(+)-ESI-MS spectrum of compound D.

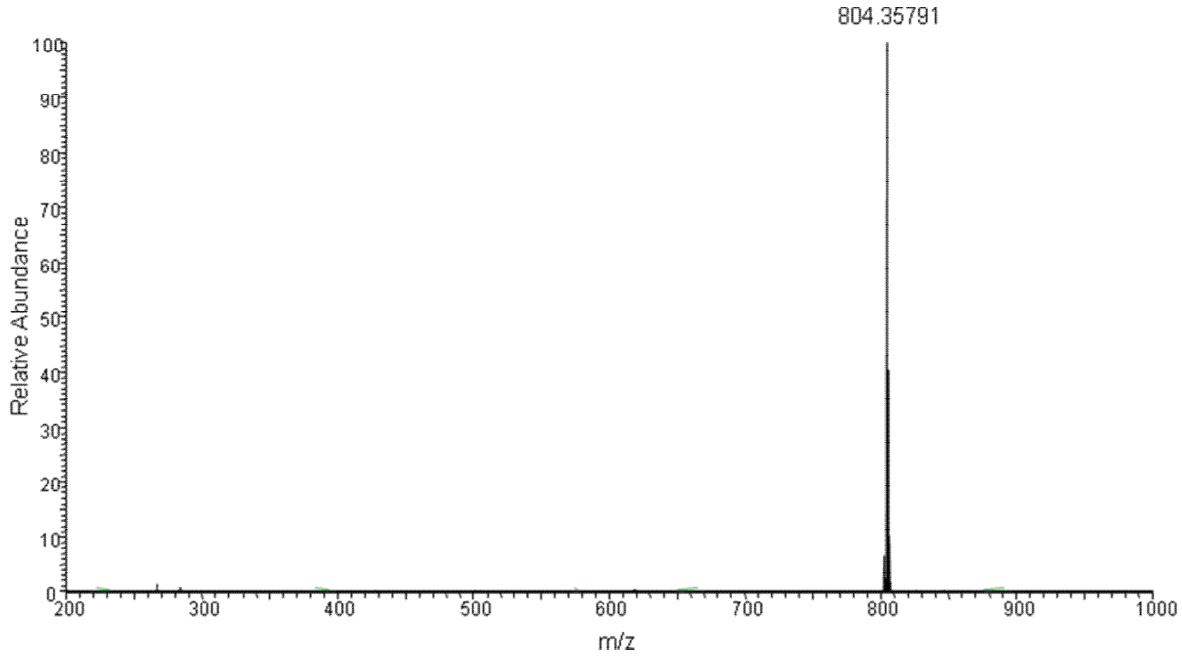

A16 Comparison of isotopic patterns of compound D with the generated molecular formula $C_{38}H_{55}N_5O_6P$.

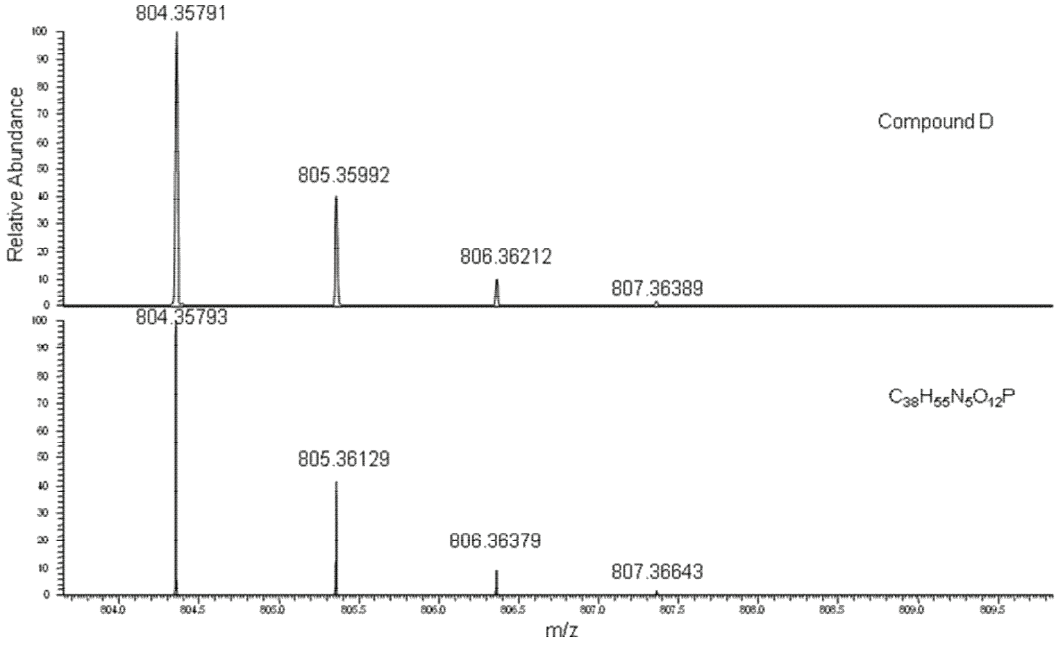

A17 ^{1}H NMR (600 MHz, d_6-DMSO, 300 K) of compound D.